

# STOCHASTIC HYBRID SYSTEMS WITH RENEWAL TRANSITIONS

by

Mohammad Soltani

A dissertation submitted to the Faculty of the University of Delaware in partial fulfillment of the requirements for the degree of Doctor of Philosophy in Electrical and Computer Engineering

Spring 2018

© 2018 Mohammad Soltani  
All Rights Reserved

**STOCHASTIC HYBRID SYSTEMS WITH RENEWAL TRANSITIONS**

by

Mohammad Soltani

Approved: \_\_\_\_\_  
Kenneth E. Barner, Ph.D.  
Chair of the Department of Electrical and Computer Engineering

Approved: \_\_\_\_\_  
Babatunde Ogunnaike, Ph.D.  
Dean of the College of Engineering

Approved: \_\_\_\_\_  
Ann L. Ardis, Ph.D.  
Senior Vice Provost for Graduate and Professional Education

I certify that I have read this dissertation and that in my opinion it meets the academic and professional standard required by the University as a dissertation for the degree of Doctor of Philosophy.

Signed: \_\_\_\_\_

Abhyudai Singh, Ph.D.  
Professor in charge of dissertation

I certify that I have read this dissertation and that in my opinion it meets the academic and professional standard required by the University as a dissertation for the degree of Doctor of Philosophy.

Signed: \_\_\_\_\_

Ryan Zurakowski, Ph.D.  
Member of dissertation committee

I certify that I have read this dissertation and that in my opinion it meets the academic and professional standard required by the University as a dissertation for the degree of Doctor of Philosophy.

Signed: \_\_\_\_\_

Javier Garcia-Frias, Ph.D.  
Member of dissertation committee

I certify that I have read this dissertation and that in my opinion it meets the academic and professional standard required by the University as a dissertation for the degree of Doctor of Philosophy.

Signed: \_\_\_\_\_

Pak-Wing Fok, Ph.D.  
Member of dissertation committee

## ACKNOWLEDGEMENTS

I want to thank my genius advisor Abhyudai Singh. I learned a lot from him and I wish I was learning more. I want to thank my friends and colleagues Cesar Vargas-Garcia, Khem Ghusinga, Saurabh Modi, and Zikai Xu for their friendship and collaborations. I hope we keep on working on exciting topics for years. I am grateful to the Dean, the Faculty, and the Staff of the Department of Electrical and Computer Engineering for providing their assistance and support through the years of my Ph.D. program.

A very special thank to my wife, Hannah E. Palmer for her support throughout my Ph.D. studies. I know I've not been a perfect partner because of the time and dedication that Ph.D. took. She tolerate this lack of attention for years and I hope that I will make it up to her in the future.

Thanks to my parents Kohzad and Manijeh, and my sister Zahra who had a huge role in my upbringing.

## TABLE OF CONTENTS

<b>LIST OF TABLES</b> . . . . .	<b>ix</b>
<b>LIST OF FIGURES</b> . . . . .	<b>x</b>
<b>ABSTRACT</b> . . . . .	<b>xviii</b>
<b>PREFACE</b> . . . . .	<b>xx</b>
<b>NOTATION</b> . . . . .	<b>xxiii</b>
 <b>Chapter</b>	
<b>1 MOMENT DYNAMICS OF STOCHASTIC HYBRID SYSTEMS WITH RENEWAL TRANSITIONS</b> . . . . .	<b>1</b>
1.1 Model Formulation . . . . .	1
1.2 Embedded Markov Chain for Event Timing . . . . .	3
1.3 Moment Dynamics of TTSHS . . . . .	5
1.4 Conclusion . . . . .	7
 <b>2 FLUCTUATIONS IN PROTEIN LEVELS FROM STOCHASTIC EXPRESSION AND NOISY CELL-CYCLE PROCESSES</b> . . . . .	 <b>8</b>
2.1 Coupling Gene Expression to Cell Division . . . . .	10
2.2 Modeling the Cell-cycle Time Using Phase-type Distributions . . . . .	11
2.3 Computing the Average Number of Protein Molecules . . . . .	13
2.4 Computing the Protein Noise Level . . . . .	15
2.4.1 Contribution from Randomness in Cell-cycle Times . . . . .	15
2.4.2 Contribution from Partitioning Errors . . . . .	17
2.4.3 Contribution from Stochastic Expression . . . . .	20
2.5 Noise in Synchronized Cells . . . . .	22
2.6 Conclusion . . . . .	23

<b>3</b>	<b>EFFECTS OF CELL-CYCLE DEPENDENT EXPRESSION ON RANDOM FLUCTUATIONS IN PROTEIN LEVELS . . . . .</b>	<b>24</b>
3.1	Model Coupling Cell Cycle to Gene Expression . . . . .	26
3.2	Mean Protein Level for Cell-cycle Driven Expression . . . . .	27
3.3	Protein Noise Level for Cell-cycle Driven Expression . . . . .	28
3.4	Optimal Cell-cycle Regulation to Minimize Noise . . . . .	30
3.5	Conclusion . . . . .	34
<b>4</b>	<b>STEADY-STATE MOMENT ANALYSIS OF STOCHASTIC HYBRID SYSTEMS . . . . .</b>	<b>38</b>
4.1	Statistical Analysis of TTSHS . . . . .	38
4.1.1	Steady-state Mean Level . . . . .	39
4.1.2	Steady-state Second-order Moments . . . . .	44
4.2	Modeling Noise in Nanosensors . . . . .	48
4.3	Quantifying Noise in Gene Expression . . . . .	50
4.3.1	Average Gene Product Level for Random Cell-cycle Times . . . . .	50
4.3.2	Stochasticity in Gene Product Levels for Random Cell-cycle Times . . . . .	51
4.3.3	Inclusion of Randomness in the Molecular Partitioning Process . . . . .	53
4.4	Conclusion . . . . .	55
<b>5</b>	<b>CONTROL DESIGN AND ANALYSIS OF A STOCHASTIC EVENT-DRIVEN SYSTEM . . . . .</b>	<b>56</b>
5.1	Stochastic Control of Event-driven Linear Systems . . . . .	57
5.2	Control Design from Steady-state Moments . . . . .	59
5.2.1	The Steady-state Mean of $\mathbf{x}$ . . . . .	59
5.2.2	The Second-order Moments of $\mathbf{x}$ . . . . .	60
5.3	Illustrative Examples . . . . .	62
5.3.1	Example 1 . . . . .	63
5.3.1.1	The Second-order Moment of the System . . . . .	63

5.3.1.2	Control Design . . . . .	66
5.3.2	Example II . . . . .	66
5.4	Conclusion . . . . .	68
<b>6</b>	<b>STOCHASTIC HYBRID SYSTEMS WITH FAMILIES OF RANDOM DISCRETE EVENTS . . . . .</b>	<b>69</b>
6.1	Model Formulation . . . . .	69
6.2	Steady-state Mean Level . . . . .	70
6.3	Steady-state Second-order Moments . . . . .	73
6.4	Noise in Protein Concentration . . . . .	74
6.5	Conclusion . . . . .	77
<b>7</b>	<b>MULTI-MODE STOCHASTIC HYBRID SYSTEMS WITH RENEWAL TRANSITIONS . . . . .</b>	<b>78</b>
7.1	Model Formulation . . . . .	78
7.2	Statistical Moments of Multi-mode Stochastic Hybrid System . . . . .	80
7.2.1	Steady-state Mean Level . . . . .	81
7.2.2	Steady-state Second-order Moments . . . . .	83
7.3	Noise in Gene Switching . . . . .	85
7.4	Conclusion . . . . .	88
<b>8</b>	<b>LINEAR NOISE APPROXIMATION FOR A CLASS OF STOCHASTIC HYBRID SYSTEMS . . . . .</b>	<b>90</b>
8.1	Comparison of Linearization and LNA in a Simple Genetic Circuit . . . . .	91
8.2	Equivalence of the Omega Expansion and Linearization Method . . . . .	94
8.3	An Alternative Representation to Systems Where Direct LNA Fails . . . . .	98
8.4	An Illustrative Example . . . . .	99
8.5	Conclusion . . . . .	102
<b>9</b>	<b>DISCUSSION . . . . .</b>	<b>103</b>
	<b>BIBLIOGRAPHY . . . . .</b>	<b>104</b>
	<b>Appendix</b>	
<b>A</b>	<b>DISCLAIMER . . . . .</b>	<b>118</b>

## LIST OF TABLES

1.1	Stochastic events in the TTSHS with timing of events described by the embedded Markov Chain in Fig. 1.2. . . . .	5
-----	--	---

## LIST OF FIGURES

- 1.1 **Schematic of a linear time-triggered stochastic hybrid system.** The state evolves according to a set of ordinary differential equation and events occur in random times. Whenever the event occurs  $\mathbf{x}$  changes via (1.2). . . . . 3
- 1.2 **A continuous-time Markov chain model for timing of events in TTSHS.** The time interval  $\tau_s \equiv t_s - t_{s-1}$  between two successive stochastic events is assumed to follow a mixture of Erlang distributions. After an event occurs, a state  $S_{i1}$ ,  $i = \{1, \dots, I\}$  is chosen with probability  $p_i$ . The system transitions through states  $S_{ij}$ ,  $j = \{1, \dots, m_i\}$  residing for an exponentially distributed time in each state. The next event occurs after exit from  $S_{im_i}$  and the above process is repeated. . . . . 4
- 2.1 **Sample trajectory of the protein level in a single cell with different sources of noise.** Stochastically expressed proteins accumulate within the cell at a certain rate. At a random point in the cell cycle, gene duplication results in an increase in production rate. Stochastic cell-division events lead to random partitioning of protein molecules between two daughter cells with each cell receiving, on average, half the number of proteins in the mother cell just before division. The steady-state protein copy number distribution obtained from a large number of trajectories is shown on the right. The total noise in the protein level, as measured by the squared Coefficient of Variation ( $CV^2$ ) can be broken into contributions from individual noise mechanisms. . . . . 9

2.2	<p><b>Stochastic models of gene expression with cell division.</b> Arrows denote stochastic events that change the protein level by discrete jumps as shown in (2.1) and (2.4). The differential equation within the circle represents the time evolution of <math>\mathbf{x}(t)</math> in between events. <b>A)</b> Model with all the different sources of noise: proteins are expressed in stochastic bursts, cell division occurs at random times, and molecules are partitioned between the two daughter cells based on (2.5). The trivial dynamics <math>\frac{d\mathbf{x}}{dt} = 0</math> signifies that the protein level is constant in-between stochastic events. <b>B)</b> Hybrid model where randomness in cell-division events is the only source of noise. Protein production is modeled deterministically through a differential equation and partitioning errors are absent, i.e., <math>b = 0</math> in (2.5). <b>C)</b> Hybrid model where noise comes from both cell-division events and partitioning errors. Protein production is considered to be deterministic as in part B. Since <math>\mathbf{x}(t)</math> is continuous here, <math>\mathbf{x}_+</math> has a positively-valued continuous distribution with same mean and variance as in (2.5) . . . . .</p>	12
2.3	<p><b>Scaling of noise as a function of the mean protein level for different mechanisms.</b> The contribution of random cell-division events to the noise in protein copy numbers (extrinsic noise) is invariant of the mean. In contrast, contributions from partitioning errors at the time of cell division (partitioning noise) and stochastic expression (production noise) scale inversely with the mean. The scaling factors are shown as a function of the protein random burst size <math>\mathbf{u}</math>, noise in cell-cycle time (<math>CV_{\tau_s}^2</math>) and magnitude of partitioning errors quantified by <math>b</math> (see (2.5)). With increasing mean level the total noise first decreases and then reaches a baseline that corresponds to extrinsic noise. For this plot, <math>\mathbf{u}</math> is assumed to be geometrically distributed with mean <math>\langle \mathbf{u} \rangle = 1.5</math>, <math>CV_{\tau_s}^2 = 0.05</math> and <math>b = 1</math> (i.e., binomial partitioning). . . . .</p>	19
3.1	<p><b>Coupling cell cycle to gene expression.</b> The outer loop shows an individual cell from birth to division passing through cell-cycle stages <math>S_1, S_2, \dots, S_I</math>, with transition rates between stages give by <math>\lambda_i</math>, <math>i \in \{1, 2, \dots, I\}</math>. The cell is born in stage <math>S_1</math> and division is initiated in <math>S_I</math>. The inner loop (transcriptional cycle) represents the rate at which protein expression bursts occur and is given by <math>k_i</math> in cell-cycle stage <math>S_i</math>. . . . .</p>	25

3.2 **Noise comparison for different strategies coupling cell cycle to gene expression.** The noise from bursty expression (left) and partitioning errors (right) as given by (3.17) are shown for five different strategies: expression only at the start of cell cycle; expression only at the cell-cycle midpoint; constant mRNA synthesis rate throughout the cell cycle; doubling of synthesis rate at the cell-cycle midpoint; expression only towards the end of cell cycle. While noise from bursty expression is minimized in the latter strategy, contribution from partitioning errors are lowest if expression occurs only at the beginning of cell cycle. The cell cycle was modeled by choosing  $I = 20$  stages with equal transition rates, i.e., stages have equal mean duration. The duration of each stage is an exponentially distributed random variable. The production rates  $k_i$  were chosen so as to have the same mean protein level per cell across all cases. Note that this plot is true for any burst size and distribution. . . . . 31

3.3 **Protein noise level from bursty expression is minimal when gene-duplication event is at the cell-cycle end, and fold-change in transcription is high.** *Left:* The rate of transcription within the cell cycle is modeled as a step function - it is equal to  $k$  ( $mk$ ) before (after) the gene-duplication event, where  $m$  is the fold-change in transcription. The event is assumed to occur at time  $\tau_g$  since the start of cell cycle, and cell division occurs at time  $\tau_s = \tau_g + \tau_d$ . After division, the rate again resets to  $k$ . The times  $\tau_g$  and  $\tau_d$  are assumed to be deterministic. *Right:* The noise contribution from bursty expression is plotted as a function of  $\tau_g/\tau_s$  and  $m$ . The value of  $k$  is changed so as to keep the mean protein level fixed. Noise levels are normalized to the noise when protein is expressed at a constant rate throughout the cell cycle ( $m = 1$ ). The plot reveals that the noise is smallest when  $\tau_g/\tau_s$  is close to 1, and  $m$  is large. . . . . 33

3.4	<p><b>Synthesis of proteins towards the end of cell cycle minimizes fluctuations in copy numbers.</b> Protein level in an individual cell across multiple cell cycles for two strategies: a fixed transcription rate throughout the cell cycle (top) and transcription increases drastically just before cell division (bottom). In both cases we assumed that there exists a small degradation of protein through the cell cycle. Trajectories obtained via Monte Carlo simulations are shown for the stochastic model (blue) and a reduced model where noise mechanisms are modeled deterministically (gray). These levels are subtracted to obtain a zero-mean stochastic process <math>\mathbf{z}(t)</math>, where fluctuations resulting from cell cycle are removed (black). Stationary distribution of <math>\mathbf{z}</math> obtained from 20,000 MC simulation runs is shown on the right, and the bottom strategy leads to lower variability in <math>\mathbf{z}</math> for the same mean protein level. Cell cycle and expression was modeled as in Fig. 3.1 and burst arrival rates were chosen so as to ensure a average protein copy number of 150 molecules per cell in both cases. . . . .</p>	35
4.1	<p><b>Schematic of stochastic hybrid systems with timer.</b> As the state evolves according to a linear system, events occur at discrete times that change the state of the system according to (1.2). The timing of events is controlled by renewal transitions defined through a timer <math>\tau</math> that linearly increases over time in between events, and is reset to zero each time an event occurs. Choosing the event arrival rate <math>h(\tau)</math> based on (4.1) ensures that the time interval between events is iid with probability distribution <math>f</math>. . . . .</p>	39
4.2	<p><b>The noise contributions show similar behavior with respect to decay rate, but contrasting behavior with respect to noise in cell-cycle times.</b> A 2D color plot of the two noise contributions in (4.70) as a function of the gene product decay rate and the noise in cell-cycle times. Increasing <math>CV_{\tau_s}^2</math> increases the noise contribution from random cell-cycle times, but decreases the contribution from random partitioning. Both noise contributions decrease monotonically with increasing decay rate. Noise levels are normalized to their value when <math>CV_{\tau_s}^2 = 0</math> and <math>\gamma_x = 0.1 \text{ hr}^{-1}</math>. We used gamma distributed <math>\tau_s</math> with a fixed mean cell-cycle time of <math>\langle \tau_s \rangle = 2 \text{ hrs}</math>. The mean of <math>\mathbf{x}</math> is fixed at 100 molecules by simultaneously changing <math>k_x</math>. . . . .</p>	52

4.3	<p><b>Gene product noise levels can both increase or decrease with increasing noise in cell-cycle times.</b> The total noise in (4.70) is plotted as a function of parameter <math>b</math> in the partitioning process and noise in cell-cycle times. While for small (large) values of <math>b</math> the noise levels increase (decrease) with increasing <math>CV_{\tau_s}^2</math>, intermediate values of <math>b</math> can make the total noise approximately invariant of <math>CV_{\tau_s}^2</math>. Noise levels are normalized to their value when <math>CV_{\tau_s}^2 = 0</math>, the mean of <math>\mathbf{x}</math> is fixed at 20 molecules by simultaneously changing <math>k_x</math>, and <math>\gamma_x = 0.1 \text{ hr}^{-1}</math>. The rest of parameters are chosen equal to their value in Fig. 4.2. . . . . .</p>	54
5.1	<p><b>Model schematic of an event-driven control loop.</b> <i>Left:</i> The controller is far from the plant hence the feedback loop is connected through a network. In between transmission times, plant uses the previous control law which is maintained in hold. Any time that connection occurs, the hold reads the new control law which is calculated based on the current values of states of the system. <i>Right:</i> The mathematical representation of system as a stochastic hybrid system. Resets are the times in which connection occurs. Any time that a transmission occurs, a new control law is applied to the plant. However due to presence of errors, an extra term <math>\eta</math> is added to the system. . . . .</p>	58
5.2	<p><b>Making transmission of the control law more random can reduce variance of <math>\mathbf{x}</math>.</b> A) Surprisingly, by increasing the mean time intervals between the transmissions, the noise in <math>\mathbf{x}</math> contributed from disturbance can reduce. On the other hand, increasing <math>\tau_s</math> will increase the noise contributed from <math>\sigma</math>. This is because the added noise by controller remains in the system for a longer time before getting corrected by a new control law. B) Noisy transmission times also can reduce the variance contributed from disturbance. Hence, when the noise added by controller is small, randomly distributed times can be used to reduce variance in <math>\mathbf{x}</math>. For this plot, we used gamma distributed time intervals and variance of <math>\mathbf{x}</math> is normalized to its value at the beginning of the plot. The noise in transmission time intervals is quantified by coefficient of variation squared <math>CV_{\tau_s}^2</math>. The parameters are selected as <math>\hat{a} = 1</math>, <math>A = -1</math>, <math>E = 0.45</math>, <math>B = 0.5</math>, <math>K = 0.5</math>, and <math>\sigma = 1</math>. Finally, 95% confidence intervals are obtained by running 1000 numerical simulations. . . . .</p>	62

- 5.3 **The control gain can be designed to obtain any desired mean as long as eigenvalues remain within the unit circle.** A) By increasing the control gain, the magnitude of eigenvalues increases resulting in the system to move toward instability. The second eigenvalue becomes greater than 1 first. This means that there exists a control gain that the mean is finite, but the variance is infinite. When the other eigenvalue becomes greater than 1 the system becomes unstable. Hence, there exists certain values of mean that we never can reach. B) The variance is finite only when absolute value of both eigenvalues are less than 1. The variance is normalized to its value when  $K = 0$ . For intermediate values of  $K$ , variance is less than the time in which there exists no control ( $K = 0$ ). In this figure, time intervals in between the resets are gamma distributed with  $\langle \tau_s \rangle = 1 \text{ min}$  and  $CV_T^2 = 0.2$ . The rest of parameters are selected as  $\hat{a} = 1.5$ ,  $A = -1$ , and  $B = -1$ . . . . . 64
- 6.1 **Schematic of a TTSHS with linear continuous dynamics and two families of random resets.** The two families of resets occurs at random times and change the state based on the linear affine maps (6.2) and (6.4). For the first reset, events happen at exponentially-distributed time intervals, while for the second reset, time intervals are generally-distributed and drawn from an arbitrary probability distribution function. The timing of the latter family of resets is regulated by a timer  $\tau$  that measures the time since the last event, and the next event occurs at a hazard rate  $h_2(\tau)$ . In between events, the state evolve according to a linear time-invariant dynamical system. . . . . 71
- 6.2 **Modeling stochasticity in the level of protein concentration using TTSHS.** *Left:* Time evolution of the protein level  $\mathbf{x} \in \mathbb{R}$  in a single cell is modeled via a SHS with two stochastic resets representing production of proteins in bursts and cell-division events. The latter is controlled by a timer  $\tau$ , and whenever it occurs the state is reset via (6.26)-(6.27). In between events, protein concentrations decay exponentially with rate  $\gamma_x$  due to cellular growth. *Right:* A sample trajectory of  $\mathbf{x}$  is shown with cell division events (dashed lines). The steady-state distribution of  $\mathbf{x}$  obtained via a large number Monte Carlo simulations is shown on the right. . . . . 75

7.1	<b>Schematic of stochastic hybrid systems with two operation modes.</b>	In each mode the states are governed via a set of stochastic differential equations according to (7.1). Resets happen at random times. Any time that an event occurs the states change their value and the system switches to another operation mode. The states after reset depend on the states before reset (eq. 7.4). A timer $\tau$ measures the time since the last even, and rest to zero after each event occurs.	79
7.2	<b>The fundamental process of gene switching can be modeled through multi-mode framework.</b>	A) Promoter randomly switches between active and inactive states. Protein synthesis only occurs when promoter is ON. Protein is subject to decay with a rate $\gamma_x$ . B) The multi-mode system presented here is perfect for modeling promoter toggling. When gene is OFF the protein dynamics are only governed via decay. when promoter becomes active the protein synthesis is modeled through a Langevin equation with a rate $k_x$ .	86
7.3	<b>The noise in protein concentration is highly affected by the gene-switching time intervals.</b>	A) Noise in gene ON time intervals will not change the mean of a protein. Moreover, it does not have an obvious effect on the protein time trend. B) The noise in protein is highly affected by the gene switching noise. While the mean of protein only depends on the ratio of gene ON and OFF times, noise is affected by the magnitude of the ON and OFF time intervals as well. For this plot the protein production rate is selected to be $k_x = 100$ , decay rate is $\gamma_x = 1 \text{ min}^{-1}$ , and mean ON and OFF time intervals are equal $\langle \tau_{on} \rangle = \langle \tau_{off} \rangle$ .	88
8.1	<b>The schematic of general SHS vs the ones in which linearization and LNA leads to the same results.</b>	Continuous dynamics of the system are governed via a set of general ordinary differential equations $g(\mathbf{x}/\Omega, t)$ . Different family of resets occur with transition intensity $h_r(\mathbf{x}/\Omega, t)$ , $r \in \{1, \dots, s\}$ . Anytime that a reaction occurs the states of SHS change via a matrix $J^r$ and a vector $A_r$ . Note that for $J^r \neq I_n$ the direct LNA using omega expansion is not valid.	95

8.2 **The fluctuations in protein  $x$  can be split into a macroscopic part and a stochastic production part.** *Left.* The large fluctuations in proteins are reflected in the macroscopic part and the smaller fluctuations correspond to the stochastic production part. *Right.* The noise in protein ( $CV_x^2$ ) can be approximated well by our omega expansion technique when the system size increases. Note that this approximation is better than simply applying moment closure on the moment dynamics of  $x$ . The 95% confidence intervals are obtained via bootstrapping based on 5,000 realizations. . . . . 100

## ABSTRACT

Stochastic dynamics of several systems can be modeled via piecewise deterministic time evolution of the state, interspersed by random discrete events. Within this general class of systems we consider time-triggered stochastic hybrid systems (TTSHS), where the state evolves continuously according to a linear dynamical system. Discrete events occur based on an underlying renewal process (timer), and the intervals between successive events follow an arbitrary continuous probability density function. Moreover, whenever the event occurs, the state is reset based on a linear affine transformation that allows for inclusion of state-dependent and independent noise terms.

Traditional analysis of stochastic hybrid systems (SHS) relies heavily on various Monte Carlo simulation techniques, which come at a significant computational cost. Since one is often interested in computing only the lower-order moments of the state variables, much time and effort can be saved by directly computing these statistical moments without having to run Monte Carlo simulations. Unfortunately, moment calculations in SHS can be non-trivial due to the problem of unclosed dynamics: the time evolution of lower-order moments of the state space depends on higher-order moments. In such cases, moments are usually approximated by employing closure schemes, that close the system of differential equations by approximating higher-order moments as nonlinear functions of lower-order moments.

The key contribution of this thesis is to develop novel methods for different classes of TTSHS for obtaining exact analytical expressions for the steady-state moments, along with derivation of necessary and sufficient conditions for the stability of statistical moments. The method developed here is applied to a wide range of problems from systems biology to nano sensors. Moreover, we used TTSHS as an efficient tool to design a controller in the presence of disturbance, noise, and random discrete events

in a system. Finally, for SHS models which cannot be solved analytically, we develop a new moment closure approach to approximate their moments with low approximation error.

## PREFACE

In chapter 1 we introduce a method for deriving moment dynamics of TTSHS systems. Our approach relies on embedding a Markov chain based on phase-type processes to model timing of events. In this case, we show that the time evolution of moments can be computed exactly by solving a system of linear differential equations. In chapter 2 we use this method to study noisy expression inside individual cells. The contribution of this part is quantifying how cell cycle-related noise sources combine with stochastic expression to drive intercellular variability in protein molecular counts. Derived formulas lead to many counterintuitive results, such as increasing randomness in the timing of cell division can lower noise in the level of a protein. In chapter 3 we used a variation of TTSHS in chapter 1 to study cell-cycle dependent expression of genes. In our model, a protein is synthesized in random bursts, and the frequency with which bursts occur varies within the cell cycle. Our model reveals an interesting trade-off: cell-cycle dependencies that amplify the noise contribution from bursty expression also attenuate the contribution from partitioning errors. We investigate existence of optimum strategies for coupling expression to the cell cycle that minimize the stochastic component. Intriguingly, results show that a zero production rate throughout the cell cycle, with expression only occurring just before cell division minimizes noise from bursty expression for a fixed mean protein level. We provide examples of regulatory proteins that are expressed only towards the end of cell cycle, and argue that such strategies enhance robustness of cell-cycle decisions to the intrinsic stochasticity of gene expression.

In chapter 4 we introduce an alternative approach to calculate the statistical moments of these systems in steady-state. The proposed method is unable to provide transient behavior of the system but, on the bright side, is applicable to a wide class of

stochastic hybrid systems. Moreover, the new method provides explicit conditions for the existence and convergence of statistical moments. We show that this broad class of systems is conveniently suited to capture the moments of unstable gene products, and derive unique formulas connecting its mean and variance to underlying model parameters and noise mechanisms. In addition, through a nano sensor example we show that the applicability of this framework is beyond systems biology. In chapter 5 we use an adaptation of the results in chapter 4 to design controller for a class of linear systems. The system is subject to external disturbances that affect the plant. The control law is applied to the system in random discrete time intervals, and the control law can contain noise and uncertainty due to faulty actuators, noise in the system, etc. Our objective is how to design the control law to have finite statistical moments of the system and reach to desired performance specifications. We derive exact solutions of the first two moments of the system, and use them to derive the stability conditions. We further design a control law that steers the system to a desired mean and variance.

Next, in chapter 6 we expand our work and consider two families of mutually independent discrete events, with one family of resets occurring at exponentially-distributed times. Our results are illustrated on protein concentration where we assumed a protein is expressed in bursts at exponentially-distributed time intervals, decays within the cell cycle, and is randomly divided among daughter cells when generally-distributed cell-division events occur. Moreover, in chapter 7 we extend our analysis to the systems in which random resets can change both dynamics and states of the system. We demonstrate our method on protein concentration in the presence of random gene switching times and random synthesis events. We observe that randomness in gene-switching time increases the total noise in protein concentration. Since the noise in gene switching time intervals is a function of the number of steps that needs to be taken before transcription starts, we discuss how noise in protein sheds light on the underlying gene expression mechanisms.

Finally, in chapter 8 we study stochastic hybrid systems in which their exact solution is not available. We extend the Linear Noise Approximation (LNA) method

to these systems. The LNA method is obtained by small noise approximation of the probability distribution solution of the master equation, and is widely used in discrete-state continuous-time models. We prove that LNA is only directly applicable to a small sub-class of SHS, and we show that for this sub-class, LNA is equivalent to calculating moments directly by linearizing nonlinearities of the system. For the systems where direct application of LNA fails to give meaningful results, we provide a novel method for approximating moments.

## NOTATION

The set of real numbers is denoted by  $\mathbb{R}$ . Constant vectors are indicated by a hat, e.g.  $\hat{a}$ , and matrices are denoted by capital letters. Further, transpose of a matrix  $A$  is given by  $A^\top$  and the  $n$ -dimensional identity matrix is denoted by  $I_n$ . We show zero vectors and matrices with the same notation, e.g.  $A = \hat{a} = 0$ . Random variables are indicated by boldsymbol letters. The expected value of a random variable  $\mathbf{x}$  is denoted by  $\langle \mathbf{x} \rangle$  and the expected value in steady-state is denoted by  $\overline{\langle \mathbf{x} \rangle} \equiv \lim_{t \rightarrow \infty} \langle \mathbf{x}(t) \rangle$ . Similarly for time varying variable  $x$ , the steady-state value is presented by  $\bar{x}$ . Moreover, the conditional expectation of  $\mathbf{x}$  given another random variable  $\mathbf{y}$  is denoted  $\langle \mathbf{x} |_{\mathbf{y}} \rangle$ . Finally, the name of species is denoted by capital non-italic letters.

## Chapter 1

### MOMENT DYNAMICS OF STOCHASTIC HYBRID SYSTEMS WITH RENEWAL TRANSITIONS

We study a class of stochastic hybrid systems (SHS) that couple continuous linear dynamics with random discrete events that occur based on an underlying renewal process. Such systems have been referred to in literature as time-triggered stochastic hybrid systems (TTSHS) [1–4], and are an important sub-class of piecewise-deterministic Markov processes (PDMP) [5–8] with applications in different disciplines. For example, TTSHS have been shown to arise ubiquitously in networked control systems, where a dynamical system is controlled over a noisy communication network, and signals are received at discrete random times [9–17]. Other TTSHS applications include modeling disturbances in nanosensors [18], capturing stochastic effects in cellular biochemical processes [19–22], and neuroscience [23]. First, we study TTSHS where the continuous dynamics was modeled by a linear time-invariant system, and the time intervals between successive discrete events are restricted to follow a phase-type distribution (i.e., mixture and/or sum of exponential random variables).

#### 1.1 Model Formulation

Here, we identify a class of SHS known as time-triggered SHS (TTSHS) that have closed moments. The main ingredients of TTSHS are as follows:

1. A continuous state  $\mathbf{x}(t) \in \mathbb{R}^{n \times 1}$  that evolves according to a set of ordinary differential equations (ODEs) as

$$\frac{d\mathbf{x}(t)}{dt} = \hat{a} + A\mathbf{x}(t), \quad (1.1)$$

where  $A \in \mathbb{R}^{n \times n}$  and  $\hat{a} \in \mathbb{R}^{n \times 1}$  are a constant matrix and vector. While exact moment computations can be easily extended to linear stochastic differential equations, we prefer to work with ODEs for the sake of simplicity.

2. Stochastic events occur at discrete times  $\mathbf{t}_s$ ,  $s \in \{1, 2, \dots\}$ , and the intervals  $\mathbf{t}_s - \mathbf{t}_{s-1}$  are independent and identical random variables drawn from a given probability density function. These events can be referred to as renewal transitions, as their timing is determined by an underlying renewal process.
3. A reset map defining the change in  $\mathbf{x}$  when the event occurs

$$\mathbf{x} \mapsto \mathbf{x}_+, \quad (1.2)$$

where  $\mathbf{x}_+$  denotes the state of the system just after the event. While prior work has considered a deterministic linear reset map

$$\mathbf{x} \mapsto J\mathbf{x} \quad (1.3)$$

[9, 11, 24], we allow for both state-dependent and state-independent noise sources in  $\mathbf{x}_+$ . We assume  $\mathbf{x}_+$  to be a random variable, whose average value is related to its value just before the event by a linear affine map

$$\langle \mathbf{x}_+ \rangle = J\mathbf{x} + \hat{r}, \quad (1.4)$$

where  $J \in \mathbb{R}^{n \times n}$  and  $\hat{r} \in \mathbb{R}^{n \times 1}$  are a constant matrix and vector, respectively. Furthermore, the covariance matrix of  $\mathbf{x}_+$  is defined by

$$\langle \mathbf{x}_+ \mathbf{x}_+^\top \rangle - \langle \mathbf{x}_+ \rangle \langle \mathbf{x}_+ \rangle^\top = Q\mathbf{x}\mathbf{x}^\top Q^\top + B\mathbf{x}\hat{c}^\top + \hat{c}\mathbf{x}^\top B^\top + D. \quad (1.5)$$

Here  $Q \in \mathbb{R}^{n \times n}$  and  $B \in \mathbb{R}^{n \times n}$  are constant matrices, and  $\hat{c} \in \mathbb{R}^{n \times 1}$  is a constant vector. Moreover  $D \in \mathbb{R}^{n \times n}$  is a constant symmetric positive semi-definite matrix. Intuitively, (1.5) formalizes the noise added to the state during the reset (event), with  $Q = B = D = \hat{c} = 0$  implying that  $\mathbf{x}_+$  is simply a deterministic linear function of  $\mathbf{x}$ . A constant state-independent noise can be incorporated through a nonzero matrix  $D$  with  $Q = B = \hat{c} = 0$ . The generality of (1.5) allows for state-dependent noise terms that can potentially be quadratic (nonzero  $Q$ ) or linear (nonzero  $B$  and  $\hat{c}$ ) functions of the state, and we will see an example of it later in the manuscript. In the following sections, we show how statistical moments of  $\mathbf{x}(t)$  can be computed exactly for TTSHS illustrated in Fig. 1.1.

Our goal is to connect moments of the continuous state to the statistics of the time interval  $\tau_s \equiv \mathbf{t}_s - \mathbf{t}_{s-1}$ . The key contribution of this chapter is to model arrival of events using phase-type processes [25], and show that the resulting systems has closed moment dynamics. More specifically, the time derivative of an appropriately selected vector of moments depends only on itself, and not on higher-order moments. As a consequence, moments can be computed exactly by solving a system of differential equations.

## 1.2 Embedded Markov Chain for Event Timing

Our strategy for exact moment computations relies on two steps: i) Modeling the timing of stochastic events through a phase-type distribution, which can be represented by embedding a continuous-time Markov chain (Fig. 1.2) and ii) Showing that the time evolution of moments in the resulting system becomes automatically closed at some high-order moment. Here we focus on phase-type distributions that consists of a mixture of Erlang distributions [25], and use them as a practical tool for modeling the timing of stochastic events in TTSHS.

Recall that an Erlang distribution of the shape  $m$  and the rate  $k$  is

$$f(\tau) = \frac{k^m \tau^{m-1} e^{-k\tau}}{(m-1)!}. \quad (1.6)$$

For this distribution mean is  $m/k$ . This Erlang distribution can be written as the sum of  $m$  independent and identical random variables that follow exponential distributions with rate  $k$

$$f(\tau) = k e^{-k\tau}, \quad (1.7)$$

where each random variable has a mean of  $1/k$ .

Here, the interval  $\tau_s$  is assumed to have an Erlang distribution of shape  $m_i$  and rate  $k_i$  with probability  $p_i$ ,  $i = \{1, \dots, I\}$  and can be represented by a continuous-time Markov chain with states  $S_{ij}$ ,  $i = \{1, \dots, I\}$ ,  $j = \{1, \dots, m_i\}$  (Fig. 1.2) [26]. Let

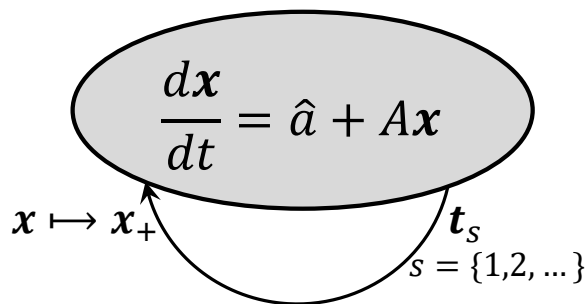


**Figure 1.1: Schematic of a linear time-triggered stochastic hybrid system.** The state evolves according to a set of ordinary differential equation and events occur in random times. Whenever the event occurs  $x$  changes via (1.2).

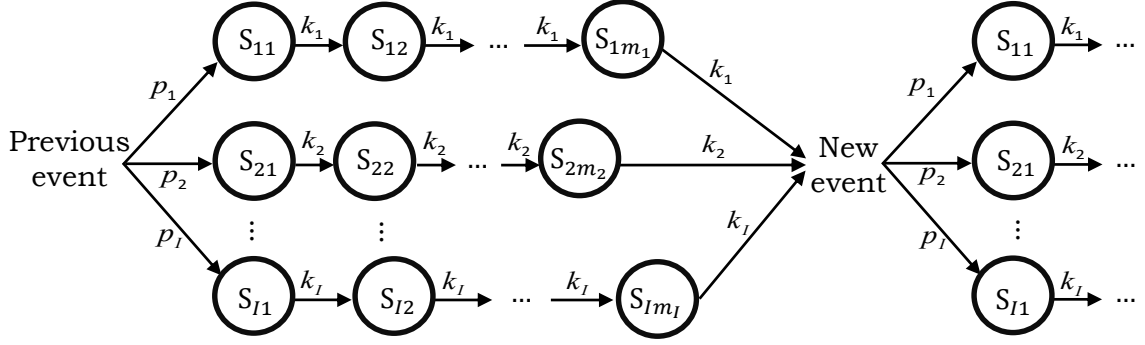


**Figure 1.2: A continuous-time Markov chain model for timing of events in TTSHS.** The time interval  $\tau_s \equiv t_s - t_{s-1}$  between two successive stochastic events is assumed to follow a mixture of Erlang distributions. After an event occurs, a state  $S_{i1}$ ,  $i = \{1, \dots, I\}$  is chosen with probability  $p_i$ . The system transitions through states  $S_{ij}$ ,  $j = \{1, \dots, m_i\}$  residing for an exponentially distributed time in each state. The next event occurs after exit from  $S_{im_i}$  and the above process is repeated.

Bernoulli random variables  $\mathbf{s}_{ij} = 1$  if the system resides in state  $S_{ij}$  and 0 otherwise. The probability of transition  $S_{ij} \rightarrow S_{i(j+1)}$  in the next infinitesimal time interval  $(t, t + dt]$  is given by  $k_i \mathbf{s}_{ij} dt$ , implying that the time spent in each state  $S_{ij}$  is exponentially distributed with mean  $1/k_i$ . To summarize, just after an event occurs a state  $S_{i1}$ ,  $i = \{1, \dots, I\}$  is chosen with probability  $p_i$  and the next event occurs after transitioning through  $m_i$  exponentially distributed steps (after an Erlang distribution of rate  $k_i$  and shape  $m_i$  which is selected with probability  $p_i$ ). Based on this formulation, the probability of a stochastic event occurring in the time interval  $(t, t + dt]$  is given by  $\sum_{j=1}^I k_j \mathbf{s}_{jj} dt$ , and whenever the event occurs, the state is reset as per (1.2). For a mixture of Erlang distributions, the moment are given by

$$\langle \tau_s^q \rangle = \sum_{i=1}^I \frac{p_i}{k_i^q} \frac{(m_i + q - 1)!}{(m_i - 1)!}, \quad q \in \{1, 2, \dots\} \quad (1.8)$$

[26]. Given a specific distribution of timing of events, the above equation can in principle be used to construct a complex enough appropriate Markov chain that matches some lower orders moments of the given distribution [27].

**Table 1.1:** Stochastic events in the TTSHS with timing of events described by the embedded Markov Chain in Fig. 1.2.

Stochastic events	Reset	Transition intensity ( $h$ )
Phase-type evolution	$\mathbf{s}_{ij}(t) \mapsto \mathbf{s}_{ij}(t) - 1,$ $\mathbf{s}_{i(j+1)}(t) \mapsto \mathbf{s}_{i(j+1)}(t) + 1$	$k_i \mathbf{s}_{ij}, j \in \{1, \dots, m_i - 1\}$
Events changing $\mathbf{x}$	$\mathbf{x} \mapsto \mathbf{x}_+,$ $\mathbf{s}_{jm_j}(\mathbf{t}_s) \mapsto 0,$ $\mathbf{s}_{i1}(\mathbf{t}_s) \mapsto \mathbf{s}_{i1}(\mathbf{t}_s) + 1$	$p_i \sum_{j=1}^n k_j \mathbf{s}_{jm_j}, i \& j \in \{1, \dots, I\}$

### 1.3 Moment Dynamics of TTSHS

The overall model is now given by the linear system

$$\frac{d\mathbf{x}(t)}{dt} = \hat{a} + A\mathbf{x}(t). \quad (1.9)$$

together with stochastic transitions associated with the embedded Markov chain illustrated in Table 1.1. The theorem below outlines the main result.

**Theorem 1** *Consider the TTSHS where timing of events are modeled through the Markov chain in Fig. 1.2, and reset are given by (1.2). Then, the time evolution of vector  $\nu$  consisting of all the first and second order moments of stochastic processes  $\mathbf{x}$  and  $\mathbf{s}_{ij}$ , and the third order moments of form  $\langle \mathbf{x}^2 \mathbf{s}_{ij} \rangle, i = \{1, \dots, I\}, j = \{2, \dots, m_i\}$  is given by a linear dynamical system*

$$\dot{\nu} = \hat{a}_\nu + A_\nu \nu, \quad (1.10)$$

for an appropriate vector  $a_\nu$  and matrix  $A_\nu$ .

**Proof:** Based on Theorem 1 of [28], time derivative of the expected value of the elements of any vector of continuously differentiable functions  $\varphi(\mathbf{x}, \mathbf{s}_{ij}) \in \mathbb{R}^F$  is given by

$$\frac{d\langle\varphi_f(\mathbf{x}, \mathbf{s}_{ij})\rangle}{dt} = \langle(L\varphi_f)(\mathbf{x}, \mathbf{s}_{ij})\rangle, \quad f = \{1, \dots, F\}, \quad (1.11)$$

where the extended generator ( $L\varphi_f$ ) for this SHS is

$$(L\varphi_f)(x, s_{ij}) = \left\langle \sum_{\text{Events}} h \times \Delta\varphi_f(x, s_{ij}) \right\rangle + \left\langle \frac{\partial\varphi_f(x, s_{ij})}{\partial x} (\hat{a} + Ax) \right\rangle. \quad (1.12)$$

Here,  $\Delta\varphi_f$  is the change in  $\varphi_f$  whenever an event occurs and  $\frac{\partial\varphi_f(x, s_{ij})}{\partial x} \in \mathbb{R}^{1 \times n}$  denotes the gradient of  $\varphi_f(x, s_{ij})$  with respect to  $x$ . Moreover,  $h$  denotes the transition intensities for the events and determine how often these events occur [28, 29].

Using the transition intensities shown in Table I, the dynamics of the means can be written by choosing  $\varphi$  to be  $x$  and  $s_{ij}$  in (1.12). For example suppose that  $\varphi_f$  is selected to be  $s_{ij}$   $j \in \{2, \dots, m_i\}$  then there are two reactions that affect  $s_{ij}$ . First one is the reaction of arriving to the state  $S_{ij}$  which happens with the transition intensity  $k_i s_{i(j-1)}$ . For this reaction the change  $\Delta\varphi_f(x, s_{ij})$  is  $+1$ . The other one is the reaction of leaving the state  $S_{ij}$  which happens with the transition intensity  $k_i s_{ij}$ . For this reaction the change  $\Delta\varphi_f(x, s_{ij})$  is  $-1$ . The moment dynamics can be compactly derived as

$$\frac{d\langle\mathbf{x}\rangle}{dt} = \hat{a} + A\langle\mathbf{x}\rangle + \sum_{j=1}^I k_j ((J - I_n)\langle\mathbf{x}\mathbf{s}_{jm_j}\rangle + \hat{r}\langle\mathbf{s}_{jm_j}\rangle), \quad (1.13a)$$

$$\frac{d\langle\mathbf{s}_{i1}\rangle}{dt} = p_i \left\langle \sum_{j=1}^I k_j \mathbf{s}_{jm_j} \right\rangle - k_i \langle\mathbf{s}_{i1}\rangle, \quad i = \{1, \dots, I\}, \quad (1.13b)$$

$$\frac{d\langle\mathbf{s}_{ij}\rangle}{dt} = k_i \langle\mathbf{s}_{i(j-1)}\rangle - k_i \langle\mathbf{s}_{ij}\rangle, \quad i = \{1, \dots, I\}, \quad j = \{2, \dots, m_i\}. \quad (1.13c)$$

Note that the first equation is not closed since it depends on the second order moments of the form  $\langle\mathbf{x}\mathbf{s}_{ij}\rangle$ . The time evolution of the moments  $\langle\mathbf{x}\mathbf{s}_{ij}\rangle$  depends on third order moments of the form  $\langle\mathbf{x}\mathbf{s}_{ij}^2\rangle$  and  $\langle\mathbf{s}_{ij}\mathbf{s}_{rq}\mathbf{x}^b\rangle$ . However, using the fact that  $\mathbf{s}_{ij}$  are Bernoulli random variables

$$\langle\mathbf{s}_{ij}^q\rangle = \langle\mathbf{s}_{ij}\rangle, \quad \langle\mathbf{s}_{ij}\mathbf{x}^b\rangle = \langle\mathbf{s}_{ij}\mathbf{x}^b\rangle, \quad q \& b \in \{1, 2, \dots\}. \quad (1.14)$$

Moreover, since only one of the states  $\mathbf{s}_{ij}$  can be 1 at a time

$$\langle \mathbf{s}_{ij} \mathbf{s}_{rq} \mathbf{x}^b \rangle = 0, \text{ if } i \neq r \text{ or } j \neq q. \quad (1.15)$$

Exploiting (1.14)-(1.15), moment dynamics of  $\langle \mathbf{x} \mathbf{s}_{ij} \rangle$  becomes automatically closed and given by

$$\frac{d\langle \mathbf{x} \mathbf{s}_{i1} \rangle}{dt} = \hat{a} \langle \mathbf{x} \mathbf{s}_{i1} \rangle + A \langle \mathbf{x} \mathbf{s}_{i1} \rangle - k_i \langle \mathbf{x} \mathbf{s}_{i1} \rangle \quad (1.16a)$$

$$+ p_i \sum_{j=1}^I k_j ((J - I_n) \langle \mathbf{x} \mathbf{s}_{jm_j} \rangle + \hat{r} \langle \mathbf{s}_{jm_j} \rangle), \quad i = \{1, \dots, I\},$$

$$\frac{d\langle \mathbf{x} \mathbf{s}_{ij} \rangle}{dt} = \hat{a} \langle \mathbf{x} \mathbf{s}_{ij} \rangle + A \langle \mathbf{x} \mathbf{s}_{ij} \rangle - k_i \langle \mathbf{x} \mathbf{s}_{ij} \rangle \quad (1.16b)$$

$$+ k_i \langle \mathbf{x} \mathbf{s}_{i(j-1)} \rangle, \quad i = \{1, \dots, I\}, \quad j = \{2, \dots, m_i\}.$$

Thus (1.13) and (1.16) represent a closed set of equations that can be used to obtain the mean dynamics  $\langle \mathbf{x} \rangle$ . A similar approach can be taken for obtaining the second order moments. Briefly, the time evolution of  $\langle \mathbf{x} \mathbf{x}^T \rangle$  would depend on moments of the form  $\langle \mathbf{x} \mathbf{x}^T \mathbf{s}_{ij} \rangle$ . Moment dynamics of  $\langle \mathbf{x} \mathbf{x}^T \mathbf{s}_{ij} \rangle$  can be closed automatically using (1.14)-(1.15). ■

## 1.4 Conclusion

In summary, our results show that if timing of events in TTSHS can be modeled via a phase-type process (as in Fig. 1.2), then time evolution of moments can be obtained by solving a linear systems of differential equations. Next, we use TTSHS model for capturing random fluctuations in the level of a protein.

## Chapter 2

### FLUCTUATIONS IN PROTEIN LEVELS FROM STOCHASTIC EXPRESSION AND NOISY CELL-CYCLE PROCESSES

The level of a protein can deviate considerably from cell-to-cell, in spite of the fact that cells are genetically-identical and are in the same extracellular environment [30–32]. This intercellular variation or noise in protein counts has been implicated in diverse processes such as corrupting functioning of gene networks [33–35], driving probabilistic cell-fate decisions [36–41], buffering cell populations from hostile changes in the environment [42–45], and causing clonal cells to respond differently to the same stimulus [46–48]. An important source of noise driving random fluctuations in protein levels is stochastic gene expression due to the inherent probabilistic nature of biochemical processes [49–52]. Recent experimental studies have uncovered additional noise sources that affect protein copy numbers. For example, the time taken to complete cell cycle (i.e., time between two successive cell-division events) has been observed to be stochastic across organisms [53–60]. Moreover, given that many proteins/mRNAs are present inside cells at low-copy numbers, errors incurred in partitioning of molecules between two daughter cells are significant [61–63]. Finally, the time at which a particular gene of interest is duplicated can also vary between cells [64, 65]. We investigate how such noise sources in the cell-cycle process combine with stochastic gene expression to generate intercellular variability in protein copy numbers (Fig. 2.1).

Prior studies that quantify the effects of cell division on the protein noise level have been restricted to specific cases. For example, noise computations have been done in stochastic gene expression models, where cell divisions occur at deterministic time intervals [61, 66, 67]. We formulate a mathematical model that couples stochastic expression of a stable protein with random cell-division events that follow a general

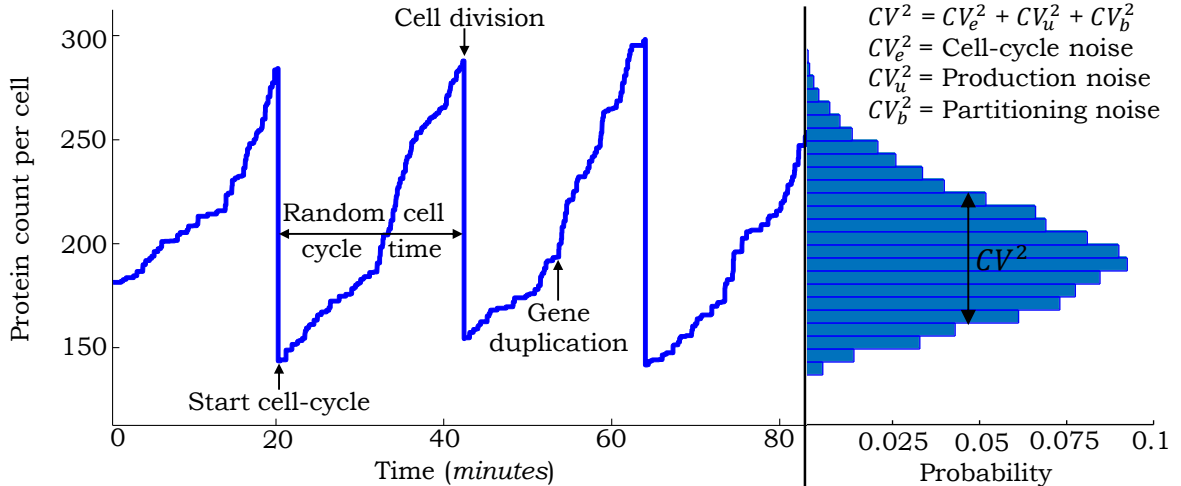


**Figure 2.1: Sample trajectory of the protein level in a single cell with different sources of noise.** Stochastically expressed proteins accumulate within the cell at a certain rate. At a random point in the cell cycle, gene duplication results in an increase in production rate. Stochastic cell-division events lead to random partitioning of protein molecules between two daughter cells with each cell receiving, on average, half the number of proteins in the mother cell just before division. The steady-state protein copy number distribution obtained from a large number of trajectories is shown on the right. The total noise in the protein level, as measured by the squared Coefficient of Variation ( $CV^2$ ) can be broken into contributions from individual noise mechanisms.

class of probability distributions. Moreover, at the time of cell division, proteins are randomly partitioned between two daughter cells based on a framework that allows the partitioning errors to be higher or lower than as predicted by binomial partitioning. For this class of models, we derive an exact analytical formula for the protein noise level as quantified by the steady-state squared Coefficient of Variation ( $CV^2$ ). This formula is further decomposed into individual components representing contributions from different noise sources. A systematic investigation of this formula leads to novel insights, such as identification of regimes where increasing randomness in the timing of cell-division events decreases the protein noise level.

## 2.1 Coupling Gene Expression to Cell Division

We consider the standard model of stochastic gene expression [68, 69], where mRNAs are transcribed at exponentially distributed time intervals from a constitutive gene with rate  $k_x$ . Assuming short-lived mRNAs, each transcription event results in a burst of proteins [69–71]. The corresponding jump in protein levels is shown as

$$\mathbf{x}(t) \mapsto \mathbf{x}(t) + \mathbf{u}, \quad (2.1)$$

where  $\mathbf{x}(t)$  is the protein population count in the mother cell at time  $t$ ,  $\mathbf{u}$  is a random burst size drawn from a positively-valued distribution and represents the number of protein molecules synthesized in a single-mRNA lifetime. Motivated by observations in *E. coli* and mammalian cells, where many proteins have half-lives considerably longer than the cell doubling time, we assume a stable protein with no active degradation [72–74]. Thus, proteins accumulate within the cell till the time of cell division, at which point they are randomly partitioned between two daughter cells.

Let cell division events occur at times  $\mathbf{t}_s$ ,  $s \in \{1, 2, \dots\}$ . The cell-cycle time

$$\tau_s \equiv \mathbf{t}_s - \mathbf{t}_{s-1}, \quad (2.2)$$

follows an arbitrary positively-valued probability distribution with the following mean and squared coefficient of variation

$$\langle \tau_s \rangle = \langle \mathbf{t}_s - \mathbf{t}_{s-1} \rangle, \quad CV_{\tau_s}^2 = \frac{\langle \tau_s^2 \rangle - \langle \tau_s \rangle^2}{\langle \tau_s \rangle^2}. \quad (2.3)$$

The random change in  $\mathbf{x}$  during cell division is given by

$$\mathbf{x} \mapsto \mathbf{x}_+, \quad (2.4)$$

where  $\mathbf{x}$  denotes the protein levels in the mother cell just before division and  $\mathbf{x}_+$  denotes the protein levels in one of the daughter cells just after division. Conditioned on  $\mathbf{x}$ ,  $\mathbf{x}_+$  is assumed to have the following statistics

$$\langle \mathbf{x}_+ \rangle = \frac{\mathbf{x}}{2}, \quad \langle \mathbf{x}_+^2 \rangle - \langle \mathbf{x}_+ \rangle^2 = \frac{b\mathbf{x}}{4}. \quad (2.5)$$

The first equation implies symmetric partitioning, i.e., on average each of the daughter cells inherits half the number protein molecules just before division. The second equation in (2.5) describes the variance of  $\mathbf{x}_+$  and quantifies the error in partitioning of molecules through the non-negative parameter  $b$ . For example,  $b = 0$  represents deterministic partitioning where  $\mathbf{x}_+ = \mathbf{x}/2$  with probability equal to one. A more realistic model for partitioning is each molecule having an equal probability of being in the each daughter cell [75–77]. This results in a binomial distribution for  $\mathbf{x}_+$

$$\text{Probability}\{\mathbf{x}_+ = j\} = \frac{\mathbf{x}!}{j!(\mathbf{x} - j)!} \left(\frac{1}{2}\right)^{\mathbf{x}}, \quad j \in \{0, 1, \dots, \mathbf{x}\}, \quad (2.6)$$

and corresponds to  $b = 1$  in (2.5). Interestingly, recent studies have shown that partitioning of proteins that form clusters or multimers can result in  $b > 1$  in (2.5), i.e., partitioning errors are much higher than as predicted by the binomial distribution [61, 67]. In contrast, if molecules push each other to opposite poles of the cell, then the partitioning errors will be smaller than as predicted by (2.6) and  $b < 1$ .

The model with all the different noise mechanisms (stochastic expression; random cell-division events and partitioning errors) is illustrated in Fig. 2.2A and referred to as the full model. We also introduce two additional hybrid models [22, 78], where protein production and partitioning are considered in their deterministic limit (Fig. 2.2B-C). Note that unlike the full model, where  $\mathbf{x}(t)$  takes non-negative integer values,  $\mathbf{x}(t)$  is continuous in the hybrid models. We will use these hybrid models for decomposing the protein noise level obtained from the full model into individual components representing contributions from different noise sources.

## 2.2 Modeling the Cell-cycle Time Using Phase-type Distributions

In order to quantify the steady-state protein mean and noise, we need to define the stochastic process that governs the timing of cell division. Variations in the duration of cell cycle can result from a variety of factors, such as cell physiology, growth rate, cell size and expression of genes that affect cell-cycle time such as FtsZ [53–60]. Given these complexities, we take a phenomenological approach to modeling cell-cycle time,

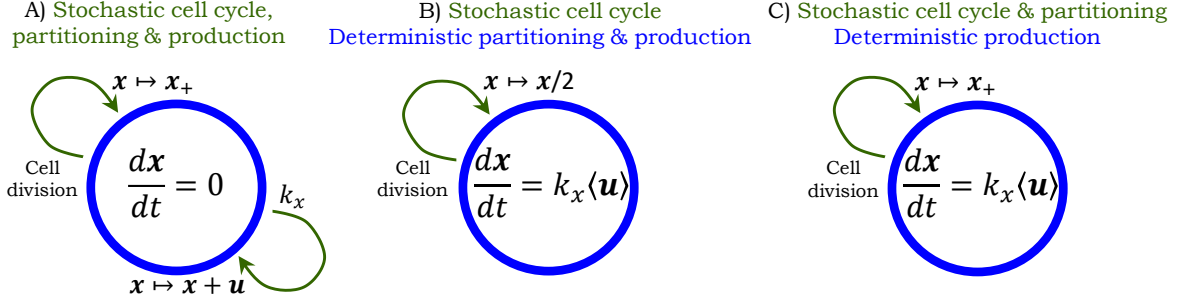


**Figure 2.2: Stochastic models of gene expression with cell division.** Arrows denote stochastic events that change the protein level by discrete jumps as shown in (2.1) and (2.4). The differential equation within the circle represents the time evolution of  $\mathbf{x}(t)$  in between events. **A)** Model with all the different sources of noise: proteins are expressed in stochastic bursts, cell division occurs at random times, and molecules are partitioned between the two daughter cells based on (2.5). The trivial dynamics  $\frac{d\mathbf{x}}{dt} = 0$  signifies that the protein level is constant in-between stochastic events. **B)** Hybrid model where randomness in cell-division events is the only source of noise. Protein production is modeled deterministically through a differential equation and partitioning errors are absent, i.e.,  $b = 0$  in (2.5). **C)** Hybrid model where noise comes from both cell-division events and partitioning errors. Protein production is considered to be deterministic as in part B. Since  $\mathbf{x}(t)$  is continuous here,  $\mathbf{x}_+$  has a positively-valued continuous distribution with same mean and variance as in (2.5)

and assume it to be an independent and identically distributed random variable that is drawn from a mixture of Erlang distributions.

In Fig. 1.2 let the probability of transition  $S_{ij} \rightarrow S_{i(j+1)}$  in the next infinitesimal time interval  $[t, t + dt)$  be given by  $k_i s_{ij} dt = ik s_{ij} dt$ , implying that the time spent in each state  $S_{ij}$  is exponentially distributed with mean  $1/ik$ . This implies that that we select  $k_i = ik$  and  $m_i = i$ . This sub-class of phase-type distributions is fairly general, in the sense that, any positively-valued distribution with  $CV_{\tau_s} \leq 1$  can be modeled via a mixture of Erlang distributions [27]. For this class of phase-type distributions, the mean, the squared coefficient of variation and the skewness of the cell-cycle time

in terms of the Markov chain parameters are given by

$$\langle \tau_s \rangle = \frac{1}{k}, \quad CV_{\tau_s}^2 = \sum_{i=1}^I \frac{p_i}{i}, \quad \text{Skewness} = \frac{\langle \tau_s^3 \rangle - 3\langle \tau_s \rangle(\langle \tau_s^2 \rangle - \langle \tau_s \rangle^2) - \langle \tau_s \rangle^3}{(\langle \tau_s^2 \rangle - \langle \tau_s \rangle^2)^{3/2}} = 2 \sum_{i=1}^I \frac{p_i}{i^2} \quad (2.7)$$

[26], where  $\langle \tau_s^3 \rangle$  is the third-order moment of the cell-cycle time. An important property of this class of distributions is that increasing  $CV_{\tau_s}^2$  also makes the distribution highly skewed, because from (2.7) both the  $CV_{\tau_s}$  and skewness are linear combinations of  $p_i$ , albeit with different linear coefficients that decrease with  $i$ . Considering that  $\sum_{i=1}^I p_i = 1$ , the only way to increase  $CV_{\tau_s}^2$  is by increasing smaller-index components and decreasing larger-index components of the distribution (i.e. increasing  $p_i$  and decreasing  $p_j$ , where  $i < j$ ). Since higher values of  $i$  are more penalized in the skewness equation, this would correspond to making the distribution more positively skewed. Hence high values of  $CV_{\tau_s}^2$  also means high values of skewness, thus occurrences of longer cell cycles are more probable. As we will shortly see, this property leads to mean protein levels being dependent on  $CV_{\tau_s}^2$ .

### 2.3 Computing the Average Number of Protein Molecules

All the models shown in Fig. 2.2 are identical in terms of finding  $\langle \mathbf{x}(t) \rangle$  and in principle any one of them could have been used. We choose to analyze the full model illustrated in Fig. 2.2A. Time evolution of the statistical moments of  $\mathbf{x}(t)$  can be obtained from (1.11)

$$\frac{d\langle \mathbf{x} \rangle}{dt} = k_x \langle \mathbf{u} \rangle - \frac{k}{2} \sum_{j=1}^I (j \langle \mathbf{x} \mathbf{s}_{jj} \rangle). \quad (2.8)$$

Note that the time-derivative of the mean protein level (first-order moment) is unclosed, in the sense that, it depends on the second-order moment  $\langle \mathbf{x} \mathbf{s}_{ij} \rangle$ . The time evolution

of  $\langle \mathbf{s}_{ij} \rangle$  and  $\langle \mathbf{x}\mathbf{s}_{ij} \rangle$  is obtained as

$$\frac{d\langle \mathbf{s}_{i1} \rangle}{dt} = kp_i \sum_{j=1}^I (j\langle \mathbf{s}_{jj} \rangle) - ik\langle \mathbf{s}_{i1} \rangle, \quad (2.9)$$

$$\frac{d\langle \mathbf{s}_{ij} \rangle}{dt} = ik\langle \mathbf{s}_{i(j-1)} \rangle - ik\langle \mathbf{s}_{ij} \rangle, \quad j = \{2, \dots, i\}, \quad (2.10)$$

$$\frac{d\langle \mathbf{x}\mathbf{s}_{i1} \rangle}{dt} = k_x\langle \mathbf{u} \rangle \langle \mathbf{s}_{i1} \rangle + \frac{k}{2}p_i \sum_{j=1}^I (j\langle \mathbf{x}\mathbf{s}_{jj} \rangle) - ik\langle \mathbf{x}\mathbf{s}_{i1} \rangle, \quad (2.11)$$

$$\frac{d\langle \mathbf{x}\mathbf{s}_{ij} \rangle}{dt} = k_x\langle \mathbf{u} \rangle \langle \mathbf{s}_{ij} \rangle - ik\langle \mathbf{x}\mathbf{s}_{ij} \rangle + ik\langle \mathbf{x}\mathbf{s}_{i(j-1)} \rangle, \quad j = \{2, \dots, i\} \quad (2.12)$$

and only depends on  $\langle \mathbf{s}_{ij} \rangle$  and  $\langle \mathbf{x}\mathbf{s}_{ij} \rangle$ . Thus, (2.8) and (2.9)-(2.12) constitute a closed system of linear differential equations from which moments can be computed exactly.

To obtain an analytical formula for the average number of proteins, we start by performing a steady-state analysis of (2.8) that yields

$$\sum_{j=1}^I \left( j \overline{\langle \mathbf{x}\mathbf{s}_{jj} \rangle} \right) = \frac{2k_x\langle \mathbf{u} \rangle}{k}, \quad (2.13)$$

where  $\overline{\langle \cdot \rangle}$  denotes the expected value in the limit  $t \rightarrow \infty$ . Using (2.13),  $\overline{\langle \mathbf{x}\mathbf{s}_{i1} \rangle}$  is determined from (2.11), and then all moments  $\overline{\langle \mathbf{x}\mathbf{s}_{ij} \rangle}$  are obtained recursively by performing a steady-state analysis of (2.12) for  $j = \{2, \dots, i\}$ . This analysis results in

$$\overline{\langle \mathbf{x}\mathbf{s}_{ij} \rangle} = \frac{k_x\langle \mathbf{u} \rangle}{ik} p_i \left( 1 + \frac{j}{i} \right). \quad (2.14)$$

Using (2.7), (2.14) and the fact that  $\sum_{i=1}^I \sum_{j=1}^i \mathbf{s}_{ij} = 1$  we obtain the following expression for the mean protein level

$$\overline{\langle \mathbf{x} \rangle} = \overline{\left\langle \mathbf{x} \sum_{i=1}^I \sum_{j=1}^i \mathbf{s}_{ij} \right\rangle} = \sum_{i=1}^I \sum_{j=1}^i \overline{\langle \mathbf{x}\mathbf{s}_{ij} \rangle} = \frac{k_x\langle \mathbf{u} \rangle \langle \tau_s \rangle (3 + CV_{\tau_s}^2)}{2}. \quad (2.15)$$

It is important to point that (2.15) holds irrespective of the complexity, i.e., the number of states  $S_{ij}$  used in the phase-type distribution to approximate the cell-cycle time distribution. As expected,  $\overline{\langle \mathbf{x} \rangle}$  increases linearly with the average cell-cycle time duration  $\langle \tau_s \rangle$  with longer cell cycles resulting in more accumulation of proteins. Consistent with previous findings, (2.15) shows that the mean protein level is also affected by

the randomness in the cell-cycle times ( $CV_{\tau_s}^2$ ) [19, 79]. For example,  $\overline{\langle \mathbf{x} \rangle}$  reduces by 25% as  $\tau_s$  changes from being exponentially distributed ( $CV_{\tau_s}^2 = 1$ ) to deterministic ( $CV_{\tau_s}^2 = 0$ ) for fixed  $\langle \tau_s \rangle$ . Next, we determine the noise in protein copy numbers, as quantified by the squared coefficient of variation.

## 2.4 Computing the Protein Noise Level

Recall that the full model introduced in Fig. 2.2A has three distinct noise mechanisms. Our strategy for computing the protein noise level is to first analyze the model with a single noise source, and then consider models with two and three sources. As shown below, this approach provides a systematic dissection of the protein noise level into components representing contributions from different mechanisms.

### 2.4.1 Contribution from Randomness in Cell-cycle Times

We begin with the model shown in Fig. 2.2B, where noise comes from a single source - random cell-division events. For this model, the time evolution of the second-order moment of the protein copy number is obtained as

$$\frac{d\langle \mathbf{x}^2 \rangle}{dt} = 2k_x \langle \mathbf{u} \rangle \langle \mathbf{x} \rangle - \frac{3k}{4} \sum_{j=1}^I (j \langle \mathbf{x}^2 \mathbf{s}_{jj} \rangle), \quad (2.16)$$

and depends on third-order moments  $\langle \mathbf{x}^2 \mathbf{s}_{jj} \rangle$ . Using the approach introduced earlier for obtaining the mean protein level, we close moment equations by writing the time evolution of moments  $\langle \mathbf{x}^2 \mathbf{s}_{ij} \rangle$

$$\frac{d\langle \mathbf{x}^2 \mathbf{s}_{i1} \rangle}{dt} = 2k_x \langle \mathbf{u} \rangle \langle \mathbf{x} \mathbf{s}_{i1} \rangle + \frac{k}{4} p_i \sum_{j=1}^I (j \langle \mathbf{x}^2 \mathbf{s}_{jj} \rangle) - ik \langle \mathbf{x}^2 \mathbf{s}_{i1} \rangle, \quad (2.17)$$

$$\frac{d\langle \mathbf{x}^2 \mathbf{s}_{ij} \rangle}{dt} = 2k_x \langle \mathbf{u} \rangle \langle \mathbf{x} \mathbf{s}_{ij} \rangle - ik \langle \mathbf{x}^2 \mathbf{s}_{ij} \rangle + ik \langle \mathbf{x}^2 \mathbf{s}_{(i-1)j} \rangle, \quad j = \{2, \dots, i\}. \quad (2.18)$$

Note that the moment dynamics for  $\langle \mathbf{x} \rangle$  and  $\langle \mathbf{x} \mathbf{s}_{ij} \rangle$  obtained in the previous section (equations (2.8), (2.11), and (2.12)) are identical for all the models in Fig. 2.2, irrespective of whether the noise mechanism is modeled deterministically or stochastically.

Equations (2.8), (2.9)-(2.12), and (2.16)-(2.18) represent a closed set of linear differential equations and their steady-state analysis yields

$$\overline{\langle \mathbf{x}^2 \mathbf{s}_{ij} \rangle} = \frac{k_x^2 \langle \mathbf{u} \rangle^2 \langle \tau_s \rangle (3 + CV_{\tau_s}^2)}{3ik} p_i + \frac{2k_x^2 \langle \mathbf{u} \rangle^2}{i^2 k^2} \left( \frac{j^2 + 2ij + j}{2i} \right) p_i. \quad (2.19)$$

From (2.19)

$$\overline{\langle \mathbf{x}^2 \rangle} = \overline{\left\langle \mathbf{x}^2 \sum_{i=1}^I \sum_{j=1}^i \mathbf{s}_{ij} \right\rangle} = \sum_{i=1}^I \sum_{j=1}^i \overline{\langle \mathbf{x}^2 \mathbf{s}_{ij} \rangle} = k_x^2 \langle \mathbf{u} \rangle^2 \frac{\langle \tau_s^3 \rangle + 4CV_{\tau_s}^2 \langle \tau_s \rangle^3 + 6\langle \tau_s \rangle^3}{3\langle \tau_s \rangle}, \quad (2.20)$$

$$\langle \tau_s^3 \rangle = \left( 1 + 3CV_{\tau_s}^2 + 2 \sum_{i=1}^I \frac{p_i}{i^2} \right) \langle \tau_s \rangle^3. \quad (2.21)$$

Using (2.20) and the mean protein count quantified in (2.15), we use the following steady-state coefficient of variation squared

$$CV^2 \equiv \frac{\overline{\langle \mathbf{x}^2 \rangle} - \langle \mathbf{x} \rangle^2}{\langle \mathbf{x} \rangle^2}, \quad \langle \mathbf{x}^i \rangle = \int_0^\infty \int_0^\infty x^i p(x, \tau) dx d\tau \quad (2.22)$$

to quantify noise. Here  $\tau$  denotes cell-cycle time, and  $p(x, \tau)$  is probability of having  $x$  molecules at cell-cycle time  $\tau$ . Note that  $\langle \mathbf{x}^i \mathbf{s}_{ij} \rangle$  in (2.11)-(2.12) and (2.17)-(2.18) can be seen as expected value conditioned on cell-cycle stage  $s_{ij}$  which is the measure of cell age  $\tau$  in our model Using this equation we have

$$CV_e^2 = \frac{1}{27} + \frac{4 \left( 9 \frac{\langle \tau_s^3 \rangle}{\langle \tau_s \rangle^3} - 9 - 6CV_{\tau_s}^2 - 7CV_{\tau_s}^4 \right)}{27 (3 + CV_{\tau_s}^2)^2}, \quad (2.23)$$

where  $CV_e^2$  represents the noise contribution from random cell-division events. Since cell division is a global event that affects expression of all genes, this noise contribution can also be referred to as *extrinsic noise* [80–83]. In reality, there would be other sources of extrinsic noise, such as, fluctuations in the gene-expression machinery that we have ignored in this analysis.

Note that  $CV_e^2 \rightarrow 1/27$  as  $\tau_s$  approaches a delta distribution, i.e., cell divisions occur at fixed time intervals. We discuss simplifications of (2.23) in various limits. For example, if the time taken to complete cell cycle is lognormally distributed, then

$$\frac{\langle \tau_s^3 \rangle}{\langle \tau_s \rangle^3} = (1 + CV_{\tau_s}^2)^3 \implies CV_e^2 = \frac{1}{27} + \frac{4 (21CV_{\tau_s}^2 + 20CV_{\tau_s}^4 + 9CV_{\tau_s}^6)}{27 (3 + CV_{\tau_s}^2)^2} \quad (2.24)$$

and extrinsic noise monotonically increases with  $CV_{\tau_s}^2$ . If fluctuations in  $\tau_s$  around  $\langle \tau_s \rangle$  are small, then using Taylor series

$$\langle \tau_s^3 \rangle / \langle \tau_s \rangle^3 \approx 1 + 3CV_{\tau_s}^2. \quad (2.25)$$

Substituting (2.25) in (2.23) and ignoring  $CV_{\tau_s}^4$  and higher order terms yields

$$CV_e^2 \approx \frac{1}{27} + \frac{28CV_{\tau_s}^2}{81}, \quad (2.26)$$

where the first term is the extrinsic noise for  $CV_{\tau_s}^2 \rightarrow 0$  and the second term is the additional noise due to random cell-division events.

#### 2.4.2 Contribution from Partitioning Errors

Next, we consider the model illustrated in Fig. 2.2C with both random cell-division events and partitioning of protein between the two daughter cells. Thus, the protein noise level here represents the contribution from both these sources. The time evolution of  $\langle \mathbf{x}^2 \rangle$  and  $\langle \mathbf{x}^2 \mathbf{s}_{ij} \rangle$  are given by

$$\frac{d\langle \mathbf{x}^2 \rangle}{dt} = 2k_x \langle \mathbf{u} \rangle \langle \mathbf{x} \rangle + \frac{k}{4} b \sum_{j=1}^I (j \langle \mathbf{x} \mathbf{s}_{jj} \rangle) - \frac{3k}{4} \sum_{j=1}^I (j \langle \mathbf{x}^2 \mathbf{s}_{jj} \rangle), \quad (2.27)$$

$$\frac{d\langle \mathbf{x}^2 \mathbf{s}_{i1} \rangle}{dt} = 2k_x \langle \mathbf{u} \rangle \langle \mathbf{x} \mathbf{s}_{i1} \rangle + \frac{k}{4} p_i \sum_{j=1}^I (j \langle \mathbf{x}^2 \mathbf{s}_{jj} \rangle) + \frac{k}{4} b p_i \sum_{j=1}^I (j \langle \mathbf{x} \mathbf{s}_{jj} \rangle) - ik \langle \mathbf{x}^2 \mathbf{s}_{i1} \rangle, \quad (2.28)$$

$$\frac{d\langle \mathbf{x}^2 \mathbf{s}_{ij} \rangle}{dt} = 2k_x \langle \mathbf{u} \rangle \langle \mathbf{x} \mathbf{s}_{ij} \rangle - ik \langle \mathbf{x}^2 \mathbf{s}_{ij} \rangle + ik \langle \mathbf{x}^2 \mathbf{s}_{(i-1)j} \rangle, \quad j = \{2, \dots, i\}. \quad (2.29)$$

Note that (2.27)-(2.28) are slightly different from their counterparts obtained in the previous section (equations (2.16) and (2.17)) with additional terms that depend on  $b$ , where  $b$  quantifies the degree of partitioning error as defined in (2.5). As expected, (2.27)-(2.28) reduces to (2.16)-(2.17) when  $b = 0$  (i.e., deterministic partitioning). Computing  $\overline{\langle \mathbf{x}^2 \mathbf{s}_{ij} \rangle}$  by performing a steady-state analysis of (2.27)-(2.29) and using a similar approach as in (2.20) we obtain

$$\overline{\langle \mathbf{x}^2 \rangle} = k_x^2 \langle \mathbf{u} \rangle^2 \frac{\langle \tau_s^3 \rangle + 4CV_{\tau_s}^2 \langle \tau_s \rangle^3 + 6\langle \tau_s \rangle^3}{3\langle \tau_s \rangle} + \frac{2bk_x \langle \mathbf{u} \rangle \langle \tau_s \rangle}{3}. \quad (2.30)$$

Finding  $CV^2$  of the protein level and subtracting the extrinsic noise ( $CV_e^2$  found in (2.23)) yields

$$CV_b^2 = \frac{4b}{3(3 + CV_{\tau_s}^2)} \frac{1}{\langle \mathbf{x} \rangle}, \quad (2.31)$$

where  $CV_b^2$  represents the contribution of partitioning errors to the protein noise level. Intriguingly, while  $CV_b^2$  increases with  $b$ , it decrease with  $CV_{\tau_s}^2$ . Thus, as cell-division times become more random for a fixed  $\langle \tau_s \rangle$  and  $\overline{\langle \mathbf{x} \rangle}$ , the noise contribution from partitioning errors decrease. It turns out that this dependence of  $CV_b^2$  on  $CV_{\tau_s}$  is a direct result of the second equation in (2.5), where stochasticity in the partitioning process increases linearly with  $\mathbf{x}$ , the number of protein molecules just before division. Based on (2.15), one needs to reduce  $k_x$  or  $\langle \mathbf{u} \rangle$  to maintain a fixed  $\overline{\langle \mathbf{x} \rangle}$  for increasing randomness in cell-division times. Since the average number of protein molecules just before division is  $2k_x \langle \mathbf{u} \rangle \langle \tau_s \rangle$ , a reduction in  $k_x$  or  $\langle \mathbf{u} \rangle$  results in a lower number of protein molecules before division, and hence, lesser noise from partitioning as per (2.5) and a smaller  $CV_b^2$ . This reasoning is supported by the fact that if we redefine the noise in the partitioning process to make it independent of  $\mathbf{x}$ , i.e. modify (2.5) as

$$\langle \mathbf{x}_+ \rangle = \frac{\mathbf{x}}{2}, \quad \langle \mathbf{x}_+^2 \rangle - \langle \mathbf{x}_+ \rangle^2 = b, \quad (2.32)$$

then the noise contribution from partitioning errors is given by

$$CV_b^2 = \frac{4b}{3} \frac{1}{\langle \mathbf{x} \rangle^2}, \quad (2.33)$$

and the dependence  $CV_b^2$  on  $CV_{\tau_s}$  disappears. Finally note that  $CV_b^2$  can be obtained from a stochastic hybrid system where cell-cycle time and production events are modeled deterministically and the only source of stochasticity is partitioning errors. For this model the noise contribution will be equal to that of the current model when the mean protein levels right before the division in both models are the same.

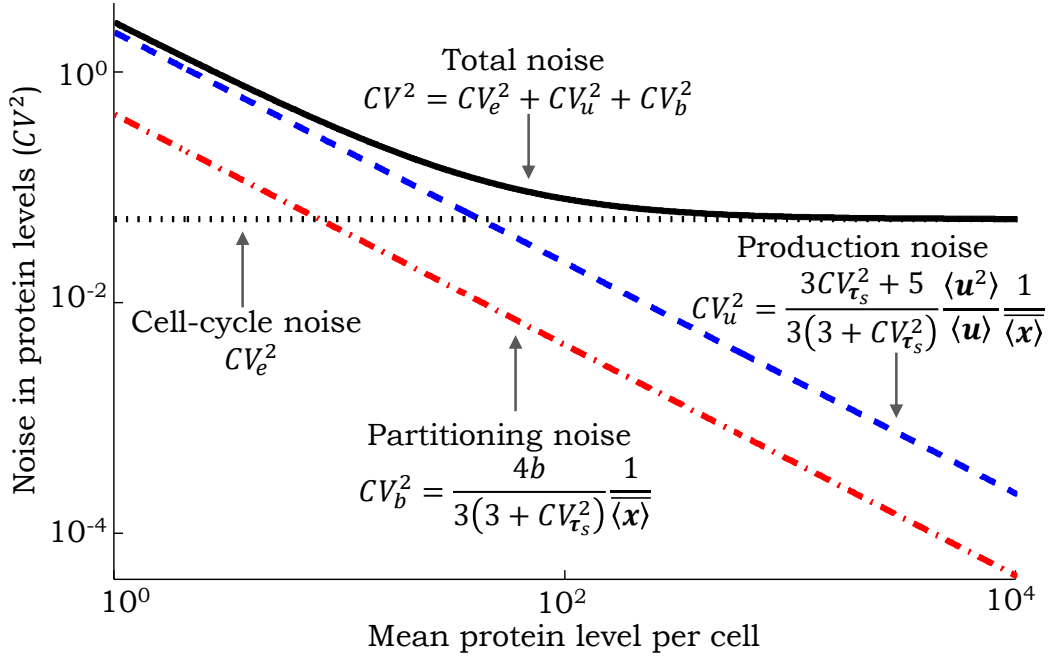


**Figure 2.3: Scaling of noise as a function of the mean protein level for different mechanisms.** The contribution of random cell-division events to the noise in protein copy numbers (extrinsic noise) is invariant of the mean. In contrast, contributions from partitioning errors at the time of cell division (partitioning noise) and stochastic expression (production noise) scale inversely with the mean. The scaling factors are shown as a function of the protein random burst size  $\mathbf{u}$ , noise in cell-cycle time ( $CV_{\tau_s}^2$ ) and magnitude of partitioning errors quantified by  $b$  (see (2.5)). With increasing mean level the total noise first decreases and then reaches a baseline that corresponds to extrinsic noise. For this plot,  $\mathbf{u}$  is assumed to be geometrically distributed with mean  $\langle \mathbf{u} \rangle = 1.5$ ,  $CV_{\tau_s}^2 = 0.05$  and  $b = 1$  (i.e., binomial partitioning).

### 2.4.3 Contribution from Stochastic Expression

Finally, we consider the full model in Fig. 2.2A with all the three different noise sources. For this model, moment dynamics is obtained as

$$\frac{d\langle \mathbf{x}^2 \rangle}{dt} = k_x \langle \mathbf{u}^2 \rangle + 2k_x \langle \mathbf{u} \rangle \langle \mathbf{x} \rangle + \frac{k}{4} b \sum_{j=1}^I (j \langle \mathbf{x} \mathbf{s}_{jj} \rangle) - \frac{3k}{4} \sum_{j=1}^I (j \langle \mathbf{x}^2 \mathbf{s}_{jj} \rangle), \quad (2.34)$$

$$\begin{aligned} \frac{d\langle \mathbf{x}^2 \mathbf{s}_{i1} \rangle}{dt} &= k_x \langle \mathbf{u}^2 \rangle \langle \mathbf{s}_{i1} \rangle + 2k_x \langle \mathbf{u} \rangle \langle \mathbf{x} \mathbf{s}_{i1} \rangle + \frac{k}{4} p_i \sum_{j=1}^I (j \langle \mathbf{x}^2 \mathbf{s}_{jj} \rangle) + \frac{k}{4} b p_i \sum_{j=1}^I (j \langle \mathbf{x} \mathbf{s}_{jj} \rangle) \\ &\quad - ik \langle \mathbf{x}^2 \mathbf{s}_{i1} \rangle, \end{aligned} \quad (2.35)$$

$$\frac{d\langle \mathbf{x}^2 \mathbf{s}_{ij} \rangle}{dt} = k_x \langle \mathbf{u}^2 \rangle \langle \mathbf{s}_{ij} \rangle + 2k_x \langle \mathbf{u} \rangle \langle \mathbf{x} \mathbf{s}_{ij} \rangle - ik \langle \mathbf{x}^2 \mathbf{s}_{ij} \rangle + ik \langle \mathbf{x}^2 \mathbf{s}_{(i-1)j} \rangle, \quad j = \{2, \dots, i\}. \quad (2.36)$$

Compared to (2.27)-(2.29), (2.34)-(2.36) has additional terms of the form  $k_x \langle \mathbf{u}^2 \rangle$ , where  $\langle \mathbf{u}^2 \rangle$  is the second-order moment of the protein burst size in (2.1). Performing an identical analysis as before we obtain

$$\overline{\langle \mathbf{x}^2 \rangle} = k_x^2 \langle \mathbf{u} \rangle^2 \frac{\langle \tau_s^3 \rangle + 4CV_{\tau_s}^2 \langle \tau_s \rangle^3 + 6\langle \tau_s \rangle^3}{3\langle \tau_s \rangle} + \frac{2bk_x \langle \mathbf{u} \rangle \langle \tau_s \rangle}{3} + \frac{k_x \langle \mathbf{u}^2 \rangle \langle \tau_s \rangle (3CV_{\tau_s}^2 + 5)}{2}, \quad (2.37)$$

which yields the following total protein noise level

$$CV^2 = CV_e^2 + CV_b^2 + CV_u^2 = CV_e^2 + \underbrace{\frac{4b}{3(3 + CV_{\tau_s}^2)} \frac{1}{\langle \mathbf{x} \rangle}}_{\text{Partitioning noise } (CV_b^2)} + \underbrace{\frac{3CV_{\tau_s}^2 + 5}{3(3 + CV_{\tau_s}^2)} \frac{\langle \mathbf{u}^2 \rangle}{\langle \mathbf{u} \rangle} \frac{1}{\langle \mathbf{x} \rangle}}_{\text{Production noise } (CV_u^2)}, \quad (2.38)$$

that can be decomposed into three terms. The first term  $CV_e^2$  represents the contribution from random cell-division events and is given by (2.23). The second term  $CV_b^2$  is the contribution from partitioning errors determined in the previous section (partitioning noise), and the final term  $CV_u^2$  is the additional noise representing the contribution from stochastic expression (production noise). A common approach to study gene expression noise is to decompose it into *intrinsic and extrinsic* components. These components are obtained experimentally using the dual-color assay that measures the correlation in the expression of two identical copies of the gene [75]. As per this definition,  $CV_e^2$  represents the extrinsic noise as random cell-division events are

common to all genes and makes expression levels more correlated in individual cells. In contrast, the contributions from noisy production and partitioning represent the intrinsic noise as they are specific to an individual gene and make expression levels less correlated.

An interesting observation from (2.38) is that  $CV_{\tau_s}^2$  has opposite effects on  $CV_b^2$  and  $CV_u^2$  (for fixed mean protein level). While  $CV_b^2$  monotonically decreases with increasing  $CV_{\tau_s}^2$ ,  $CV_u^2$  increases with  $CV_{\tau_s}^2$ . Thus, if  $\langle \mathbf{x} \rangle$  is small and  $b$  is large, then the noise contributed from partitioning dominates the total noise, and making cell-cycle duration more random will reduce the total noise. However, since both  $CV_e^2$  and  $CV_u^2$  are monotonically increasing functions of  $CV_{\tau_s}^2$ , the total noise will begin to increase with  $CV_{\tau_s}^2$  once these noise sources become dominant. It turns out that in certain cases the intrinsic noise becomes invariant of  $CV_{\tau_s}^2$ . For example, when  $\mathbf{u} = 1$  with probability one, i.e., proteins are synthesized one at a time at exponentially distributed time intervals and  $b = 1$  (binomial partitioning)

$$CV^2 = CV_e^2 + \frac{4}{3(3 + CV_{\tau_s}^2)} \frac{1}{\langle \mathbf{x} \rangle} + \frac{3CV_{\tau_s}^2 + 5}{3(3 + CV_{\tau_s}^2)} \frac{1}{\langle \mathbf{x} \rangle} = CV_e^2 + \frac{1}{\langle \mathbf{x} \rangle}. \quad (2.39)$$

In this limit the intrinsic noise is always  $1/\text{Mean}$  irrespective of the cell-cycle time distribution  $\tau_s$  [61]. Note that the average number of proteins itself depends on  $\tau_s$  as shown in (2.15). Another important limit is  $CV_{\tau_s}^2 \rightarrow 0$ , in which case (2.38) reduces to

$$CV^2 \approx \underbrace{\frac{CV_e^2}{27}}_{\text{Extrinsic noise}} + \underbrace{\frac{CV_b^2}{9} \frac{1}{\langle \mathbf{x} \rangle} + \frac{CV_u^2}{9} \frac{\langle \mathbf{u}^2 \rangle}{\langle \mathbf{u} \rangle} \frac{1}{\langle \mathbf{x} \rangle}}_{\text{Intrinsic noise}}, \quad (2.40)$$

and is similar to the result obtained in [66] for deterministic cell-division times and binomial partitioning.

Fig. 2.3 shows how different protein noise components change as a function of the mean protein level as the gene's transcription rate  $k_x$  is modulated. The extrinsic noise is primarily determined by the distribution of the cell-cycle time and is completely independent of the mean. In contrast, both  $CV_b^2$  and  $CV_u^2$  scale inversely with

the mean, albeit with different scaling factors (Fig. 2.3). This observation is particularly important since many single-cell studies in *E. coli*, yeast and mammalian cells have found the protein noise levels to scale inversely with the mean across different genes [84–87]. Based on this scaling it is often assumed that the observed cell-to-cell variability in protein copy numbers is a result of stochastic expression. However, as our results show, noise generated thorough partitioning errors is also consistent with these experimental observations and it may be impossible to distinguish between these two noise mechanisms based on protein  $CV^2$  versus mean plots unless  $b$  is known.

## 2.5 Noise in Synchronized Cells

The mathematical framework introduced for modeling timing of cell division can be easily used to compute noise in synchronized cells. For example, let the cell-cycle duration be an Erlang distribution with shape parameter  $I$  and rate parameter  $Ik$  (i.e.,  $p_I = 1$  in Fig. 1.2), which can be biologically interpreted as cells moving through  $I$  cell-cycle stages  $S_{I1}, S_{I2}, \dots, S_{II}$ . Statistical moments conditioned on the cell-cycle stage  $S_{Ij}$  can be obtained using

$$\overline{\langle \mathbf{x}^m |_{s_{Ij}=1} \rangle} = \frac{\overline{\langle \mathbf{s}_{Ij} \mathbf{x}^m \rangle}}{\overline{\langle \mathbf{s}_{Ij} \rangle}}, \quad m \in \{1, 2\}. \quad (2.41)$$

Using (2.41) and moments  $\overline{\langle \mathbf{x}^m \mathbf{s}_{Ij} \rangle}$  obtained from (2.14) and (2.34)-(2.36), yields the following conditional mean

$$\overline{\langle \mathbf{x} |_{s_{Ij}=1} \rangle} = k_x \langle \mathbf{u} \rangle \langle \boldsymbol{\tau}_s \rangle \left( 1 + \frac{j}{I} \right), \quad (2.42)$$

which increases with cell-cycle stage (i.e., higher values of  $j$ ). The protein noise level given that cells are in stage  $S_{Ij}$  is given by

$$\begin{aligned} CV^2|_{s_{Ij}=1} &:= \frac{\overline{\langle \mathbf{x}^2 |_{s_{Ij}=1} \rangle} - \overline{\langle \mathbf{x} |_{s_{Ij}=1} \rangle}^2}{\overline{\langle \mathbf{x} |_{s_{Ij}=1} \rangle}^2} \\ &= \underbrace{\frac{CV_e^2}{I + 3j}}_{\text{Extrinsic noise}} + \underbrace{\frac{CV_b^2}{3(I+j)} \frac{1}{\overline{\langle \mathbf{x} |_{s_{Ij} \rangle}}}}_{\text{Intrinsic noise}} + \underbrace{\frac{CV_u^2}{3(I+j)} \frac{\langle \mathbf{u}^2 \rangle}{\langle \mathbf{u} \rangle} \frac{1}{\overline{\langle \mathbf{x} |_{s_{Ij} \rangle}}}}_{\text{Intrinsic noise}}. \end{aligned} \quad (2.43)$$

Note that if  $I$  is large then the first term, which represents the noise contribution from the cell-cycle process, is negligible and can be dropped. Interestingly, while the noise contribution from partitioning errors  $CV_b^2$  decreases with cell-cycle stage, the noise contribution from stochastic expression  $CV_u^2$  increases with  $j$ . Moreover, for  $\mathbf{u} = 1$  with probability 1 and  $b = 1$ , the intrinsic noise is always  $1/\text{Mean}$  irrespective of  $j$ . Assuming high  $I$ , the noise at cell birth ( $j = 1$ ) and division ( $j = I$ ) are obtained as

$$CV^2|_{s_{I1}=1} = \underbrace{\frac{\overbrace{2b}^{CV_b^2} \cdot 1}{3 \langle \mathbf{x}|_{s_{I1}} \rangle} + \frac{\overbrace{1 \cdot \langle \mathbf{u}^2 \rangle}^{CV_u^2} \cdot 1}{3 \langle \mathbf{u} \rangle \langle \mathbf{x}|_{s_{I1}} \rangle}}_{\text{Intrinsic noise}} \quad (2.44)$$

$$CV^2|_{g_{nn}=1} = \underbrace{\frac{\overbrace{b}^{CV_b^2} \cdot 1}{3 \langle \mathbf{x}|_{s_{II}} \rangle} + \frac{\overbrace{2 \langle \mathbf{u}^2 \rangle}^{CV_u^2} \cdot 1}{3 \langle \mathbf{u} \rangle \langle \mathbf{x}|_{s_{II}} \rangle}}_{\text{Intrinsic noise}}, \quad (2.45)$$

respectively. Thus, measurements of (2.44) and (2.45) by synchronizing cells (or by using cell size as a proxy for cell-cycle stage) can be used to quantify  $b$  and  $\langle \mathbf{u}^2 \rangle / \langle \mathbf{u} \rangle$ , providing a novel way to separate these noise contributions.

## 2.6 Conclusion

In this chapter TTSHS were used to model stochasticity in protein levels affected by cell-division events. Our analysis reveals that the noise in protein levels can decrease with increasing randomness in cell-division events. Our study presents exciting avenues for future research. The current formulation of TTSHS considers time intervals between events to be independent. It will be interesting to add some form of correlation between successive events. This is particularly important for cell division, where the cell-cycle lengths of mother and daughter cells are generally correlated.

## Chapter 3

### EFFECTS OF CELL-CYCLE DEPENDENT EXPRESSION ON RANDOM FLUCTUATIONS IN PROTEIN LEVELS

Advances in experimental technologies over the last decade have provided important insights into gene expression at a single-molecule and single-cell resolution. An important (but not surprising) revelation is the stochastic expression of genes inside individual cells across different organisms [30–32, 50, 51, 88–93]. In many cases, stochastic expression is characterized by random burst-like synthesis of gene products during transcription and translation. At the transcriptional level, promoters randomly switch to an active state, producing a burst of RNAs before becoming inactive [22, 94–98]. At the translational level, a relatively unstable mRNA degrades after synthesizing a burst of protein molecules [69, 70, 84, 99]. Bursty expression drives intercellular variability in gene product levels across isogenic cells, significantly impacting biological pathways and phenotypes [40, 42, 49, 86, 100–103].

Mathematical models have played a key role in predicting the impact of bursty expression on noise in the level of a given protein. However, these studies have primarily relied on models where synthesis rates are assumed to be constant and invariant of cell-cycle processes. While such an assumption is clearly violated for cell-cycle regulated genes [104], replication-associated changes in gene dosage can alter expression parameters genome wide [64, 105–107]. It is not clear how such cell-cycle dependent expression affects the stochastic dynamics of protein levels in single cells. To systematically investigate this question, we formulate a model where a cell passes through multiple cell-cycle stages from birth to division. Cell cycle is coupled to bursty expression of a stable protein and the rate at which bursts occur depend arbitrarily on the cell-cycle stage (Fig. 3.1). In addition to stochastic expression in bursts, the model

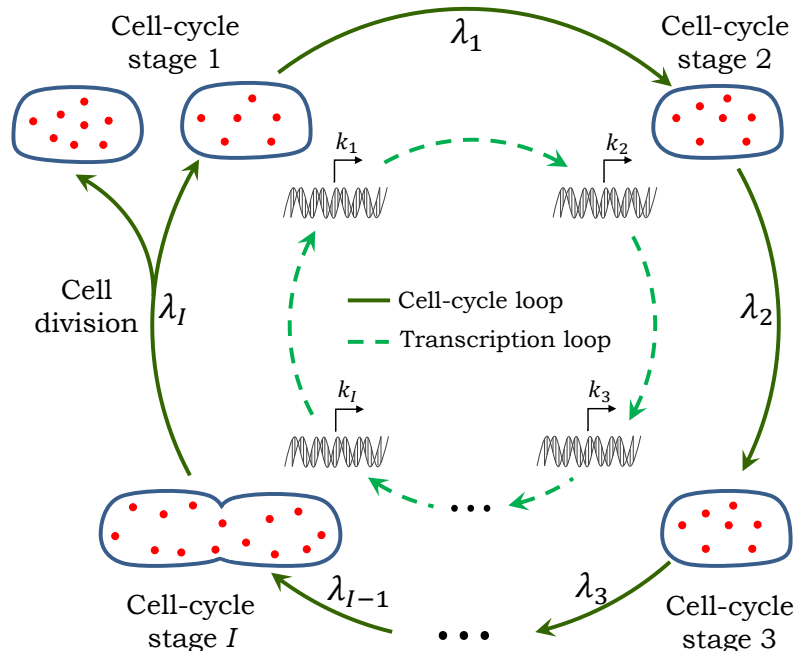


**Figure 3.1: Coupling cell cycle to gene expression.** The outer loop shows an individual cell from birth to division passing through cell-cycle stages  $S_1, S_2, \dots, S_I$ , with transition rates between stages give by  $\lambda_i, i \in \{1, 2, \dots, I\}$ . The cell is born in stage  $S_1$  and division is initiated in  $S_I$ . The inner loop (transcriptional cycle) represents the rate at which protein expression bursts occur and is given by  $k_i$  in cell-cycle stage  $S_i$ .

incorporates other physiological noise sources, such as variability in the duration of cell-cycle times and random partitioning of molecules between daughter cells at the time of division [53, 56–63].

In the proposed model, some cell-to-cell variability or noise in the protein level is simply a result of cells being in different cell-cycle stages (i.e., asynchronous population). We illustrate a novel approach that takes into account such cell-cycle effects, and quantifies the noise contribution just from bursty expression and partitioning errors. Formulas obtained using this approach reveal that cell-cycle dependent expression considerably alters noise, always affecting contributions from bursty expression and partitioning errors in opposite ways. Intriguingly, our results show existence of optimal strategies to synthesize a protein within the cell cycle that minimize noise

contributions for a fixed mean protein level. For example, the noise contribution from bursty expression is minimal when the protein is synthesized only towards the end of cell cycle. We discuss intuitive reasoning behind these optimal strategies, and provide examples of proteins that are expressed in this fashion to enhance fidelity of cell-cycle decisions.

### 3.1 Model Coupling Cell Cycle to Gene Expression

Similar to chapter 2, we adopt a phenomenological approach to model cell cycle and divided it into  $I$  stages  $S_1, S_2, \dots, S_I$ . A newborn cell is in stage  $S_1$  and transitions from  $S_i$  to  $S_{i+1}$  with rate  $\lambda_i$ . In stage  $S_I$ , cell division is initiated with rate  $\lambda_I$ , and upon division the cell returns to  $S_1$ . In the stochastic formulation of this model, the cell resides in stage  $S_i$  for an exponentially distributed time interval with mean  $1/\lambda_i$ , and cell-cycle duration is a sum of  $I$  independent, but not necessarily identical, exponential random variables. These stages can be mathematically characterized by Bernoulli processes  $\mathbf{s}_1(t), \mathbf{s}_2(t), \dots, \mathbf{s}_I(t)$ , where  $\mathbf{s}_i(t) = 1$  when the cell is in stage  $S_i$  and  $\mathbf{s}_i(t) = 0$  otherwise.

We assume that gene-expression bursts occur at a Poisson rate  $k_i$  in cell-cycle stage  $S_i$ . Using the above-defined Bernoulli processes, the burst arrival rate can be compactly written as  $\sum_{i=1}^I k_i \mathbf{s}_i(t)$ . Let  $\mathbf{x}(t)$  denote the number of protein molecules in a single cell at time  $t$ . Then, whenever burst events occur, the protein level is reset as

$$\mathbf{x}(t) \mapsto \mathbf{x}(t) + \mathbf{u}, \quad (3.1)$$

where the protein burst size  $\mathbf{u} \in \{0, 1, 2, \dots\}$  is a random variable independently drawn from an arbitrary distribution, and reflects the net contribution of transcriptional and translational bursting. The partitioning of protein molecules is similar to (2.5). The overall model coupling cell cycle to expression is illustrated in Fig. 3.1 together with a representative trajectory of  $\mathbf{x}(t)$ .

### 3.2 Mean Protein Level for Cell-cycle Driven Expression

In the first step we obtain differential equations describing the time evolution of the statistical moments for  $\mathbf{x}(t)$  and  $\mathbf{s}_i(t)$

$$\frac{d\langle \mathbf{s}_1 \rangle}{dt} = \lambda_I \langle \mathbf{s}_I \rangle - \lambda_1 \langle \mathbf{s}_1 \rangle, \quad \frac{d\langle \mathbf{s}_i \rangle}{dt} = \lambda_{c-i} \langle \mathbf{s}_{i-1} \rangle - \lambda_i \langle \mathbf{s}_i \rangle, \quad i \in \{2, 3, \dots, I\}, \quad (3.2a)$$

$$\frac{d\langle \mathbf{x} \rangle}{dt} = \left( \sum_{i=1}^I k_i \langle \mathbf{s}_i \rangle \right) \langle \mathbf{u} \rangle - \frac{\lambda_I}{2} \langle \mathbf{x} \mathbf{s}_I \rangle. \quad (3.2b)$$

Steady-state analysis of (3.2a) yields the average value of Bernoulli processes as

$$\overline{\langle \mathbf{s}_i \rangle} = \frac{1}{\sum_{j=1}^I \frac{1}{\lambda_j}}, \quad (3.3)$$

which can be interpreted as the fraction of time spent in the cell-cycle stage  $S_i$ . Next we add the time evolution of moments of the form  $\langle \mathbf{x} \mathbf{s}_i \rangle$

$$\frac{d\langle \mathbf{x} \mathbf{s}_1 \rangle}{dt} = k_1 \langle \mathbf{u} \rangle \langle \mathbf{s}_1 \rangle + \frac{\lambda_I}{2} \langle \mathbf{x} \mathbf{s}_I \rangle - \frac{\lambda_I}{2} \langle \mathbf{x} \mathbf{s}_1 \mathbf{s}_I \rangle - \lambda_1 \langle \mathbf{x} \mathbf{s}_1 \rangle, \quad (3.4a)$$

$$\frac{d\langle \mathbf{x} \mathbf{s}_i \rangle}{dt} = k_i \langle \mathbf{u} \rangle \langle \mathbf{s}_i \rangle - \lambda_i \langle \mathbf{x} \mathbf{s}_i \rangle + \lambda_{i-1} \langle \mathbf{x} \mathbf{s}_{i-1} \rangle. \quad j \in \{2, \dots, n\}. \quad (3.4b)$$

At steady-state, the linear equations can be solved recursively to yield

$$\overline{\langle \mathbf{x} \mathbf{s}_i \rangle} = \frac{\langle \mathbf{u} \rangle}{\lambda_i} \frac{\sum_{j=1}^I \frac{k_j}{\lambda_j} + \sum_{j=1}^i \frac{k_j}{\lambda_j}}{\sum_{j=1}^I \frac{1}{\lambda_j}}. \quad (3.5)$$

Since  $\mathbf{s}_i$ 's are binary random variables, the mean protein level conditioned on the cell-cycle stage (i.e., synchronized cell population) can be obtained as

$$\overline{\langle \mathbf{x} | \mathbf{s}_i \rangle} = \frac{\overline{\langle \mathbf{x} \mathbf{s}_i \rangle}}{\overline{\langle \mathbf{s}_i \rangle}} = \langle \mathbf{u} \rangle \left( \sum_{j=1}^I \frac{k_j}{\lambda_j} + \sum_{j=1}^i \frac{k_j}{\lambda_j} \right). \quad (3.6)$$

Furthermore, using (3.5) and the fact that  $\sum_{i=1}^I \mathbf{s}_i = 1$ ,

$$\overline{\langle \mathbf{x} \rangle} = \sum_{j=1}^I \overline{\langle \mathbf{x} \mathbf{s}_j \rangle} = \frac{\langle \mathbf{u} \rangle}{\sum_{j=1}^I \frac{1}{\lambda_j}} \left( \sum_{i=1}^I \sum_{j=1}^I \frac{k_j}{\lambda_i \lambda_j} + \sum_{i=1}^I \sum_{j=1}^i \frac{k_j}{\lambda_i \lambda_j} \right). \quad (3.7)$$

Next, we investigate the mean protein level  $\overline{\langle \mathbf{x} \rangle}$  in some limiting cases. Consider equal transition rates between cell-cycle stages  $\lambda_i = I / \langle \tau_s \rangle$ , which corresponds to an

Erlang distributed cell-cycle duration with mean  $\langle \tau_s \rangle$  and shape parameter  $I$ . In this scenario

$$\overline{\langle \mathbf{x} \rangle} = \frac{\langle \mathbf{u} \rangle \langle \tau_s \rangle \left( \sum_{i=1}^I \sum_{j=1}^I k_j + \sum_{i=1}^I \sum_{j=1}^i k_j \right)}{I^2}, \quad (3.8)$$

and further reduces to

$$\overline{\langle \mathbf{x} \rangle} = k \langle \mathbf{u} \rangle \langle \tau_s \rangle \left( \frac{3}{2} + \frac{1}{2I} \right) \quad (3.9)$$

when the rate of expression bursts  $k_i = k$  is constant throughout the cell cycle. Finally, in the limit of deterministic cell-cycle durations of length  $\tau_s$  ( $I \rightarrow \infty$ )

$$\overline{\langle \mathbf{x} \rangle} = \frac{3 \langle \mathbf{u} \rangle \langle \tau_s \rangle k}{2}. \quad (3.10)$$

### 3.3 Protein Noise Level for Cell-cycle Driven Expression

The mathematical approach illustrated above is now used to obtain the noise in protein copy numbers. By noise (cell-to-cell variability), we mean the magnitude of fluctuations in  $\mathbf{x}(t)$  that can be attributed to two stochastic mechanisms: bursty expression and random partitioning. Note that even in the absence of these mechanisms, there will be cell-cycle related fluctuations with protein molecules accumulating over time and dividing by half at random cell-division times. To correct for such cell-cycle driven fluctuations, we define another stochastic process  $\mathbf{y}(t)$  that estimates the protein level if expression and partitioning were modeled deterministically. More specifically, within the cell cycle  $\mathbf{y}(t)$  evolves according to the following differential equation

$$\frac{d\mathbf{y}}{dt} = \langle \mathbf{u} \rangle \sum_{i=1}^I k_i \mathbf{s}_i(t). \quad (3.11)$$

At the time of cell division, the level is divided exactly by half

$$\mathbf{y}(t) \mapsto \frac{\mathbf{y}(t)}{2} \quad (3.12)$$

with zero partitioning errors, i.e.,  $b = 0$  in (2.5). This allows us to define a new zero-mean stochastic process  $\mathbf{z}(t)$  corrected for cell-cycle effects

$$\mathbf{z}(t) \equiv \mathbf{x}(t) - \mathbf{y}(t) \quad (3.13)$$

that measures the deviation in the protein count in the original stochastic model ( $\mathbf{x}$ ) from its expected levels if noise mechanisms were modeled deterministically ( $\mathbf{y}$ ). The protein noise level can now be defined through the dimensionless quantify

$$CV^2 := \frac{\overline{\langle \mathbf{z}^2 \rangle}}{\overline{\langle \mathbf{x} \rangle}^2}, \quad (3.14)$$

measuring the steady-state variance in  $\mathbf{z}(t)$  normalized by the square of the mean level. Since  $\overline{\langle \mathbf{x} \rangle} = \overline{\langle \mathbf{y} \rangle}$  and  $\overline{\langle \mathbf{x} \mathbf{y} \rangle} = \overline{\langle \mathbf{y}^2 \rangle}$ , it can be rewritten as

$$CV^2 = \frac{\overline{\langle (\mathbf{x} - \mathbf{y})^2 \rangle}}{\overline{\langle \mathbf{x} \rangle}^2} = \frac{\overline{\langle \mathbf{x}^2 \rangle}}{\overline{\langle \mathbf{x} \rangle}^2} - \frac{\overline{\langle \mathbf{y}^2 \rangle}}{\overline{\langle \mathbf{y} \rangle}^2}. \quad (3.15)$$

In the context of previous chapter,  $\overline{\langle \mathbf{y}^2 \rangle} / \overline{\langle \mathbf{y} \rangle}^2 - 1$  is interpreted as the ‘‘extrinsic noise’’ in gene expression resulting from cell-cycle effects. In contrast,  $CV^2$  is the ‘‘intrinsic noise’’ resulting from stochasticity in gene expression and partitioning processes, and is measured by subtracting the extrinsic noise from the total noise  $\overline{\langle \mathbf{x}^2 \rangle} / \overline{\langle \mathbf{x} \rangle}^2 - 1$ .

Having appropriately defined the noise level, we next compute it using moment equations. The time evolution of the moments  $\langle \mathbf{z}^2 \rangle$  and  $\langle \mathbf{z}^2 \mathbf{s}_i \rangle$  are given by

$$\frac{d\langle \mathbf{z}^2 \rangle}{dt} = \langle \mathbf{u}^2 \rangle \sum_{i=1}^I k_i \langle \mathbf{s}_i \rangle + \frac{b\lambda_I}{4} \langle \mathbf{x} \mathbf{s}_I \rangle + \frac{\lambda_I}{4} \langle \mathbf{z}^2 \mathbf{s}_1 \mathbf{s}_I \rangle - \frac{3}{4} \lambda_I \langle \mathbf{z}^2 \mathbf{s}_I \rangle \quad (3.16a)$$

$$\frac{d\langle \mathbf{z}^2 \mathbf{s}_1 \rangle}{dt} = k_1 \langle \mathbf{u}^2 \rangle + \frac{b\lambda_I}{4} \langle \mathbf{x} \mathbf{s}_I \rangle + \frac{\lambda_I}{4} \langle \mathbf{z}^2 \mathbf{s}_I \rangle - \lambda_1 \langle \mathbf{z}^2 \mathbf{s}_1 \rangle, \quad (3.16b)$$

$$\frac{d\langle \mathbf{z}^2 \mathbf{s}_i \rangle}{dt} = k_i \langle \mathbf{u}^2 \rangle - \lambda_i \langle \mathbf{z}^2 \mathbf{s}_i \rangle + \lambda_{i-1} \langle \mathbf{z}^2 \mathbf{s}_{i-1} \rangle, \quad i = \{2, \dots, I\}. \quad (3.16c)$$

and depend on the fourth-order moments  $\langle \mathbf{z}^2 \mathbf{s}_1 \mathbf{s}_I \rangle$ . Exploiting the model structure as before, it follows that  $\langle \mathbf{z}^2 \mathbf{s}_1 \mathbf{s}_I \rangle = 0$ , and (3.2), (3.4), (3.16) constitute a ‘‘closed’’ set of linear differential equations. Steady-state analysis yields the following noise level

$$CV^2 = \underbrace{\left( \frac{1}{3} + \frac{2}{3} \frac{1}{1 + \beta} \right) \frac{\langle \mathbf{u}^2 \rangle}{\langle \mathbf{u} \rangle} \frac{1}{\overline{\langle \mathbf{x} \rangle}}}_{\text{Bursty synthesis}} + \underbrace{\frac{2b}{3} \frac{\beta}{1 + \beta} \frac{1}{\overline{\langle \mathbf{x} \rangle}}}_{\text{Partitioning errors}} \quad (3.17)$$

that is inversely proportional to the mean  $\overline{\langle \mathbf{x} \rangle}$ . The noise can be decomposed into two terms: the first term represents the contribution from protein synthesis in random bursts and depends on the statistical moments of the protein burst size  $\mathbf{u}$ . The

second term is the contribution from partitioning errors and depends linearly on  $b$ . Interestingly, results show that the effect of cell-cycle regulation on the noise level can be quantified through a single dimensionless parameter

$$\beta = \frac{\sum_{i=1}^I \sum_{j=1}^I \frac{k_j}{\lambda_i \lambda_j}}{\sum_{i=1}^I \sum_{j=1}^i \frac{k_j}{\lambda_i \lambda_j}}, \quad (3.18)$$

that is uniquely determined by the number of cell-cycle stages in the model ( $I$ ), transition rates between stages ( $\lambda_i$ ), and protein synthesis rates across stages ( $k_i$ ). Note from (3.17) that  $\beta$  affects the noise terms in opposite ways – any coupling of cell-cycle to expression that increases  $\beta$  will attenuate the contribution from bursty expression but amplifies the contribution from partitioning errors. Finally, we point out that in the case of non-bursty expression ( $\mathbf{u} = 1$  with probability one) and binomial partitioning ( $b = 1$ )

$$CV^2 = \frac{1}{\langle \mathbf{x} \rangle}. \quad (3.19)$$

and the noise level is always consistent with that of a Poisson distribution irrespective of the value of  $\beta$ , and hence the form of cell-cycle regulation.

### 3.4 Optimal Cell-cycle Regulation to Minimize Noise

We explore how different forms of cell-cycle regulation affect  $CV^2$  and begin with the simplest case of a constant synthesis rate  $k_i = k$ ,  $i \in \{1, 2, \dots, I\}$  throughout the cell cycle. This case would correspond to a scenario where the net rate of expression (across all copies of a gene) remains invariant to replication-associated changes in gene dosage, as has recently been shown in different organisms [106, 107]. Further assuming equal transition rates  $\lambda_i = I/\langle \tau_s \rangle$  (Erlang distributed cell-cycle durations)

$$\beta = \frac{2I}{I+1}, \quad (3.20)$$

which reduces to  $\beta = 2$  as  $I \rightarrow \infty$ . Thus, in this important limit of no cell-cycle regulation (equal  $k_i$ 's) and deterministic cell-cycle duration (large  $I$ ),

$$CV^2 = \frac{5}{9} \frac{\langle \mathbf{u}^2 \rangle}{\langle \mathbf{u} \rangle} \frac{1}{\langle \mathbf{x} \rangle} + \frac{4b}{9} \frac{1}{\langle \mathbf{x} \rangle} \quad \text{for } \beta = 2. \quad (3.21)$$

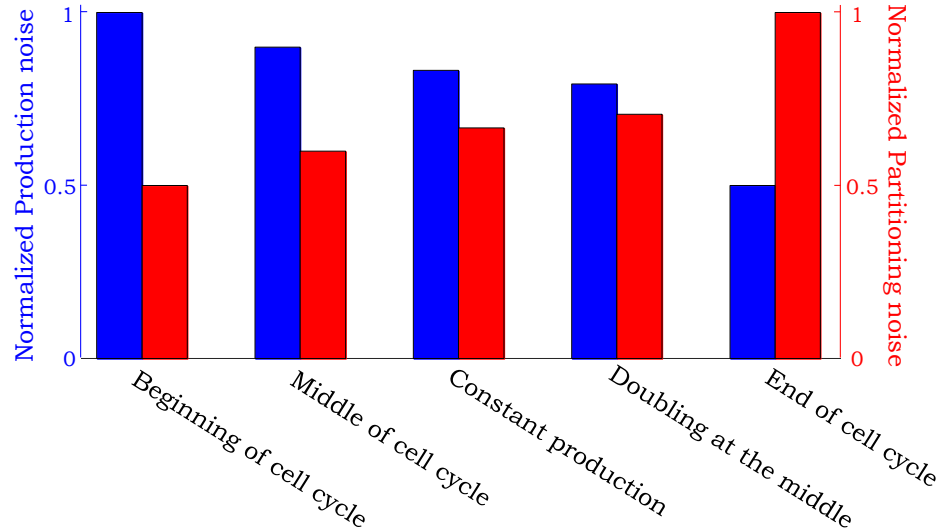


**Figure 3.2: Noise comparison for different strategies coupling cell cycle to gene expression.** The noise from bursty expression (left) and partitioning errors (right) as given by (3.17) are shown for five different strategies: expression only at the start of cell cycle; expression only at the cell-cycle midpoint; constant mRNA synthesis rate throughout the cell cycle; doubling of synthesis rate at the cell-cycle midpoint; expression only towards the end of cell cycle. While noise from bursty expression is minimized in the latter strategy, contribution from partitioning errors are lowest if expression occurs only at the beginning of cell cycle. The cell cycle was modeled by choosing  $I = 20$  stages with equal transition rates, i.e., stages have equal mean duration. The duration of each stage is an exponentially distributed random variable. The production rates  $k_i$  were chosen so as to have the same mean protein level per cell across all cases. Note that this plot is true for any burst size and distribution.

Next, consider the following strategies for coupling cell cycle to gene expression:

1. The burst arrival rate is assumed to increase by two-fold at the cell-cycle midpoint due to gene duplication. Assuming even  $n$ , this corresponds to

$$k_i = k, \quad i \in \left\{1, \dots, \frac{I}{2}\right\} \quad (3.22a)$$

$$k_i = 2k, \quad i \in \left\{\frac{I}{2}, \dots, I\right\} \quad (3.22b)$$

2. Expression only occurs at the start of cell cycle, i.e.,  $k_1 = k$  and all other  $k_i$ 's are zero.

3. Expression only occurs at the end of cell cycle, i.e.,  $k_I = k$  and all other  $k_i$ 's are zero.
4. Expression only occurs at the cell cycle midpoint, i.e.,  $k_{\frac{I}{2}} = k$  and all other  $k_i$ 's are zero.

For a mathematically controlled comparison, the parameter  $k$  is adjusted using (3.7) from case-to-case so as to maintain a fixed average number protein molecules. It is important to point out that strategies 2–4 above correspond to expression only occurring at specific instants in the cell-cycle, with expression turned off for the remainder of the cycle. Our results show that the noise contribution from bursty expression is different depending on when the proteins are synthesized, and it is the highest (lowest) when expression occurs at the start (end) of the cell cycle (Fig. 3.2). Furthermore, as expected from (3.17), the noise contribution from partitioning errors exhibits a completely opposite trend.

Interestingly, a two-fold increase in the protein expression rate (due to gene duplication) at the cell-cycle midpoint leads to a lower noise contribution from bursty synthesis, as compared to a constant rate throughout the cell-cycle (Fig. 3.2). Is it possible to further reduce noise levels by changing the timing of genome-duplication? This question is particularly relevant since genes can be duplicated at different times in the cell cycle, and depending on dosage-compensation mechanisms, have different fold-changes in transcription rates upon duplication [64]. To investigate this scenario, we consider a  $m$ -fold change in the synthesis rate (from  $k$  to  $mk$ ) that occurs at some time  $\tau_g$  from the start of cell cycle. Noise is investigated as a function of  $\tau_g$  and  $m$ , while keeping a fixed average protein level through alterations in  $k$  (Fig. 3.3). Intriguingly, our analysis reveals that for a fixed  $\tau_g$ , noise contribution from bursty synthesis always decreases with increasing  $m$  (Fig. 3.3). Moreover, the minimal noise is obtained when  $m$  is as large as possible, and the duplication event occurs close to the cell-cycle end, i.e., the protein is expressed at a small basal rate within the cell cycle, and the rate is increased for a small time window just before division (Fig. 3.3).

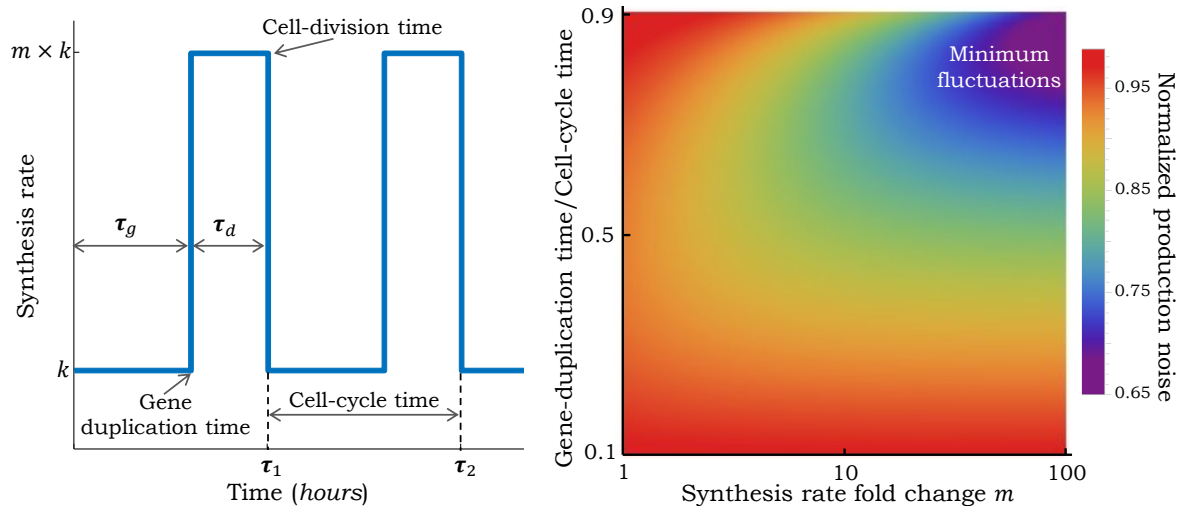


**Figure 3.3: Protein noise level from bursty expression is minimal when gene-duplication event is at the cell-cycle end, and fold-change in transcription is high.** *Left:* The rate of transcription within the cell cycle is modeled as a step function - it is equal to  $k$  ( $mk$ ) before (after) the gene-duplication event, where  $m$  is the fold-change in transcription. The event is assumed to occur at time  $\tau_g$  since the start of cell cycle, and cell division occurs at time  $\tau_s = \tau_g + \tau_d$ . After division, the rate again resets to  $k$ . The times  $\tau_g$  and  $\tau_d$  are assumed to be deterministic. *Right:* The noise contribution from bursty expression is plotted as a function of  $\tau_g/\tau_s$  and  $m$ . The value of  $k$  is changed so as to keep the mean protein level fixed. Noise levels are normalized to the noise when protein is expressed at a constant rate throughout the cell cycle ( $m = 1$ ). The plot reveals that the noise is smallest when  $\tau_g/\tau_s$  is close to 1, and  $m$  is large.

Above results motivate a related but more general question: Is there an optimal way to express a protein during the cell cycle that maximizes/minimizes protein noise levels? Since the form of cell-cycle regulation impacts  $CV^2$  through  $\beta$ , this amounts to choosing  $k_i$ 's so as to maximize/minimize it. Our result show that  $\beta$  is bounded from both below and above

$$1 \leq \beta \leq \beta_{max} = \frac{\frac{1}{\lambda_1} + \frac{1}{\lambda_2} + \dots + \frac{1}{\lambda_I}}{\frac{1}{\lambda_I}}. \quad (3.23)$$

The minimal value of  $\beta = 1$  is attained when expression only occurs at the start of cell cycle, i.e., a non-zero  $k_1$  and all other  $k_i$ 's are zero. In this case

$$CV^2 = \frac{2}{3} \frac{\langle \mathbf{u}^2 \rangle}{\langle \mathbf{u} \rangle} \frac{1}{\langle \mathbf{x} \rangle} + \frac{b}{3} \frac{1}{\langle \mathbf{x} \rangle} \quad \text{for } \beta = 1. \quad (3.24)$$

with the lowest noise contribution from partitioning errors, but the highest contribution from bursty synthesis. In contrast, the maximum value of  $\beta = \beta_{max}$  is attained when expression only occurs at the end of cell cycle, i.e., a non-zero  $k_I$ , and all other  $k_i$ 's are relatively small or zero. Note from (3.23) that  $\beta_{max} \rightarrow \infty$  as  $\lambda_I \rightarrow \infty$  (time spent in stage  $S_I$  approaches zero), in which case

$$CV^2 = \frac{1}{3} \frac{\langle \mathbf{u}^2 \rangle}{\langle \mathbf{u} \rangle} \frac{1}{\langle \mathbf{x} \rangle} + \frac{2b}{3} \frac{1}{\langle \mathbf{x} \rangle} \quad \text{for } \beta = \infty. \quad (3.25)$$

and the noise contribution from bursty synthesis is minimal.

In summary, consistent with finding of Fig. 3.3, if bursty expression is the dominant source of noise (high  $\mathbf{u}$  and low  $b$ ), then  $CV^2$  is minimized for a given  $\overline{\langle \mathbf{x} \rangle}$  when the protein is made in the shortest time window just before cell division (Fig. 3.4). On the other hand, if randomness in partitioning error is dominant (low  $\mathbf{u}$  and high  $b$ ), the optimal strategy is to make the protein just after cell division.

### 3.5 Conclusion

Theoretical model of stochastic gene expression have played a pivotal role in understanding how noise mechanisms and biologically relevant parameters generate differences in protein/mRNA population counts between isogenic cells [108–112]. Here

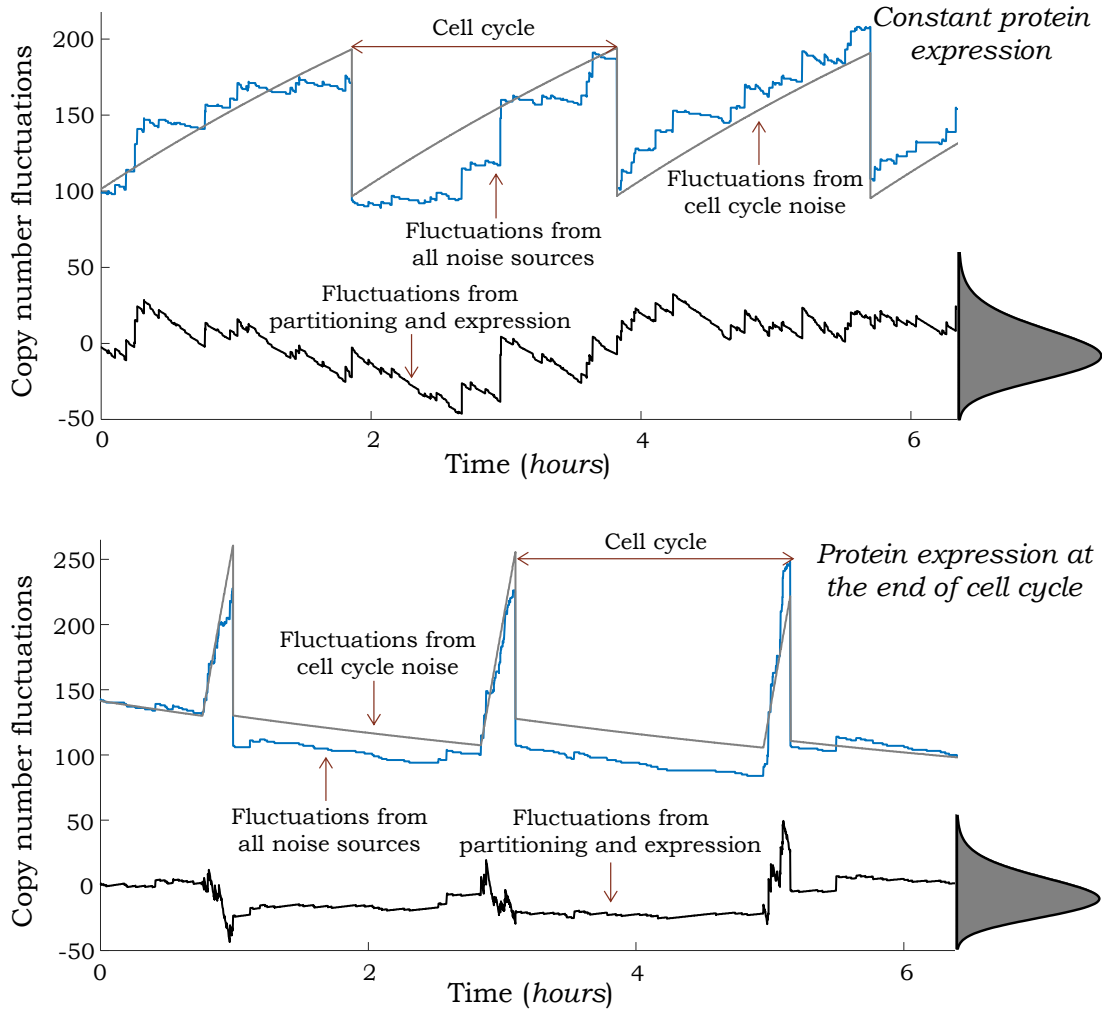


**Figure 3.4: Synthesis of proteins towards the end of cell cycle minimizes fluctuations in copy numbers.** Protein level in an individual cell across multiple cell cycles for two strategies: a fixed transcription rate throughout the cell cycle (top) and transcription increases drastically just before cell division (bottom). In both cases we assumed that there exists a small degradation of protein through the cell cycle. Trajectories obtained via Monte Carlo simulations are shown for the stochastic model (blue) and a reduced model where noise mechanisms are modeled deterministically (gray). These levels are subtracted to obtain a zero-mean stochastic process  $z(t)$ , where fluctuations resulting from cell cycle are removed (black). Stationary distribution of  $z$  obtained from 20,000 MC simulation runs is shown on the right, and the bottom strategy leads to lower variability in  $z$  for the same mean protein level. Cell cycle and expression was modeled as in Fig. 3.1 and burst arrival rates were chosen so as to ensure a average protein copy number of 150 molecules per cell in both cases.

we have expanded this theory to consider cell-cycle regulated genes. Our approach involves a general model of cell cycle, where a cell transitioning through an arbitrary number of stages from birth to division. The protein is assumed to be expressed in random bursts, and the rate at which bursts arrive varies arbitrarily with cell-cycle stage. In the case of translational bursting of proteins from mRNA, the burst arrive rate corresponds to the mRNA synthesis (transcription) rate. In contrast, for transcriptional bursting of mRNAs, the burst arrive rate corresponds to the frequency with which a promoter become transcriptionally active. The key contribution of this work is derivation of (3.7) and (3.17) that predict the protein mean and noise levels for a given form of cell-cycle regulation.

Derivation of noise formulas enable uncovering of optimal cell-cycle regulation strategies to minimize  $CV^2$  for a fixed mean protein level. In the physiological case of large bursts ( $\langle \mathbf{u} \rangle \gg 1$ ) and binomial partitioning of proteins between daughter cells ( $b = 1$ ), the contribution from bursty synthesis dominates  $CV^2$ . Our results show that in this scenario, expression of the protein just before division is the optimal strategy (Fig. 3.3). Intuitively, such a strategy can be understood in the context of the number of burst events from birth to division needed to maintain a given  $\overline{\langle \mathbf{x} \rangle}$  throughout the cell-cycle. It turns out that this number is highly dependent on the form of cell-cycle regulation. Hence, any strategy that requires more burst events to maintain the same mean protein level, lowers noise through more effective averaging of the underlying bursty process, albeit being more energy inefficient. For example, if protein production only occurs at the end of cell cycle, then on average,  $\overline{\langle \mathbf{x} \rangle}$  number of proteins must to added just before cell division. This corresponds to  $\overline{\langle \mathbf{x} \rangle} / \langle \mathbf{u} \rangle$  number of burst events per cell cycle. If proteins were only expressed at the start of cell cycle, then one needs to add only  $\overline{\langle \mathbf{x} \rangle} / 2$  number of molecules, half as much as the earlier strategy. If proteins were made at a constant synthesis rate throughout the cell cycle, then on average,  $2\overline{\langle \mathbf{x} \rangle} / 3$  number of protein are added per cell cycle, which is higher than the early-expression strategy but lower than the late-expression strategy. In summary, gene product synthesis just before division requires production of the most number

of protein molecules to maintain a fixed mean level within the cell-cycle, and hence, provides the most effective noise buffering through averaging of burst events. Next, we provide two recent examples of proteins that are indeed expressed in this fashion.

The green alga *C. reinhardtii* has a prolonged  $G_1$  phase, where the size of a newborn cell increases by more than 2-fold. This long  $G_1$  phase is followed by an  $S/M$  phase. Here the cell undergoes multiple DNA replication and fission cycles creating  $2^d$  daughter cells, where  $d$  is number of rounds of division. Recent studies suggest that the number of rounds of division is controlled by a protein CDKG1, that is only expressed just before exit from  $G_1$  [113]. Another example, is the protein Whi5 in budding yeast *S. cerevisiae* and its level controls the transition of cells past the Start checkpoint. This protein is not expressed in  $G_1$ , and is only synthesized late in the cell cycle [114, 115]. While such selective expression of these proteins plays a critical role in coupling cell size to cell-cycle decision, it may also minimize intrinsic fluctuations in protein levels from the innate stochasticity in gene expression. Clearly, a more systematic study exploring the role of noisy expression on the fidelity of these cell-cycle decisions is warranted.

## Chapter 4

### STEADY-STATE MOMENT ANALYSIS OF STOCHASTIC HYBRID SYSTEMS

In this chapter a new method for deriving steady-state moments of TTSHS is presented. The key contributions of this method are derivation of necessary and sufficient conditions for the stability of statistical moments, along with exact analytical expressions for the steady-state moments. These results are illustrated on an example from cell biology, where deterministic synthesis and decay of a gene product (RNA or protein) is coupled to random timing of cell-division events. As experimentally observed, cell-division events occur based on an internal timer that measures the time elapsed since the start of cell cycle (i.e., last event). Upon division, the gene product level is halved, together with a state-dependent noise term that arises due to randomness in the partitioning of molecules between two daughter cells.

#### 4.1 Statistical Analysis of TTSHS

A convenient approach to implement the TTSHS represented by (1.1)-(1.5) is via a timer  $\tau$  that measures the time elapsed since the last event (Fig. 4.1). The timer increases between events, and resets to zero whenever the events occur. Let the probability that an event occurs in the next infinitesimal time  $(t, t + dt]$  be  $h(\tau)dt$ , where

$$h(\tau) \equiv \frac{f(\tau)}{1 - \int_{y=0}^{\tau} f(y)dy} \quad (4.1)$$

is the event arrival rate (hazard rate). Then,  $\tau_s$  follows the continuous positively-valued pdf

$$\tau_s \sim f(\tau) = h(\tau)e^{-\int_0^{\tau} h(y)dy} \quad (4.2)$$

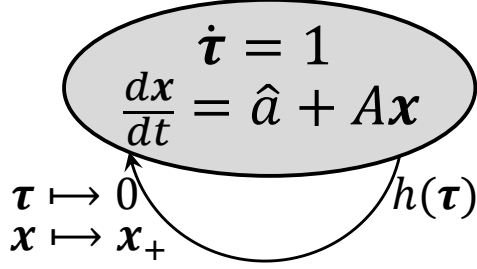


**Figure 4.1: Schematic of stochastic hybrid systems with timer.** As the state evolves according to a linear system, events occur at discrete times that change the state of the system according to (1.2). The timing of events is controlled by renewal transitions defined through a timer  $\tau$  that linearly increases over time in between events, and is reset to zero each time an event occurs. Choosing the event arrival rate  $h(\tau)$  based on (4.1) ensures that the time interval between events is iid with probability distribution  $f$ .

[116–118], and at steady-state, the timer follows the continuous positively-valued pdf

$$\tau \sim p(\tau) = \frac{1}{\langle \tau_s \rangle} e^{-\int_0^\tau h(y) dy} \quad (4.3)$$

[119]. As a simple example, a constant (timer independent) hazard rate  $h(\tau) = 1/\langle \tau_s \rangle$  leads to exponentially-distributed  $\tau_s$ . Similarly, a monomial function

$$h(\tau) = \frac{k}{\lambda} \left( \frac{\tau}{\lambda} \right)^{k-1}, \quad (4.4)$$

with positive constants  $k$  and  $\lambda$  results in a Weibull distribution for  $\tau_s$  with pdf

$$f(\tau) = \frac{k}{\lambda} \left( \frac{\tau}{\lambda} \right)^{k-1} e^{-(\tau/\lambda)^k} \quad (4.5)$$

and mean  $\langle \tau_s \rangle = \lambda \Gamma(1 + 1/k)$ , where  $\Gamma$  is the gamma function. Having defined the probability distributions of  $\tau_s$  and  $\tau$ , we next summarize our main results in different theorems and corollaries.

#### 4.1.1 Steady-state Mean Level

In general, the expected value of  $x$  depends on the entire distribution of  $\tau_s$ , to derive the steady-state mean we first introduce the following lemmas.

**Lemma 1:** Existence of  $\langle e^{A\tau_s} \rangle$  is a sufficient condition for existence of  $\langle e^{A\tau_s} \int_0^{\tau_s} e^{-Al} \hat{a} dl \rangle$ .

**Proof:** The fact that a matrix exponential  $e^{A\tau}$  can be written as

$$e^{A\tau} = \sum_{i=0}^{\infty} A^i \frac{\tau^i}{i!} \quad (4.6)$$

means that  $A$  and  $e^{A\tau}$  can commute. Thus

$$\begin{aligned} A \left\langle e^{A\tau_s} \int_0^{\tau_s} e^{-Al} \hat{a} dl \right\rangle &= A \int_0^{\infty} f(\tau) e^{A\tau} \int_0^{\tau} e^{-As} \hat{a} dl d\tau \\ &= \int_0^{\infty} f(\tau) e^{A\tau} \int_0^{\tau} e^{-As} A \hat{a} dl d\tau = \int_0^{\infty} f(\tau) e^{A\tau} (I_n - e^{-A\tau}) \hat{a} d\tau \\ &= -(I_n - \langle e^{A\tau_s} \rangle) \hat{a}, \end{aligned} \quad (4.7)$$

■

**Lemma 2:** Existence of  $\langle e^{A\tau_s} \rangle$  is a sufficient condition for existence of  $\langle e^{A\tau} \rangle$ .

**Proof:** We show that when all the elements of  $\langle e^{A\tau_s} \rangle$  are bounded then  $\langle e^{A\tau} \rangle$  exists and is finite

$$\begin{aligned} \langle e^{A\tau_s} \rangle &= \int_0^{\infty} h(\tau) e^{-\int_0^{\tau} h(y) dy} e^{A\tau} d\tau \\ &= \left( -e^{-\int_0^{\tau} h(y) dy} e^{A\tau} \right)_0^{\infty} + \int_0^{\infty} e^{-\int_0^{\tau} h(y) dy} e^{A\tau} A d\tau = I_n + \langle \tau_s \rangle \langle e^{A\tau} \rangle A, \end{aligned} \quad (4.8)$$

where we used the fact that  $\lim_{\tau \rightarrow \infty} e^{-\int_0^{\tau} h(y) dy} e^{A\tau} = 0$ . For the sake of simplicity of mathematical notation we proof this for scalar case of  $A = a$ . From (4.3) it follows that

$$\int_0^{\infty} p(\tau) d\tau = 1 \Rightarrow \int_0^{\infty} e^{-\int_0^{\tau} h(y) dy} d\tau = \langle \tau_s \rangle < \infty \Rightarrow \lim_{\tau \rightarrow \infty} e^{-\int_0^{\tau} h(y) dy} = 0. \quad (4.9)$$

In the next, assume that  $\lim_{\tau \rightarrow \infty} e^{a\tau}$  is infinite, hence

$$\lim_{\tau \rightarrow \infty} e^{-\int_0^{\tau} h(y) dy} e^{a\tau} = 0 \times \infty. \quad (4.10)$$

We use L'Hopital's rule

$$\lim_{\tau \rightarrow \infty} e^{-\int_0^{\tau} h(y) dy} e^{a\tau} = -\frac{1}{a} \lim_{\tau \rightarrow \infty} h(\tau) e^{-\int_0^{\tau} h(y) dy} e^{a\tau}. \quad (4.11)$$

Finally, note that we assumed moment generating function exists, hence

$$\langle e^{a\tau_s} \rangle < \infty \Rightarrow \lim_{\tau \rightarrow \infty} h(\tau) e^{-\int_0^{\tau} h(y) dy} e^{a\tau} = 0 \quad (4.12)$$

and this completes our proof. ■

By using these lemmas, the steady-state mean of protein is provided in the following theorem.

**Theorem 2** *For the TTSHS (1.1)-(1.5) the steady-state mean of  $\mathbf{x}$  exists and is given by*

$$\overline{\langle \mathbf{x} \rangle} = \langle e^{A\tau} \rangle (I_n - J \langle e^{A\tau_s} \rangle)^{-1} \left( J \left\langle e^{A\tau_s} \int_0^{\tau_s} e^{-Al} \hat{a} dl \right\rangle + \hat{r} \right) + \left\langle e^{A\tau} \int_0^{\tau} e^{-Al} \hat{a} dl \right\rangle \quad (4.13)$$

*if and only if the expected value*

$$\langle e^{A\tau_s} \rangle = \int_0^{\infty} f(\tau) e^{A\tau} d\tau \quad (4.14)$$

*exists and all the eigenvalues of the matrix  $J \langle e^{A\tau_s} \rangle$  are inside the unit circle.*

**Proof:** Using (1.1), the states of TTSHS right before  $s^{th}$  event  $\mathbf{x}(\mathbf{t}_s)$  is related to the states of TTSHS right after  $s - 1^{th}$  event  $\mathbf{x}_+(\mathbf{t}_{s-1})$  as

$$\mathbf{x}(\mathbf{t}_s) = e^{A\tau_s} \int_0^{\tau_s} e^{-Al} \hat{a} dl + e^{A\tau_s} \mathbf{x}_+(\mathbf{t}_{s-1}). \quad (4.15)$$

Thus, by using (1.1), the mean of the states after  $s^{th}$  event is

$$\langle \mathbf{x}_+(\mathbf{t}_s) \rangle = J \left\langle e^{A\tau_s} \int_0^{\tau_s} e^{-Al} \hat{a} dl \right\rangle + J \langle e^{A\tau_s} \rangle \langle \mathbf{x}_+(\mathbf{t}_{s-1}) \rangle + \hat{r}. \quad (4.16)$$

In order to have a finite  $\langle \mathbf{x}_+(\mathbf{t}_s) \rangle$  in (4.16),  $\langle e^{A\tau_s} \int_0^{\tau_s} e^{-Al} \hat{a} dl \rangle$  and  $\langle e^{A\tau_s} \rangle$  should be finite. Based on Lemma 1,  $\langle e^{A\tau_s} \rangle$  being finite means that  $\langle e^{A\tau_s} \int_0^{\tau_s} e^{-Al} \hat{a} dl \rangle$  is also finite.

Moreover, from (4.16) the mean of the states right after an event in steady-state ( $s \rightarrow \infty$ ) exists if and only and if eigenvalues of  $J \langle e^{A\tau_s} \rangle$  are inside the unite circle. In this limit the steady-state mean of the states ( $s \rightarrow \infty$ ) right after an event can be written as

$$\lim_{s \rightarrow \infty} \langle \mathbf{x}_+(\mathbf{t}_s) \rangle = (I_n - J \langle e^{A\tau_s} \rangle)^{-1} \left( J \left\langle e^{A\tau_s} \int_0^{\tau_s} e^{-Al} \hat{a} dl \right\rangle + \hat{r} \right). \quad (4.17)$$

Let  $\overline{\langle \mathbf{x} |_{\tau=\tau} \rangle}$  denotes the steady-state mean of the states in between events at a given  $\tau = \tau$ . By using equation (1.1) and (4.17),  $\overline{\langle \mathbf{x} |_{\tau=\tau} \rangle}$  is

$$\overline{\langle \mathbf{x} |_{\tau=\tau} \rangle} = e^{A\tau} (I_n - J \langle e^{A\tau_s} \rangle)^{-1} \left( J \left\langle e^{A\tau_s} \int_0^{\tau_s} e^{-Al} \hat{a} dl \right\rangle + \hat{r} \right) + e^{A\tau} \int_0^{\tau} e^{-Al} \hat{a} dl. \quad (4.18)$$

The mean of the states can be obtained by unconditioning (4.18) with respect to  $\tau$  by using (4.3). Moreover, based on Lemma 1 and 2 when  $\langle e^{A\tau_s} \rangle$  is finite then  $\langle e^{A\tau} \rangle$  and  $\langle e^{A\tau} \int_0^{\tau} e^{-Al} \hat{a} dl \rangle$  are also finite. Hence, existence of  $\langle e^{A\tau_s} \rangle$  means that all the matrices in (4.13) exists.  $\blacksquare$

While Theorem 2 represents the most general result, we consider simplifications of (4.13) in special cases.

**Corollary 1** *If the TTSHS (1.1)-(1.5) satisfies Theorem 2 and the matrix  $A$  is invertible, then*

$$\begin{aligned} \overline{\langle \mathbf{x} \rangle} &= \frac{1}{\langle \tau_s \rangle} (I_n - \langle e^{A\tau_s} \rangle) A^{-1} (I_n - J \langle e^{A\tau_s} \rangle)^{-1} (J (I_n - \langle e^{A\tau_s} \rangle) A^{-1} \hat{a} + \hat{r}) \\ &\quad - \frac{1}{\langle \tau_s \rangle} (I_n - \langle e^{A\tau_s} \rangle) A^{-2} \hat{a} - A^{-1} \hat{a}. \end{aligned} \quad (4.19)$$

**Proof:** Taking integral by parts,  $\langle e^{A\tau} \rangle$  can be written as

$$\begin{aligned} \langle e^{A\tau} \rangle &= \frac{1}{\langle \tau_s \rangle} \int_0^{\infty} e^{-\int_0^{\tau} h(y) dy} e^{A\tau} d\tau = \frac{1}{\langle \tau_s \rangle} \left( e^{-\int_0^{\tau} h(y) dy} e^{A\tau} A^{-1} \right)_0^{\infty} \\ &\quad + \frac{1}{\langle \tau_s \rangle} \int_0^{\infty} h(\tau) e^{-\int_0^{\tau} h(y) dy} e^{A\tau} A^{-1} d\tau = \frac{-1}{\langle \tau_s \rangle} (I_n - \langle e^{A\tau_s} \rangle) A^{-1}. \end{aligned} \quad (4.20)$$

Moreover

$$\left\langle e^{A\tau_s} \int_0^{\tau_s} e^{-Al} \hat{a} dl \right\rangle = \langle e^{A\tau_s} (I_n - e^{-A\tau_s}) A^{-1} \hat{a} \rangle = -(I_n - \langle e^{A\tau_s} \rangle) A^{-1} \hat{a}. \quad (4.21)$$

Finally, the last integral in (4.13) can be written as

$$\begin{aligned} \int_0^{\infty} e^{-\int_0^{\tau} h(y) dy} e^{A\tau} \int_0^{\tau} e^{-As} \hat{a} dl d\tau &= \int_0^{\infty} e^{-\int_0^{\tau} h(y) dy} e^{A\tau} (I_n - e^{-A\tau}) A^{-1} \hat{a} d\tau \\ &= -(I_n - \langle e^{A\tau_s} \rangle) A^{-2} \hat{a} - \langle \tau_s \rangle A^{-1} \hat{a}. \end{aligned} \quad (4.22)$$

$\blacksquare$

Thus, for an invertible matrix  $A$ , the steady-state expected value can directly be computed from the moment generating function  $\langle e^{A\tau_s} \rangle$ . Interestingly, there are some

scenarios where knowing a few lower-order moments of  $\boldsymbol{\tau}_s$  are sufficient to determine  $\overline{\langle \boldsymbol{x} \rangle}$ .

**Corollary 2** Consider the TTSHS (1.1)-(1.5) with  $A = 0$ , and all eigenvalues of the matrix  $J$  are inside the unit circle, then

$$\overline{\langle \boldsymbol{x} \rangle} = (I_n - J)^{-1} (J \langle \boldsymbol{\tau}_s \rangle \hat{a} + \hat{r}) + \frac{\langle \boldsymbol{\tau}_s^2 \rangle}{2 \langle \boldsymbol{\tau}_s \rangle} \hat{a}. \quad (4.23)$$

only depends on the first- and the second-order moments of  $\boldsymbol{\tau}_s$ .

**Proof:** When  $A = 0$  we have the following

$$e^{A\tau} = I_n, \quad e^{A\tau} \int_0^\tau e^{-Al} \hat{a} dl = \tau \hat{a}. \quad (4.24)$$

Further

$$\frac{1}{\langle \boldsymbol{\tau}_s \rangle} \left( \int_0^\infty e^{-\int_0^\tau h(y) dy} \right) = \int_0^\infty p(\tau) d\tau = 1. \quad (4.25)$$

Hence (4.13) simplifies to

$$\overline{\langle \boldsymbol{x} \rangle} = J (I_n - J)^{-1} \langle \boldsymbol{\tau}_s \rangle \hat{a} + (I_n - J)^{-1} \hat{r} + \frac{1}{\langle \boldsymbol{\tau}_s \rangle} \int_0^\infty \tau e^{-\int_0^\tau h(y) dy} d\tau \hat{a}. \quad (4.26)$$

Moreover, from equation (4.1) we can calculate the second-order moment  $\langle \boldsymbol{\tau}_s^2 \rangle$  as

$$\langle \boldsymbol{\tau}_s^2 \rangle = \int_0^\infty \tau^2 h(\tau) e^{-\int_0^\tau h(y) dy} d\tau, \quad (4.27)$$

in which integrating by parts results in

$$\langle \boldsymbol{\tau}_s^2 \rangle = 2 \int_0^\infty \tau e^{-\int_0^\tau h(y) dy} d\tau. \quad (4.28)$$

Hence from (4.3) we have the following

$$\langle \boldsymbol{\tau} \rangle = \frac{1}{\langle \boldsymbol{\tau}_s \rangle} \int_0^\infty \tau e^{-\int_0^\tau h(y) dy} d\tau = \frac{\langle \boldsymbol{\tau}_s^2 \rangle}{2 \langle \boldsymbol{\tau}_s \rangle}, \quad (4.29)$$

and (4.26) simplifies to (4.23). ■

We will revisit this corollary later on, as it is pertinent to the example of gene expression.

### 4.1.2 Steady-state Second-order Moments

In order to calculate the second-order moments, we start by deriving the dynamics of  $\mathbf{x}\mathbf{x}^\top$  in between two successive events

$$\frac{d(\mathbf{x}\mathbf{x}^\top)}{dt} = \frac{d\mathbf{x}}{dt}\mathbf{x}^\top + \mathbf{x}\frac{d\mathbf{x}^\top}{dt} = A\mathbf{x}\mathbf{x}^\top + \mathbf{x}\mathbf{x}^\top A^\top + \hat{a}\mathbf{x}^\top + \mathbf{x}\hat{a}^\top. \quad (4.30)$$

To proceed further, we introduce a new transformation named ‘‘vectorization’’, i.e., a linear transformation that converts a matrix into a column vector. For instance

$$A = \begin{bmatrix} a_{11} & a_{12} \\ a_{21} & a_{22} \end{bmatrix} \Rightarrow \text{vec}(A) = \begin{bmatrix} a_{11} & a_{21} & a_{12} & a_{22} \end{bmatrix}^\top, \quad (4.31)$$

where  $\text{vec}()$  stands for the vectorization of a matrix. By putting all the columns of the matrix  $\mathbf{x}\mathbf{x}^\top$  into one vector  $\text{vec}(\mathbf{x}\mathbf{x}^\top) \in \mathbb{R}^{n^2 \times 1}$ , (4.30) can be transformed as

$$\frac{d\text{vec}(\mathbf{x}\mathbf{x}^\top)}{dt} = (I_n \otimes A + A \otimes I_n)\text{vec}(\mathbf{x}\mathbf{x}^\top) + (I_n \otimes \hat{a} + \hat{a} \otimes I_n)\mathbf{x}, \quad (4.32)$$

where  $\otimes$  denotes the Kronecker product. Note that in transforming (4.30) to (4.32) we used the fact that for three matrices  $M_1$ ,  $M_2$ , and  $M_3$

$$\begin{aligned} \text{vec}(M_1 M_2 M_3) &= (M_3^\top \otimes M_1)\text{vec}(M_2) \\ \Rightarrow \begin{cases} \text{vec}(A\mathbf{x}\mathbf{x}^\top) = \text{vec}(A\mathbf{x}\mathbf{x}^\top I_n) = (I_n \otimes A)\text{vec}(\mathbf{x}\mathbf{x}^\top), \\ \text{vec}(\mathbf{x}\mathbf{x}^\top A^\top) = \text{vec}(I_n \mathbf{x}\mathbf{x}^\top A^\top) = (A \otimes I_n)\text{vec}(\mathbf{x}\mathbf{x}^\top), \\ \text{vec}(\hat{a}\mathbf{x}^\top) = \text{vec}(\hat{a}\mathbf{x}^\top I_n) = (I_n \otimes \hat{a})\mathbf{x}, \\ \text{vec}(\mathbf{x}\hat{a}^\top) = \text{vec}(I_n \mathbf{x}\hat{a}^\top) = (\hat{a} \otimes I_n)\mathbf{x} \end{cases} \end{aligned} \quad (4.33)$$

[120]. It turns out that if we define a vector  $\boldsymbol{\mu} \equiv \begin{bmatrix} \mathbf{x}^\top & \text{vec}(\mathbf{x}\mathbf{x}^\top)^\top \end{bmatrix}^\top \in \mathbb{R}^{(n+n^2) \times 1}$ , its time evolution can also be represented by a TTSHS, albeit a more complex one. More specifically,

$$\frac{d\boldsymbol{\mu}}{dt} = \hat{a}_\mu + A_\mu \boldsymbol{\mu}, \quad (4.34)$$

in between two successive events, where

$$A_\mu \equiv \left[ \begin{array}{c|c} A & 0 \\ \hline I_n \otimes \hat{a} + \hat{a} \otimes I_n & I_n \otimes A + A \otimes I_n \end{array} \right], \hat{a}_\mu \equiv \begin{bmatrix} \hat{a} \\ 0 \end{bmatrix}. \quad (4.35)$$

Furthermore, whenever an event occurs,  $\boldsymbol{\mu}$  is reset as

$$\boldsymbol{\mu} \mapsto \boldsymbol{\mu}_+, \quad (4.36)$$

where the expected value of  $\boldsymbol{\mu}_+$  is given by

$$\langle \boldsymbol{\mu}_+ \rangle = J_\mu \boldsymbol{\mu} + \hat{r}_\mu, \quad (4.37a)$$

$$J_\mu \equiv \left[ \begin{array}{c|c} J & 0 \\ \hline B \otimes \hat{c} + J \otimes \hat{r} & J \otimes J + Q \otimes Q \\ \hline +\hat{c} \otimes B + \hat{r} \otimes J & \end{array} \right], \hat{r}_\mu \equiv \left[ \begin{array}{c} \hat{r} \\ \hline \text{vec}(D + \hat{r}\hat{r}^\top) \end{array} \right]. \quad (4.37b)$$

In summary, we have recast the stochastic dynamic of  $\boldsymbol{\mu}$  as a TTSHS (4.34) -(4.37), and a similar analysis as in Theorem 2 leads to the following result.

**Theorem 3** *Assuming the original TTSHS given by (1.1)-(1.5) satisfies Theorem 2.*

*Then*

$$\begin{aligned} \overline{\langle \boldsymbol{\mu} \rangle} &= \left\langle e^{A_\mu \tau} \int_0^\tau e^{-A_\mu l} \hat{a}_\mu dl \right\rangle \\ &+ \langle e^{A_\mu \tau} \rangle (I_{n^2+n} - J_\mu \langle e^{A_\mu \tau_s} \rangle)^{-1} \left( J_\mu \left\langle e^{A_\mu \tau_s} \int_0^{\tau_s} e^{-A_\mu l} \hat{a}_\mu dl \right\rangle + \hat{r}_\mu \right) \end{aligned} \quad (4.38)$$

*if and only if all the eigenvalues of the matrix  $(J \otimes J + Q \otimes Q) \langle e^{A\tau_s} \otimes e^{A\tau_s} \rangle$  are inside the unit circle.*

**Proof:** Let us define

$$\mathbf{u} \equiv e^{A\tau_s} \int_0^{\tau_s} e^{-Al} \hat{a} dl. \quad (4.39)$$

Using (4.15), the  $\mathbf{x}\mathbf{x}^\top$  right before  $s^{\text{th}}$  event ( $\mathbf{x}(\mathbf{t}_s)\mathbf{x}^\top(\mathbf{t}_s)$ ) is related to  $\mathbf{x}_+(\mathbf{t}_{s-1})$  as

$$\begin{aligned} \mathbf{x}(\mathbf{t}_s)\mathbf{x}^\top(\mathbf{t}_s) &= \mathbf{u}\mathbf{u}^\top + \mathbf{u} (e^{A\tau_s} \mathbf{x}_+(\mathbf{t}_{s-1}))^\top + (e^{A\tau_s} \mathbf{x}_+(\mathbf{t}_{s-1})) \mathbf{u}^\top \\ &+ (e^{A\tau_s} \mathbf{x}_+(\mathbf{t}_{s-1})) (e^{A\tau_s} \mathbf{x}_+(\mathbf{t}_{s-1}))^\top. \end{aligned} \quad (4.40)$$

Thus the mean of the second-order moment of the states after  $s^{th}$  event is

$$\begin{aligned}
\langle \mathbf{x}_+(\mathbf{t}_s) \mathbf{x}_+^\top(\mathbf{t}_s) \rangle &= Q \langle \mathbf{u} \mathbf{u}^\top \rangle Q^\top + J \langle \mathbf{u} \mathbf{u}^\top \rangle J^\top \\
&+ Q \left( \left\langle \mathbf{u} \mathbf{x}_+(\mathbf{t}_{s-1})^\top e^{A^\top \tau_s} \right\rangle + \left\langle \mathbf{u} \mathbf{x}_+(\mathbf{t}_{s-1})^\top e^{A^\top \tau_s} \right\rangle^\top \right) Q^\top \\
&+ J \left( \left\langle \mathbf{u} \mathbf{x}_+(\mathbf{t}_{s-1})^\top e^{A^\top \tau_s} \right\rangle + \left\langle \mathbf{u} \mathbf{x}_+(\mathbf{t}_{s-1})^\top e^{A^\top \tau_s} \right\rangle^\top \right) J^\top \\
&+ Q \left\langle e^{A \tau_s} \mathbf{x}_+(\mathbf{t}_{s-1}) \mathbf{x}_+^\top(\mathbf{t}_{s-1}) e^{A^\top \tau_s} \right\rangle Q^\top \\
&+ J \left\langle e^{A \tau_s} \mathbf{x}_+(\mathbf{t}_{s-1}) \mathbf{x}_+^\top(\mathbf{t}_{s-1}) e^{A^\top \tau_s} \right\rangle J^\top + B \langle \mathbf{u} \rangle \hat{c}^\top \\
&+ B \langle e^{A \tau_s} \mathbf{x}_+(\mathbf{t}_{s-1}) \rangle \hat{c}^\top + J \langle \mathbf{u} \rangle \hat{r}^\top + J \langle e^{A \tau_s} \mathbf{x}_+(\mathbf{t}_{s-1}) \rangle \hat{r}^\top \\
&+ \hat{c} \langle \mathbf{u}^\top \rangle B^\top + \hat{c} \langle \mathbf{x}_+^\top(\mathbf{t}_{s-1}) e^{A^\top \tau_s} \rangle B^\top \\
&+ \hat{r} \langle \mathbf{u}^\top \rangle J^\top + \hat{r} \langle \mathbf{x}_+^\top(\mathbf{t}_{s-1}) e^{A^\top \tau_s} \rangle J^\top + D + \hat{r} \hat{r}^\top.
\end{aligned} \tag{4.41}$$

By using vectorization, we have

$$\begin{aligned}
\text{vec}(\langle \mathbf{x}_+(\mathbf{t}_s) \mathbf{x}_+^\top(\mathbf{t}_s) \rangle) &= (J \otimes J + Q \otimes Q) \langle e^{A \tau_s} \otimes e^{A \tau_s} \rangle \text{vec}(\langle \mathbf{x}_+(\mathbf{t}_{s-1}) \mathbf{x}_+^\top(\mathbf{t}_{s-1}) \rangle) \\
&+ O(\langle \mathbf{x}_+(\mathbf{t}_{s-1}) \rangle),
\end{aligned} \tag{4.42}$$

where

$$\begin{aligned}
O(\langle \mathbf{x}_+(\mathbf{t}_{s-1}) \rangle) &= (J \otimes J + Q \otimes Q) (\langle e^{A \tau_s} \otimes \mathbf{u} \rangle + \langle \mathbf{u} \otimes e^{A \tau_s} \rangle) \langle \mathbf{x}_+(\mathbf{t}_{s-1}) \rangle \\
&+ ((B \otimes \hat{c} + J \otimes \hat{r}) \langle e^{A \tau_s} \rangle + (\hat{c} \otimes B + \hat{r} \otimes J) \langle e^{A \tau_s} \rangle) \langle \mathbf{x}_+(\mathbf{t}_{s-1}) \rangle \\
&+ \text{vec}(Q \langle \mathbf{u} \mathbf{u}^\top \rangle Q^\top + J \langle \mathbf{u} \mathbf{u}^\top \rangle J^\top + B \langle \mathbf{u} \rangle \hat{c}^\top + J \langle \mathbf{u} \rangle \hat{r}^\top \\
&+ \hat{c} \langle \mathbf{u}^\top \rangle B^\top + \hat{r} \langle \mathbf{u}^\top \rangle J^\top + D + \hat{r} \hat{r}^\top).
\end{aligned} \tag{4.43}$$

Hence, the steady-state moments of vector  $\boldsymbol{\mu}$  right after an event exists if and only if all the eigenvalues of  $(J \otimes J + Q \otimes Q) \langle e^{A \tau_s} \otimes e^{A \tau_s} \rangle$  are inside the unit circle. The rest of the proof is similar to that of Theorem 2.  $\blacksquare$

**Remark 1:** Theorems 2 and 3 provide sufficient conditions for the existence of the first two moments of  $\mathbf{x}$ .

Moreover in the case of Hurwitz  $A$ , i.e., the real parts of all eigenvalues of  $A$  are negative, we have the following remark.

**Remark 2:** If  $A$  is a Hurwitz matrix (i.e., the deterministic continuous dynamics

is by itself stable),  $J$  is a diagonal positive definite matrix and all of its eigenvalues are inside the unit circle, then the steady-state mean of  $\mathbf{x}$  exists. Moreover, if  $Q$  is diagonal,  $J \otimes J + Q \otimes Q$  is positive definite and all of its eigenvalues are inside the unit circle, then the second-order moments of  $\mathbf{x}$  also exists. Note that in these cases the first two moments of  $\mathbf{x}$  remain bounded even though higher-order moments of  $\boldsymbol{\tau}_s$  may be unbounded.

**Proof:** Based on Corollary 11 of [121], for a negative definite symmetric matrix  $M_1$  and a positive semidefinite matrix  $M_2$  we have

$$\lambda_{\min}(M_1 M_2) \geq \lambda_{\min}(M_1) \lambda_{\max}(M_2), \quad (4.44)$$

where  $\lambda_{\min}$  and  $\lambda_{\max}$  denote the smallest and largest eigenvalue of a matrix, respectively. Based on the fact that exponential of a Hurwitz matrix is positive definite and  $-J$  is symmetric negative definite ( $J$  is diagonal positive definite) we have

$$\lambda_{\min}(-J \langle e^{A\boldsymbol{\tau}_s} \rangle) \geq \lambda_{\min}(-J) \lambda_{\max}(e^{A\boldsymbol{\tau}_s}). \quad (4.45)$$

Given the fact that  $\lambda_{\min}(-J) = -\lambda_{\max}(J)$  and  $\lambda_{\min}(-J \langle e^{A\boldsymbol{\tau}_s} \rangle) = -\lambda_{\max}(J \langle e^{A\boldsymbol{\tau}_s} \rangle)$ , we have

$$\lambda_{\max}(J \langle e^{A\boldsymbol{\tau}_s} \rangle) \leq \lambda_{\max}(J) \lambda_{\max}(e^{A\boldsymbol{\tau}_s}). \quad (4.46)$$

The proof of the second part of this remark is from the fact that eigenvalues of Kronecker product of two matrices are the multiplication of their eigenvalues [122].  $\blacksquare$

The different corollaries of Theorem 2 that consider special cases can also be generalized to Theorem 3. For instance, if  $A_\mu$  is invertible then similar to Corollary 1, the steady-state mean of vector  $\boldsymbol{\mu}$  takes the form

$$\begin{aligned} \overline{\langle \boldsymbol{\mu} \rangle} &= \frac{1}{\langle \boldsymbol{\tau}_s \rangle} (I_{n^2+n} - \langle e^{A_\mu \boldsymbol{\tau}_s} \rangle) A_\mu^{-1} (I_{n^2+n} - J_\mu \langle e^{A_\mu \boldsymbol{\tau}_s} \rangle)^{-1} \times \\ & (J_\mu (I_{n^2+n} - \langle e^{A_\mu \boldsymbol{\tau}_s} \rangle) A_\mu^{-1} \hat{\mathbf{a}} + \hat{\mathbf{r}}_\mu) - \frac{1}{\langle \boldsymbol{\tau}_s \rangle} (I_{n^2+n} - \langle e^{A_\mu \boldsymbol{\tau}_s} \rangle) A_\mu^{-2} \hat{\mathbf{a}}_\mu - A_\mu^{-1} \hat{\mathbf{a}}_\mu. \end{aligned} \quad (4.47)$$

Moreover, as an extension of Corollary 2, when  $A = 0$ ,  $\langle \mathbf{x}\mathbf{x}^\top \rangle$  only depends on the first three moments of  $\boldsymbol{\tau}_s$ . In this limit,  $\langle e^{A_\mu \boldsymbol{\tau}_s} \rangle$  in (4.38) simplifies to

$$A_\mu = \left[ \begin{array}{c|c} 0 & 0 \\ \hline I_n \otimes \hat{a} + \hat{a} \otimes I_n & 0 \end{array} \right], \Rightarrow \langle e^{A_\mu \boldsymbol{\tau}_s} \rangle = \left[ \begin{array}{c|c} I & 0 \\ \hline (I_n \otimes \hat{a} + \hat{a} \otimes I_n) \langle \boldsymbol{\tau}_s \rangle & I \end{array} \right]. \quad (4.48)$$

Moreover

$$\left\langle e^{A_\mu \boldsymbol{\tau}_s} \int_0^{\boldsymbol{\tau}_s} e^{-A_\mu l} \hat{a}_\mu dl \right\rangle = \left[ \begin{array}{c|c} \hat{a} \langle \boldsymbol{\tau}_s \rangle & \\ \hline \frac{1}{2} (I_n \otimes \hat{a} + \hat{a} \otimes I_n) \hat{a} \langle \boldsymbol{\tau}_s^2 \rangle & \end{array} \right]. \quad (4.49)$$

Similarly

$$\langle e^{A_\mu \boldsymbol{\tau}_s} \rangle = \left[ \begin{array}{c|c} I & 0 \\ \hline (I_n \otimes \hat{a} + \hat{a} \otimes I_n) \langle \boldsymbol{\tau} \rangle & I \end{array} \right], \quad (4.50)$$

$$\left\langle e^{A_\mu \boldsymbol{\tau}_s} \int_0^{\boldsymbol{\tau}_s} e^{-A_\mu l} \hat{a}_\mu dl \right\rangle = \left[ \begin{array}{c|c} \hat{a} \langle \boldsymbol{\tau} \rangle & \\ \hline \frac{1}{2} (I_n \otimes \hat{a} + \hat{a} \otimes I_n) \hat{a} \langle \boldsymbol{\tau}^2 \rangle & \end{array} \right].$$

Moreover, from equation (4.1) we can calculate  $\langle \boldsymbol{\tau}_s^3 \rangle$  as

$$\langle \boldsymbol{\tau}_s^3 \rangle = \int_0^\infty \tau^3 h(\tau) e^{-\int_0^\tau h(y) dy} d\tau, \quad (4.51)$$

in which integrating by parts results in

$$\langle \boldsymbol{\tau}_s^3 \rangle = 3 \int_0^\infty \tau^2 e^{-\int_0^\tau h(y) dy} d\tau. \quad (4.52)$$

Hence, from (4.3) we have the following

$$\langle \boldsymbol{\tau}^2 \rangle = \frac{1}{\langle \boldsymbol{\tau}_s \rangle} \int_0^\infty \tau^2 e^{-\int_0^\tau h(y) dy} d\tau = \frac{\langle \boldsymbol{\tau}_s^3 \rangle}{3 \langle \boldsymbol{\tau}_s \rangle}. \quad (4.53)$$

Together with (4.29) we see that all the terms in (4.38) are only depending on the first three moments of  $\boldsymbol{\tau}_s$ . We next illustrate the theory developed for TTSHS to a nano sensor and the biological example of gene expression.

## 4.2 Modeling Noise in Nanosensors

Nanomechanical resonators are increasingly being used for diverse applications, such as, atomic force microscope tips, sensing forces at the atomic level, and chemical sensors [123]. A major source of noise in these systems is the random collisions between

surrounding gas molecules and the sensor [124]. These sensors are often kept in rarefied atmospheres, where the time interval between collisions can be long enough for model approximations based on Brownian noise to fail [124]. We present a TTSHS model that mechanistically captures the noise due to gas-molecule collisions. Nanosensor dynamics is modeled through the following mass-spring system with displacement ( $\mathbf{x}_1$ ) and velocity ( $\mathbf{x}_2$ )

$$\begin{bmatrix} \dot{\mathbf{x}}_1 \\ \dot{\mathbf{x}}_2 \end{bmatrix} = \begin{bmatrix} 0 & 1 \\ -\omega_n^2 & -2\zeta\omega_n \end{bmatrix} \begin{bmatrix} \mathbf{x}_1 \\ \mathbf{x}_2 \end{bmatrix}, \quad (4.54)$$

where  $\omega_n$  denotes the natural frequency, and  $\zeta$  the damping ratio [125]. Let gas molecules strike the sensor at times  $\mathbf{t}_s$  with intervals between subsequent strikes  $\boldsymbol{\tau}_s$  assumed to be independent and identical random variables with an arbitrary distribution. Whenever collisions occur, the velocity resets as

$$\mathbf{x}_2(\mathbf{t}_s) \mapsto \mathbf{x}_2(\mathbf{t}_s) + \boldsymbol{\eta}, \quad (4.55)$$

where  $\boldsymbol{\eta}$  is drawn from an arbitrary distribution with zero mean and variance  $\sigma^2$ . Intuitively,  $\sigma^2$  depends on the velocity of the impinging gas molecules, which in turn is determined by the gas temperature. Writing (4.55) in terms of TTSHS model results in

$$\langle \mathbf{x}_+(\mathbf{t}_s) \rangle = \mathbf{x}(\mathbf{t}_s), \quad \mathbf{x} = [\mathbf{x}_1 \ \mathbf{x}_2]^\top \quad (4.56a)$$

$$\langle \mathbf{x}_+(\mathbf{t}_s) \mathbf{x}_+^\top(\mathbf{t}_s) \rangle - \langle \mathbf{x}_+(\mathbf{t}_s) \rangle \langle \mathbf{x}_+(\mathbf{t}_s) \rangle^\top = E = \begin{bmatrix} 0 & 0 \\ 0 & \sigma^2 \end{bmatrix}, \quad (4.56b)$$

with  $Q = B = \hat{c} = 0$ . Using Theorem 3 yields the following steady-state variances of the sensor displacement and velocity

$$\overline{\langle \mathbf{x}_1^2 \rangle} = \frac{\sigma^2}{4\langle \boldsymbol{\tau}_s \rangle \zeta \omega_n^3}, \quad \overline{\langle \mathbf{x}_2^2 \rangle} = \frac{\sigma^2}{4\langle \boldsymbol{\tau}_s \rangle \zeta \omega_n}, \quad (4.57)$$

respectively. Here  $\sigma^2$  is the collision impact, and is quantified by the variance of the noise term  $\boldsymbol{\eta}$  in (4.55). Intriguingly, (4.57) shows that the magnitude of fluctuations in the sensor displacement/velocity are inversely dependent on  $\langle \boldsymbol{\tau}_s \rangle$ , and invariant of

higher-order moments of  $\tau_s$ . Thus, making the timing of collisions more random (for a fixed  $\langle \tau_s \rangle$ ) has no effect on  $\langle \mathbf{x}_1^2 \rangle$  and  $\langle \mathbf{x}_2^2 \rangle$ . Furthermore, measurement of  $\langle \mathbf{x}_1^2 \rangle$  and  $\langle \mathbf{x}_2^2 \rangle$  cannot discriminate between infrequent high-impact strikes (large  $\sigma^2$  and  $\langle \tau_s \rangle$ ), and frequent low-impact strikes (small  $\sigma^2$  and  $\langle \tau_s \rangle$ ). It is important to point out that (4.57) determines the sensor's limit of detection. For example, consider a simple displacement sensor, where the sensor's position is read out based on an external force. Then, the sensor's displacement by random chance determines the lowest force that can be accurately measured.

### 4.3 Quantifying Noise in Gene Expression

In chapter 2 we studied the contribution of noisy cell-cycle times in driving stochastic variations of a stable protein, i.e., protein with no active degradation [20]. Exploiting the TTSHS framework, we present a novel unified theory of how noisy cell-cycle times combine with randomness in the molecular partitioning process to shape variations in the level of gene product with an arbitrary decay rate.

#### 4.3.1 Average Gene Product Level for Random Cell-cycle Times

Consider a gene product synthesized at a constant rate  $k_x > 0$ , and degrades via first-order kinetics with rate  $\gamma_x > 0$ . Then, its level  $\mathbf{x}(t)$  within the cell at time  $t$  evolves as

$$\frac{d\mathbf{x}}{dt} = k_x - \gamma_x \mathbf{x}(t). \quad (4.58)$$

Cell division events occur at times  $\mathbf{t}_s$ ,  $s \in \{1, 2, \dots\}$  with cell-cycle times  $\tau_s \equiv \mathbf{t}_s - \mathbf{t}_{s-1}$  being iid random variables. Assuming perfect partitioning of molecules between two daughters for now, the level is exactly halved at the time of division

$$\mathbf{x}_+ = \frac{\mathbf{x}}{2} \text{ with probability one.} \quad (4.59)$$

In the context of the original TTSHS (1.1)-(1.5) this corresponds to  $A = -\gamma_x$ ,  $\hat{a} = k_x$ ,  $J = 1/2$  and  $\hat{r} = Q = B = \hat{c} = D = 0$ .

Since  $A = -\gamma_x < 0$  and  $J < 1$ , then as per Remark 1 the mean of  $\mathbf{x}$  exists, and using Corollary 1

$$\overline{\langle \mathbf{x} \rangle} = \frac{k_x}{\gamma_x} - \frac{k_x}{2\gamma_x^2 \langle \tau_s \rangle} \frac{1 - \langle e^{-\gamma_x \tau_s} \rangle}{1 - \frac{1}{2} \langle e^{-\gamma_x \tau_s} \rangle}. \quad (4.60)$$

If the gene product happens to be a protein whose half-life is much longer than the average cell-cycle time ( $1/\gamma_x \gg \langle \tau_s \rangle$ ), then taking the limit  $\gamma_x \rightarrow 0$  in (4.60) yields

$$\overline{\langle \mathbf{x} \rangle} = \frac{k_x \langle \tau_s \rangle (3 + CV_{\tau_s}^2)}{2}. \quad (4.61)$$

Note that (4.61) could also have been derived directly from Corollary 2. These results exemplify the earlier point that while in general, the average gene product level depends on the entire distribution of the cell-cycle time, in some limiting cases it is completely characterized by just the first two moments of  $\tau_s$ .

### 4.3.2 Stochasticity in Gene Product Levels for Random Cell-cycle Times

In order to calculate the second-order moments, we define a new vector  $\boldsymbol{\mu} = [\mathbf{x} \ \mathbf{x}^2]^T$ , whose time evolution can also be described by a TTSHS. From (4.34) it follows that

$$\frac{d\boldsymbol{\mu}}{dt} = \hat{a}_\mu + A_\mu \boldsymbol{\mu}, \quad A_\mu = \begin{bmatrix} -\gamma_x & 0 \\ 2k_x & -2\gamma_x \end{bmatrix}, \quad \hat{a}_\mu = \begin{bmatrix} k_x \\ 0 \end{bmatrix}, \quad (4.62)$$

and at the time of division

$$\langle \boldsymbol{\mu}_+ \rangle = J_\mu \boldsymbol{\mu} + \hat{r}_\mu, \quad J_\mu = \begin{bmatrix} 1/2 & 0 \\ 0 & 1/4 \end{bmatrix}, \quad \hat{r}_\mu = 0. \quad (4.63)$$

Since  $A = -\gamma_x < 0$ ,  $J = 1/2$ ,  $Q = 0$ , and  $J \otimes J + Q \otimes Q = 1/4 < 1$ , then based on Remark 1 the steady-state second-order moment of  $\mathbf{x}$  exists. We derive the terms needed in Theorem 3

$$\begin{aligned} \langle e^{A_\mu \tau_s} \rangle &= \begin{bmatrix} \langle e^{-\gamma_x \tau_s} \rangle & 0 \\ 2\frac{k_x}{\gamma_x} (\langle e^{-\gamma_x \tau_s} \rangle + \langle e^{-2\gamma_x \tau_s} \rangle) & \langle e^{-2\gamma_x \tau_s} \rangle \end{bmatrix}, \\ \left\langle e^{A_\mu \tau_s} \int_0^{\tau_s} e^{-A_\mu l} \hat{a}_\mu dl \right\rangle &= \begin{bmatrix} \frac{k_x}{\gamma_x} (1 - \langle e^{-\gamma_x \tau_s} \rangle) \\ \frac{k_x^2}{\gamma_x^2} (\langle e^{-2\gamma_x \tau_s} \rangle - 2 \langle e^{-\gamma_x \tau_s} \rangle + 1) \end{bmatrix}, \end{aligned} \quad (4.64)$$

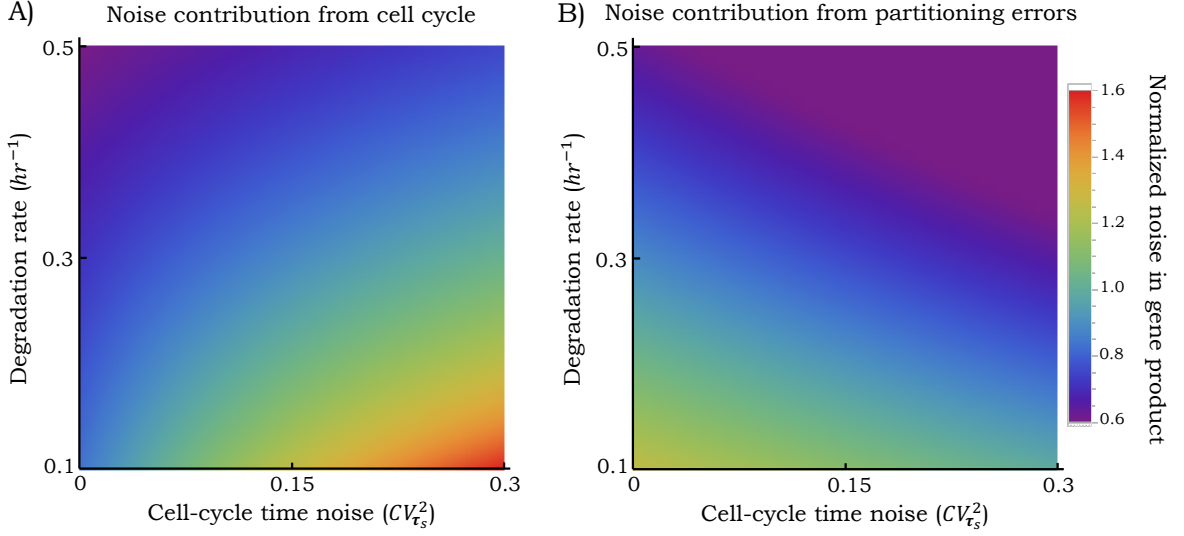


**Figure 4.2:** The noise contributions show similar behavior with respect to decay rate, but contrasting behavior with respect to noise in cell-cycle times. A 2D color plot of the two noise contributions in (4.70) as a function of the gene product decay rate and the noise in cell-cycle times. Increasing  $CV_{\tau_s}^2$  increases the noise contribution from random cell-cycle times, but decreases the contribution from random partitioning. Both noise contributions decrease monotonically with increasing decay rate. Noise levels are normalized to their value when  $CV_{\tau_s}^2 = 0$  and  $\gamma_x = 0.1 \text{ hr}^{-1}$ . We used gamma distributed  $\tau_s$  with a fixed mean cell-cycle time of  $\langle \tau_s \rangle = 2 \text{ hrs}$ . The mean of  $\mathbf{x}$  is fixed at 100 molecules by simultaneously changing  $k_x$ .

and

$$\langle e^{A_\mu \tau} \rangle = \begin{bmatrix} \langle e^{-\gamma_x \tau} \rangle & 0 \\ 2 \frac{k_x}{\gamma_x} (\langle e^{-\gamma_x \tau} \rangle + \langle e^{-2\gamma_x \tau} \rangle) & \langle e^{-2\gamma_x \tau} \rangle \end{bmatrix}, \quad (4.65)$$

$$\left\langle e^{A_\mu \tau} \int_0^\tau e^{-A_\mu l} \hat{a}_\mu dl \right\rangle = \begin{bmatrix} \frac{k_x}{\gamma_x} (1 - \langle e^{-\gamma_x \tau} \rangle) \\ \frac{k_x^2}{\gamma_x^2} (\langle e^{-2\gamma_x \tau} \rangle - 2 \langle e^{-\gamma_x \tau} \rangle + 1) \end{bmatrix}.$$

Using the fact that

$$\langle e^{-\gamma_x \tau} \rangle = \frac{1}{\langle \tau_s \rangle} \frac{1}{\gamma_x} (1 - \langle e^{-\gamma_x \tau_s} \rangle), \quad \langle e^{-2\gamma_x \tau} \rangle = \frac{1}{\langle \tau_s \rangle} \frac{1}{2\gamma_x} (1 - \langle e^{-2\gamma_x \tau_s} \rangle), \quad (4.66)$$

equation (4.65) can be changed to just contain expected values with respect to  $\tau_s$ .

Putting these matrices and vectors back in Theorem 3 we derive  $\overline{\langle \mathbf{x}^2 \rangle}$  as

$$\overline{\langle \mathbf{x}^2 \rangle} = \frac{k_x^2}{\gamma_x^2} + \frac{k_x^2}{16\gamma_x^3 \langle \tau_s \rangle} \frac{-14 + 17\langle e^{-\gamma_x \tau_s} \rangle + \langle e^{-2\gamma_x \tau_s} \rangle (2 - 5\langle e^{-\gamma_x \tau_s} \rangle)}{\left(1 - \frac{1}{4}\langle e^{-2\gamma_x \tau_s} \rangle\right) \left(1 - \frac{1}{2}\langle e^{-\gamma_x \tau_s} \rangle\right)}. \quad (4.67)$$

Using the coefficient of variation squared to quantify the noise in  $\mathbf{x}$

$$\begin{aligned} CV_e^2 &\equiv \frac{\overline{\langle \mathbf{x}^2 \rangle} - \overline{\langle \mathbf{x} \rangle}^2}{\overline{\langle \mathbf{x} \rangle}^2} \\ &= \frac{-8 \left(1 - \frac{1}{4}\langle e^{-2\gamma_x \tau_s} \rangle\right) \left(1 - \langle e^{-\gamma_x \tau_s} \rangle\right)^2 + 4\gamma_x \langle \tau_s \rangle \left(1 - \frac{1}{4}\langle e^{-\gamma_x \tau_s} \rangle^2\right) \left(1 - \langle e^{-2\gamma_x \tau_s} \rangle\right)}{8 \left(1 - \frac{1}{4}\langle e^{-2\gamma_x \tau_s} \rangle\right) \left(-1 + \langle e^{-\gamma_x \tau_s} \rangle + 2\gamma_x \langle \tau_s \rangle \left(1 - \frac{1}{2}\langle e^{-\gamma_x \tau_s} \rangle\right)\right)^2}, \end{aligned} \quad (4.68)$$

where  $CV_e^2$  denotes the noise in the gene product level due to randomness in cell-cycle times. Before analyzing this formulas further, we next consider another physiologically relevant noise source that arises from molecular partitioning errors.

### 4.3.3 Inclusion of Randomness in the Molecular Partitioning Process

As mentioned before, biomolecules in the mother cell are probabilistically partitioned between the two daughters at the time of division. Randomness in the partitioning process can be incorporated in the TTSHS framework with each division event resetting  $\mathbf{x} \mapsto \mathbf{x}_+$  as shown in (2.5).

With the above modification we have a TTSHS where  $A = -\gamma_x$ ,  $\hat{a} = k_x$ ,  $J = 1/2$ ,  $B = b$ ,  $\hat{c} = 1/8$ , and  $\hat{r} = Q = D = 0$ . While the steady-state mean of gene product level is still the same as (4.60), inclusion of the nontrivial noise term in (2.5) leads to (from Theorem 3)

$$\begin{aligned} \overline{\langle \mathbf{x}^2 \rangle} &= \frac{bk_x}{8\gamma_x^2 \langle \tau_s \rangle} \frac{1 - \langle e^{-2\gamma_x \tau_s} \rangle}{1 - \frac{1}{4}\langle e^{-2\gamma_x \tau_s} \rangle} \frac{1 - \langle e^{-\gamma_x \tau_s} \rangle}{1 - \frac{1}{2}\langle e^{-\gamma_x \tau_s} \rangle} \\ &+ \frac{k_x^2}{\gamma_x^2} + \frac{k_x^2}{16\gamma_x^3 \langle \tau_s \rangle} \frac{-14 + 17\langle e^{-\gamma_x \tau_s} \rangle + \langle e^{-2\gamma_x \tau_s} \rangle (2 - 5\langle e^{-\gamma_x \tau_s} \rangle)}{\left(1 - \frac{1}{4}\langle e^{-2\gamma_x \tau_s} \rangle\right) \left(1 - \frac{1}{2}\langle e^{-\gamma_x \tau_s} \rangle\right)}, \end{aligned} \quad (4.69)$$

which yields the following elegant decomposition for gene product noise levels

$$\begin{aligned} \text{Total Noise} &= \frac{\overline{\langle \mathbf{x}^2 \rangle} - \overline{\langle \mathbf{x} \rangle}^2}{\overline{\langle \mathbf{x} \rangle}^2} = CV_e^2 + CV_b^2, \\ CV_b^2 &= b \frac{1 - \langle e^{-2\gamma_x \tau_s} \rangle}{4 - \langle e^{-2\gamma_x \tau_s} \rangle} \frac{1 - \langle e^{-\gamma_x \tau_s} \rangle}{-1 + \langle e^{-\gamma_x \tau_s} \rangle + 2\gamma_x \langle \tau_s \rangle \left(1 - \frac{1}{2}\langle e^{-\gamma_x \tau_s} \rangle\right)} \frac{1}{\overline{\langle \mathbf{x} \rangle}}. \end{aligned} \quad (4.70)$$

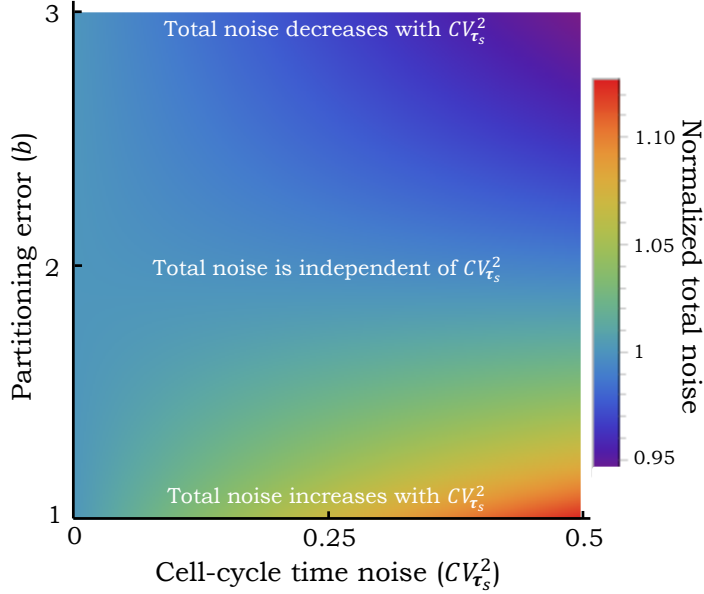


**Figure 4.3: Gene product noise levels can both increase or decrease with increasing noise in cell-cycle times.** The total noise in (4.70) is plotted as a function of parameter  $b$  in the partitioning process and noise in cell-cycle times. While for small (large) values of  $b$  the noise levels increase (decrease) with increasing  $CV_{\tau_s}^2$ , intermediate values of  $b$  can make the total noise approximately invariant of  $CV_{\tau_s}^2$ . Noise levels are normalized to their value when  $CV_{\tau_s}^2 = 0$ , the mean of  $\mathbf{x}$  is fixed at 20 molecules by simultaneously changing  $k_x$ , and  $\gamma_x = 0.1 \text{ hr}^{-1}$ . The rest of parameters are chosen equal to their value in Fig. 4.2.

Here  $CV_e^2$  is the noise contribution for random cell-cycle times as determined earlier, and the new term  $CV_b^2$ , quantifies the contribution from partitioning noise. Note that unlike  $CV_e^2$ ,  $CV_b^2$  is inversely related to the mean  $\overline{\langle \mathbf{x} \rangle}$ , and would become the dominating noise term at low molecular levels.

Both noise contributions  $CV_e^2$  and  $CV_b^2$  monotonically decrease to zero with increasing degradation rate  $\gamma_x$ , for a fixed mean  $\overline{\langle \mathbf{x} \rangle}$  (Fig. 4.2). This makes intuitive sense, as rapid turnover rates allow for faster convergence to mean levels after random perturbations. In the limit of fast decay rate ( $\gamma_x \rightarrow \infty$ ), we obtain the following asymptotes

$$CV_e^2 \approx \frac{1}{8\gamma_x \langle \tau_s \rangle}, \quad CV_b^2 \approx \frac{1}{8\gamma_x \langle \tau_s \rangle} \frac{b}{\overline{\langle \mathbf{x} \rangle}}, \quad (4.71)$$

which only depend on the mean cell-cycle times and show very similar scaling that differ by a factor of  $b$  over mean. Interestingly, noise contributions show contrasting behavior to increasing noise in cell-cycle times – increasing  $CV_{\tau_s}^2$  for fixed  $\tau_s$  increases  $CV_e^2$ , but decreases  $CV_b^2$  (Fig. 4.2B) This implies that depending on the degree of randomness in partitioning (parameter  $b$ ), the total noise may decrease, increase, or remain somewhat invariant of  $CV_{\tau_s}^2$  (Fig. 4.3). Finally, taking the limit  $\gamma_x \rightarrow 0$  in (4.70), we recover our prior result for stable gene products [20]

$$\text{Total noise} = \frac{1}{27} + \frac{\overbrace{4 \left( 9 \frac{\langle \tau_s^3 \rangle}{\langle \tau_s \rangle^3} - 9 - 6CV_{\tau_s}^2 - 7CV_{\tau_s}^4 \right)}^{CV_e^2}}{27 (3 + CV_{\tau_s}^2)^2} + \frac{\overbrace{\frac{1}{4b}}^{CV_b^2}}{3(3 + CV_{\tau_s}^2) \langle \mathbf{x} \rangle}. \quad (4.72)$$

#### 4.4 Conclusion

Our main results (Theorems 2 and 3) connect these moments to the system dynamics and the distribution of event arrival times. While knowledge of the entire distribution of  $\tau_s$  is generally needed to compute the moments, but if  $A = 0$  then the mean of  $\mathbf{x}$  just depends on the first two moments of  $\tau_s$ , and the second-order moments of  $\mathbf{x}$  depend on the first three moments of  $\tau_s$  (Corollary 2).

## Chapter 5

### CONTROL DESIGN AND ANALYSIS OF A STOCHASTIC EVENT-DRIVEN SYSTEM

We considered a feedback loop which is subject to different sources of noise and stochasticity: 1) The plant dynamics are subject to external disturbances. 2) The controller is not always interacting with the plant and is only connected to the plant in random times. 3) The control law is not precise and contains noise. Applying the control law in specific times is a promising method for reducing the energy and resource consumption [12, 126, 127]. Previous works have dealt with designing control strategies to improve system performance. In particular, different strategies are desired that reduce the number of times a control component needs to communicate with the plant. Examples of such strategies include event-driven control, where the new control law applied when the state of the system meets a certain condition [13, 14, 128, 129]; self-driven control, where the state of the system at the time of applying the control law is used to determine the next control time [15, 17, 130, 131]; time-driven control, where the control law is applied at fixed times [132–134].

It turns out a variation of TTSHS is an efficient tool to study the aforementioned control loop. We consider a system whose states are modeled as Stochastic Differential Equations (SDEs). These SDEs naturally capture the disturbances in the system. For example, if the disturbance is state independent (dependent) then the corresponding drift and diffusion terms of the SDEs could be taken as state independent (dependent). Further, to capture the randomness in the control times, we model them using a renewal process.

The framework presented here can be used to study time-driven control. Moreover, we have previously shown that some biological systems where resets happen

because states satisfy a certain condition (event-driven) can be transformed to such framework [23, 135]. Since here the system under study is subject to random disturbance, the time intervals at which states meet a certain value is random with weak correlation between them. Hence we can assume that they happen in independent and identically distributed time intervals based on an underlying renewal process. This means that the current framework is fairly general and can model a large set of systems.

We provide the necessary and sufficient conditions on stability of first- and second-order moments of the states of system. Further, we quantify the contribution of each noise source to the states of system. We show that the exact results combined with stability conditions can be used to design controllers to meet desired performance criterion. Finally, we demonstrate our method via different examples. An interesting observation is that while rare and randomly transmission times are expected to increase noise in a system, these might even reduce the noise in the system in some parameter regimes.

## 5.1 Stochastic Control of Event-driven Linear Systems

Let the states of the system  $\mathbf{x} \in \mathbb{R}^{n \times 1}$  evolve according to the following stochastic differential equation

$$d\mathbf{x} = (\hat{\mathbf{a}} + A\mathbf{x}(t) + B\mathbf{u}(t)) dt + (E + D\mathbf{x}(t)\mathbf{1}_n)d\mathbf{w}_n, \quad (5.1)$$

where  $\mathbf{u}(t) \in \mathbb{R}^{m \times 1}$  denotes the controller. Here  $\hat{\mathbf{a}} \in \mathbb{R}^{n \times 1}$  is a constant vector, and  $A \in \mathbb{R}^{n \times n}$ ,  $B \in \mathbb{R}^{n \times m}$ ,  $E \in \mathbb{R}^{n \times n}$ ,  $D \in \mathbb{R}^{n \times n}$  are constant matrices;  $\mathbf{1}_n$  is a  $1 \times n$  unit matrix. In addition  $\mathbf{w}_n$  is a  $n$ -dimensional Wiener process satisfying

$$\langle d\mathbf{w}_n \rangle = 0, \quad \langle d\mathbf{w}_n d\mathbf{w}_n^\top \rangle = I_n dt. \quad (5.2)$$

While the first part in the right-hand side of (5.1) determines dynamics of the plant, the second part represents the contribution of disturbance to the system. The state-independent disturbance is modeled through  $E$ , and  $D\mathbf{x}(t)\mathbf{1}_n$  presents state-dependent disturbance.

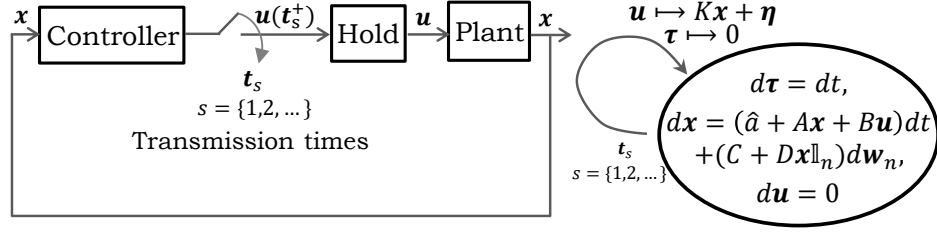


**Figure 5.1: Model schematic of an event-driven control loop.** *Left:* The controller is far from the plant hence the feedback loop is connected through a network. In between transmission times, plant uses the previous control law which is maintained in hold. Any time that connection occurs, the hold reads the new control law which is calculated based on the current values of states of the system. *Right:* The mathematical representation of system as a stochastic hybrid system. Resets are the times in which connection occurs. Any time that a transmission occurs, a new control law is applied to the plant. However due to presence of errors, an extra term  $\eta$  is added to the system.

The controller connects to the plant in random times  $t_s$ ,  $s \in \{1, 2, \dots\}$  as shown in Fig. 5.1, and the time interval between transmission times

$$\tau_s \equiv t_s - t_{s-1} \quad (5.3)$$

is an independent and identically distributed (iid) random variable that follows a continuous positively-valued probability density function  $f$ .

The controller is designed based on state feedback, i.e., the full state  $\mathbf{x}$  is available and the input  $\mathbf{u}$  is a function of  $\mathbf{x}$  [136]. Whenever the controller communicates with the plant, the control law resets as

$$\mathbf{u}_+ \mapsto K\mathbf{x} + \boldsymbol{\eta}, \quad K \in \mathbb{R}^{m \times n}. \quad (5.4)$$

Here  $K$  is the matrix of controller gains and  $\boldsymbol{\eta}$  denotes the noise in the control law. We assume that  $\boldsymbol{\eta}$  is a vector of zero-mean noise terms and  $\langle \boldsymbol{\eta}\boldsymbol{\eta}^\top \rangle = \Sigma \in \mathbb{R}^{m \times m}$ , where  $\Sigma$  is a diagonal matrix. In between the connections, the control law remains constant.

## 5.2 Control Design from Steady-state Moments

Motivated by control designs for such system [137–139], we define the main goal as obtaining a control law that derive the system to the desired mean level while minimizing the variance of system. We can set up this problem as an optimization problem

$$\text{Minimize}_K \left( \sum_{i=1}^n \lambda_i \left( \overline{\langle \mathbf{x}_i^2 \rangle} - \overline{\langle \mathbf{x}_i \rangle}^2 \right) \right), \quad (5.5a)$$

$$\text{Subject to } \overline{\langle \mathbf{x} \rangle} = \text{Constant}, \quad (5.5b)$$

where  $\lambda_i$  are weights, and  $\mathbf{x}_i$  denotes the  $i^{\text{th}}$  state. The controller matrix  $K$  has  $n^2$  elements and the number of constraints (number of mean values) is  $n$ . Hence there will be  $n^2 - n$  degree of freedom in the system. Solving such optimization problem is generally convoluted specifically if  $n$  is large.

Moreover, due to physical constraints, this is possible that degree of freedom in controller is zero. For example, consider a scalar system, for this system one can design the controller to reach to a specific mean, but then controller is unable of changing variance to a desired level because the degree of freedom is zero. However, such physical constraints can also be helpful, i.e. assume a controller which have  $n + 1$  non-zero elements in the matrix  $K$ . Then this is straightforward to solve (5.5), because we only will have one degree of freedom. Regardless of the complexity level, in order to solve (5.5), we need to derive exact solutions of steady-state mean and variance.

### 5.2.1 The Steady-state Mean of $\mathbf{x}$

We first introduce a new vector that contains both the states and the controller  $\mathbf{y} \equiv [\mathbf{x}^\top \mathbf{u}^\top]^\top \in \mathbb{R}^{(n+m) \times 1}$ . Dynamics of this vector is obtained from (5.1) as

$$d\mathbf{y} = (\hat{a}_y + A_y \mathbf{y}(t)) dt + (E_y + D_y \mathbf{y}(t) \mathbf{1}_{n+m}) d\mathbf{w}_{n+m}, \quad (5.6)$$

where

$$\hat{a}_y \equiv \begin{bmatrix} \hat{a} \\ \dots \\ 0 \end{bmatrix}, \quad A_y \equiv \begin{bmatrix} A & B \\ \dots & \dots \\ 0 & 0 \end{bmatrix}, \quad E_y \equiv \begin{bmatrix} E & 0 \\ \dots & \dots \\ 0 & 0 \end{bmatrix}, \quad D_y \equiv \begin{bmatrix} D & 0 \\ \dots & \dots \\ 0 & 0 \end{bmatrix}, \quad d\mathbf{w}_{n+m} \equiv \begin{bmatrix} d\mathbf{w}_n \\ \dots \\ 0 \end{bmatrix}. \quad (5.7)$$

Further, any time that the controller transmits a new control law, the states of  $\mathbf{y}$  change as

$$\langle \mathbf{y}_+ \rangle = J_y \mathbf{y}, \quad J_y \equiv \left[ \begin{array}{c|c} I_n & 0 \\ \hline K & 0 \end{array} \right], \quad (5.8)$$

where we used (5.4) and the fact that states of the system will not change instantaneously during the transmissions ( $\langle \mathbf{x}_+(t_s) \rangle = \mathbf{x}(t_s)$ ). By this definition, this system falls into the category of stochastic hybrid systems that we introduced in the earlier chapters, and we can generalize our results to this system.

**Theorem 4** *The steady-state mean of vector  $\mathbf{y}$  is*

$$\begin{aligned} \overline{\langle \mathbf{y} \rangle} &= \langle e^{A_y \tau} \rangle (I_{n+m} - J_y \langle e^{A_y \tau_s} \rangle)^{-1} J_y \left\langle e^{A_y \tau_s} \int_0^{\tau_s} e^{-A_y r} \hat{a}_y dr \right\rangle \\ &+ \left\langle e^{-A_y \tau} \int_0^{\tau} e^{-A_y r} \hat{a}_y dr \right\rangle, \end{aligned} \quad (5.9)$$

*if and only if the expected value  $\langle e^{A_y \tau_s} \rangle$  exists and all the eigenvalues of matrix  $J_y \langle e^{A_y \tau_s} \rangle$  are inside the unit circle.*

In the next part, we provide a novel approach for deriving the second-order moments of system.

### 5.2.2 The Second-order Moments of $\mathbf{x}$

Similar to previous chapters, our strategy is to transform the second-order moments to a similar form as in (5.6)-(5.8). To do so, we introduce a new vector

$$\boldsymbol{\mu} \equiv [\mathbf{x}^\top \quad \mathbf{u}^\top \quad \text{vec}(\mathbf{x}\mathbf{x}^\top)^\top \quad \text{vec}(\mathbf{x}\mathbf{u}^\top)^\top \quad \text{vec}(\mathbf{u}\mathbf{x}^\top)^\top \quad \text{vec}(\mathbf{u}\mathbf{u}^\top)^\top]. \quad (5.10)$$

Dynamics of  $\boldsymbol{\mu}$  between the events is given by

$$d\boldsymbol{\mu} = (\hat{a}_\mu + A_\mu \boldsymbol{\mu}(t))dt + (E_\mu + D_\mu \boldsymbol{\mu}(t) \mathbf{1}_l) d\mathbf{w}_l, \quad (5.11)$$

where  $l = n^2 + m^2 + 2mn + m + n$ . Further

$$\hat{a}_\mu \equiv \left[ \begin{array}{c|c|c|c|c|c} \hat{a} & 0 & \text{vec}(EE^\top) & 0 & 0 & 0 \end{array} \right], \quad (5.12)$$

and

$$A_\mu \equiv \begin{bmatrix} A & B & 0 & 0 & 0 & 0 \\ 0 & 0 & 0 & 0 & 0 & 0 \\ M_1 & 0 & M_2 & M_3 & M_4 & 0 \\ 0 & I_m \otimes \hat{a} & 0 & I_m \otimes A & 0 & I_m \otimes B \\ 0 & \hat{a} \otimes I_m & 0 & 0 & A \otimes I_m & B \otimes I_m \\ 0 & 0 & 0 & 0 & 0 & 0 \end{bmatrix}, \quad (5.13)$$

$$M_1 \equiv I_n \otimes \hat{a} + \hat{a} \otimes I_n + D \otimes E \mathbf{1}_n^\top + E^\top \mathbf{1}_n^\top \otimes D,$$

$$M_2 \equiv I_n \otimes A + A \otimes I_n + nD \otimes D, \quad M_3 \equiv I_n \otimes B + B \otimes I_n.$$

We did not give definitions of  $E_\mu$  and  $D_\mu$  because as we will see in Theorem 2, they have no role in defining the mean of vector  $\boldsymbol{\mu}$ . Finally, in the time of transmission, the states of vector  $\boldsymbol{\mu}(\mathbf{t}_s)$  change to  $\boldsymbol{\mu}(\mathbf{t}_s^+)$ , where

$$\langle \boldsymbol{\mu}_+(\mathbf{t}_s) \rangle = J_\mu \boldsymbol{\mu}(\mathbf{t}_s) + R_\mu, \quad J_\mu \equiv \begin{bmatrix} I_n & 0 & 0 & 0 & 0 & 0 \\ K & 0 & 0 & 0 & 0 & 0 \\ 0 & 0 & I_{n+m} & 0 & 0 & 0 \\ 0 & 0 & K \otimes I_n & 0 & 0 & 0 \\ 0 & 0 & I_n \otimes K & 0 & 0 & 0 \\ 0 & 0 & K \otimes K & 0 & 0 & 0 \end{bmatrix}, \quad R_\mu \equiv \begin{bmatrix} \hat{a} \\ 0 \\ 0 \\ 0 \\ 0 \\ \text{vec}(\Sigma) \end{bmatrix}. \quad (5.14a)$$

Deterministic dynamics (7.24) and stochastic resets (5.14) are similar to (5.6) and (5.8). Hence with a similar analysis as in previous part, we have the following theorem.

**Theorem 5** *Suppose that a system satisfies the hypothesis of Theorem 1. Then the steady-state mean of vector  $\boldsymbol{\mu}$  is*

$$\begin{aligned} \overline{\langle \boldsymbol{\mu} \rangle} &= \langle e^{A_\mu \tau} \rangle (I_l - J_\mu \langle e^{A_\mu \tau_s} \rangle)^{-1} \left( J_\mu \left\langle e^{A_\mu \tau_s} \int_0^{\tau_s} e^{-A_\mu r} \hat{a}_\mu dr \right\rangle + R_\mu \right) \\ &+ \left\langle e^{-A_\mu \tau} \int_0^\tau e^{-A_\mu r} \hat{a}_\mu dr \right\rangle, \end{aligned} \quad (5.15)$$

*if and only if all the eigenvalues of the matrix  $J_\mu \langle e^{A_\mu \tau_s} \rangle$  are inside the unit circle.*

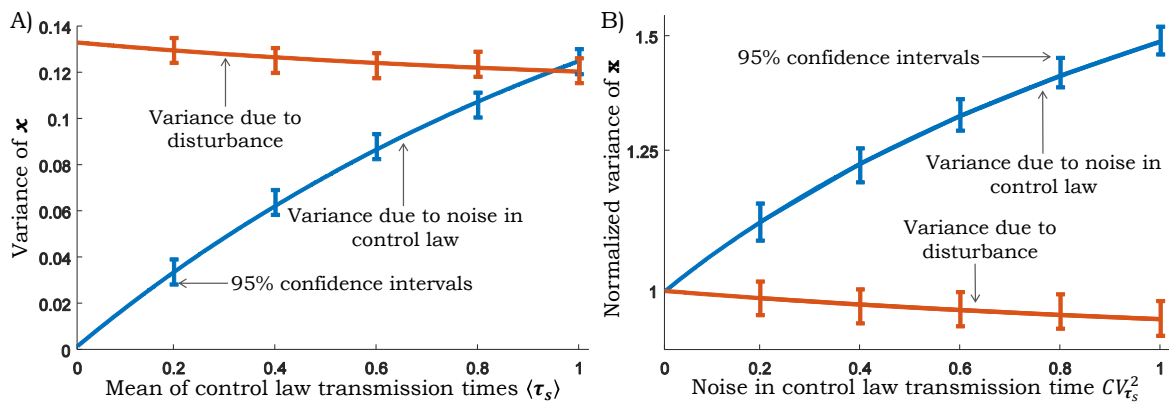


**Figure 5.2: Making transmission of the control law more random can reduce variance of  $\mathbf{x}$ .** A) Surprisingly, by increasing the mean time intervals between the transmissions, the noise in  $\mathbf{x}$  contributed from disturbance can reduce. On the other hand, increasing  $\tau_s$  will increase the noise contributed from  $\sigma$ . This is because the added noise by controller remains in the system for a longer time before getting corrected by a new control law. B) Noisy transmission times also can reduce the variance contributed from disturbance. Hence, when the noise added by controller is small, randomly distributed times can be used to reduce variance in  $\mathbf{x}$ . For this plot, we used gamma distributed time intervals and variance of  $\mathbf{x}$  is normalized to its value at the beginning of the plot. The noise in transmission time intervals is quantified by coefficient of variation squared  $CV_{\tau_s}^2$ . The parameters are selected as  $\hat{a} = 1$ ,  $A = -1$ ,  $E = 0.45$ ,  $B = 0.5$ ,  $K = 0.5$ , and  $\sigma = 1$ . Finally, 95% confidence intervals are obtained by running 1000 numerical simulations.

Mean of  $\boldsymbol{\mu}$  contains all the second-order moments of vector  $\mathbf{x}$ . Finally, by having closed form expression for the mean and the second-order moments, we can design the matrix of controller gains  $K$  to reach to the desired mean and to minimize the variance.

### 5.3 Illustrative Examples

We illustrate our results in two examples. While the first example is a general system that can be used to model any engineering or natural system, the second one is motivated from systems biology.

### 5.3.1 Example 1

Suppose that the state of a system  $\mathbf{x} \in \mathbb{R}$  is governed via a one dimensional SDE as

$$d\mathbf{x} = (\hat{a} + A\mathbf{x}(t) + B\mathbf{u}(t)) dt + E d\mathbf{w}, \quad (5.16)$$

and the control law in the time of resets is

$$\mathbf{u}(t_s^+) \mapsto K\mathbf{x}(t_s^-) + \boldsymbol{\eta}, \quad (5.17)$$

where  $\boldsymbol{\eta}$  is a zero mean noise term with variance  $\sigma^2$ . Based on (5.6), the vector  $\mathbf{y} = [\mathbf{x} \ \mathbf{u}]^\top$  is governed via

$$d\mathbf{y} = (\hat{a}_y + A_y\mathbf{y}(t)) dt + E_y d\mathbf{w}_2, \quad (5.18)$$

where

$$\hat{a}_y = \begin{bmatrix} \hat{a} \\ 0 \end{bmatrix}, \quad A_y = \begin{bmatrix} A & B \\ 0 & 0 \end{bmatrix}, \quad E_y = \begin{bmatrix} E & 0 \\ 0 & 0 \end{bmatrix}. \quad (5.19)$$

Further, at the time of a transmission, the states reset as (5.8) with  $J_y = \begin{bmatrix} 1 & 0 \\ K & 0 \end{bmatrix}$ .

Hence based on Theorem 1, the mean of  $\mathbf{x}$  in steady-state is

$$\overline{\langle \mathbf{x} \rangle} = -\frac{\hat{a}}{A + BK}. \quad (5.20)$$

Interestingly, the mean of  $\mathbf{x}$  in steady-state is independent of  $\tau_s$ . Hence, as far as system is stable, having rare connections between the controller and the plant does not change the mean of  $\mathbf{x}$ .

#### 5.3.1.1 The Second-order Moment of the System

In order to derive the second-order moments, we define

$$\boldsymbol{\mu} = [\mathbf{x} \ \mathbf{u} \ \mathbf{x}^2 \ \mathbf{x}\mathbf{u} \ \mathbf{u}^2]. \quad (5.21)$$

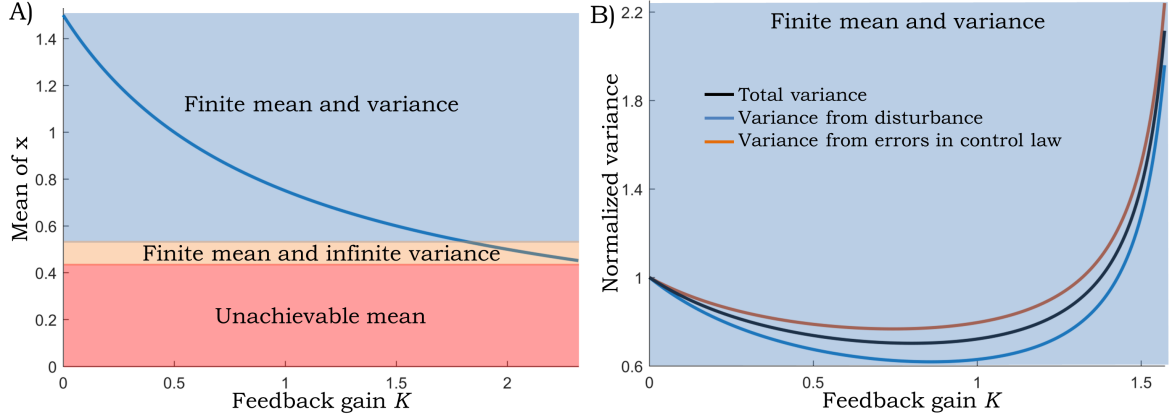


**Figure 5.3:** The control gain can be designed to obtain any desired mean as long as eigenvalues remain within the unit circle. A) By increasing the control gain, the magnitude of eigenvalues increases resulting in the system to move toward instability. The second eigenvalue becomes greater than 1 first. This means that there exists a control gain that the mean is finite, but the variance is infinite. When the other eigenvalue becomes greater than 1 the system becomes unstable. Hence, there exists certain values of mean that we never can reach. B) The variance is finite only when absolute value of both eigenvalues are less than 1. The variance is normalized to its value when  $K = 0$ . For intermediate values of  $K$ , variance is less than the time in which there exists no control ( $K = 0$ ). In this figure, time intervals in between the resets are gamma distributed with  $\langle \tau_s \rangle = 1 \text{ min}$  and  $CV_T^2 = 0.2$ . The rest of parameters are selected as  $\hat{a} = 1.5$ ,  $A = -1$ , and  $B = -1$ .

By this selection,  $\hat{a}_\mu$  and  $A_\mu$  in (5.12)-(5.13) are defined as

$$a_\mu = \begin{bmatrix} \hat{a} \\ 0 \\ E^2 \\ 0 \\ 0 \end{bmatrix}, \quad A_\mu = \begin{bmatrix} A & B & 0 & 0 & 0 \\ 0 & 0 & 0 & 0 & 0 \\ 2\hat{a} & 0 & 2A & 0 & 0 \\ 2B & \hat{a} & 0 & A & B \\ 0 & 0 & 0 & 0 & 0 \end{bmatrix}. \quad (5.22)$$

Further, anytime that connection occurs the states of system reset to

$$\langle \boldsymbol{\mu}_+(\mathbf{t}_s) \rangle = J_\mu \boldsymbol{\mu}(\mathbf{t}_s) + R_\mu, \quad J_\mu = \begin{bmatrix} 1 & 0 & 0 & 0 & 0 \\ K & 0 & 0 & 0 & 0 \\ 0 & 0 & 1 & 0 & 0 \\ 0 & 0 & K & 0 & 0 \\ 0 & 0 & K^2 & 0 & 0 \end{bmatrix}, \quad R_\mu = \begin{bmatrix} 0 \\ 0 \\ 0 \\ 0 \\ \sigma^2 \end{bmatrix}. \quad (5.23)$$

By using these matrices, the non-zero eigenvalues of  $J_\mu \langle e^{A\mu\tau_s} \rangle$  are

$$\text{spec}(J_\mu \langle e^{A\mu\tau_s} \rangle) = \left[ \frac{A \langle e^{A\tau_s} \rangle + BK \langle e^{A\tau_s} \rangle - BK}{A}, \right. \\ \left. \frac{A \langle e^{2A\tau_s} \rangle (A + BK)^2 + BK(BK - 2A \langle e^{A\tau_s} \rangle (A + BK))}{A^2} \right]. \quad (5.24)$$

If these eigenvalues are inside the unit circle then the mean and the variance of  $\mathbf{x}$  are given by (5.20) and

$$\text{var}(\mathbf{x}) = \overline{\langle \mathbf{x}^2 \rangle} - \overline{\langle \mathbf{x} \rangle}^2 = \sigma^2 \frac{\overbrace{B^2(A \langle \tau_s \rangle - \langle e^{A\tau_s} \rangle + 1) (A^2 \langle e^{A\tau_s} \rangle + 1) \langle \tau_s \rangle + 2BK \langle e^{A\tau_s} \rangle (A \langle \tau_s \rangle - 1) + 1)}^{\text{Fluctuations contributed from noise in control law}}}{A^3 \langle \tau_s \rangle^2 (A + BK)(A \langle e^{A\tau_s} \rangle + 1) + BK(\langle e^{A\tau_s} \rangle - 1)} + \\ \frac{\overbrace{E^2 (-A^4 (\langle e^{A\tau_s} \rangle + 1) \langle \tau_s \rangle^2 + A^2 BK \langle \tau_s \rangle (-2A \langle e^{A\tau_s} \rangle \langle \tau_s \rangle + \langle e^{2A\tau_s} \rangle - 1) + 2B^2 K^2 (-A \langle \tau_s \rangle + \langle e^{A\tau_s} \rangle - 1) (\langle e^{A\tau_s} \rangle (A \langle \tau_s \rangle - 1)))}^{\text{Fluctuations contributed from disturbance}}}{2A^3 \langle \tau_s \rangle^2 (A + BK)(A \langle e^{A\tau_s} \rangle + 1) + BK(\langle e^{A\tau_s} \rangle - 1)}. \quad (5.25)$$

Note that the variance can be written as the sum of two terms: 1) Variance contributed from the noise in control law ( $\sigma$ ). 2) Variance contributed from the disturbance ( $E$ ). Timing of transmissions affects both of these terms.

Interestingly, in some parameter regimes rare control of the system reduces the variance. For example, suppose that disturbance is large ( $E$  is large) and the fluctuations due to disturbance are dominant. In this limit, rare control of the system can reduce the noise as shown in Fig. 5.2. Surprisingly, the variance of  $\mathbf{x}$  in this limit is less than

$$-\frac{E^2}{A + BK} \quad (5.26)$$

which is the variance for the case in which the controller and the plant are connected all the time. This means that rare transmissions of the control law not only saves resources, but also reduces the variance in  $\mathbf{x}$ .

Moreover, in Fig. 5.2 we also illustrated the effect of noise in transmission times on variance of  $\mathbf{x}$ . As expected, increasing the noise in the timing of transmissions increases fluctuations contributed from noise in the control law (raised from  $\sigma$ ). However, again these noisy transmission times can be used to reduce the effect of fluctuations contributed from disturbance. It is important to point that the aforementioned results just occurs in specific parameter regimes. In most of the cases, by increasing the mean time intervals or randomness in the timing of transmissions, the variance of  $\mathbf{x}$  increases.

### 5.3.1.2 Control Design

For this system, the non-zero eigenvalues of the matrix  $J_y \langle e^{A\tau_s} \rangle$  are given by (5.24). Hence in order to have finite mean and variance of  $\mathbf{x}$ , it is necessary and sufficient that

$$\left| \frac{A \langle e^{A\tau_s} \rangle + BK \langle e^{A\tau_s} \rangle - BK}{A} \right| < 1, \quad (5.27a)$$

$$\left| \frac{A \langle e^{2A\tau_s} \rangle (A + BK)^2}{A^2} + \frac{BK(BK - 2A \langle e^{A\tau_s} \rangle (A + BK))}{A^2} \right| < 1, \quad (5.27b)$$

where  $||$  denotes the magnitude. In addition, we can design the controller for having the desired mean of state by choosing  $K$  as

$$K = -\frac{\hat{a} + A \overline{\langle \mathbf{x} \rangle}_{\text{desired}}}{B \overline{\langle \mathbf{x} \rangle}_{\text{desired}}}. \quad (5.28)$$

However, satisfying (5.27) means that reaching to a desired  $\mathbf{x}$  may not be possible. The interplay between the control gain and the stability of mean and variance of is shown in Fig. 5.3.

### 5.3.2 Example II

Consider a system with two states  $\mathbf{x} = [\mathbf{x}_1 \ \mathbf{x}_2]^\top$ , in which its dynamics is given by

$$d\mathbf{x} = (\hat{a} + A\mathbf{x}(t) + B\mathbf{u}) + E d\mathbf{w}_2, \quad (5.29)$$

where

$$\hat{a} = \begin{bmatrix} a_1 \\ 0 \end{bmatrix}, \quad A = \begin{bmatrix} -\gamma_1 & 0 \\ a_2 & -\gamma_2 \end{bmatrix}, \quad B = \begin{bmatrix} 1 & 0 \\ 0 & 1 \end{bmatrix}, \quad C = \begin{bmatrix} \sqrt{a_1} & 0 \\ 0 & 0 \end{bmatrix}. \quad (5.30)$$

This example is motivated from biochemical reactors, i.e., assume that  $\mathbf{x}_1$  and  $\mathbf{x}_2$  are levels of species 1 and 2, respectively. Here we assumed that molecules of species 1 are produced at a constant rate  $a_1$ . Later molecules of species 2 are produced from species 1, i.e., its production rate is  $a_2\mathbf{x}_1$ . We assumed that count level of species 2 is considerably higher than species 1. Hence the production of species  $\mathbf{x}_1$  is noisy and we used a Langevin approximation of this reaction [140]. Finally, molecules of  $\mathbf{x}_1$  and  $\mathbf{x}_2$  degrade with rates  $\gamma_1$  and  $\gamma_2$ , respectively.

This biochemical reactor is controlled through a network. Any time that transmission happens, the control law changes as

$$\langle \mathbf{u}_+(\mathbf{t}_s) \rangle = K\mathbf{x}(\mathbf{t}_s), \quad K = \begin{bmatrix} -k_1 & -k_2 \\ 0 & -k_3 \end{bmatrix}. \quad (5.31)$$

This reactor is controlled in two different ways: 1- A UV radiation that increases death rate of molecules [141, 142]. This control law is implemented by manipulating  $k_1$  and  $k_3$ . 2- The resources need to produce species 1 is controlled based on levels of species 2 through the parameter  $k_2$ . Such negative feedback loops are common motifs in biological systems [72, 143, 144].

By introducing  $\mathbf{y} = [\mathbf{x}^\top \mathbf{u}^\top]^\top \in \mathbb{R}^{4 \times 1}$ , this system can be written in the form of (5.6). Hence the methods explained in this paper can be applied, which results in

$$\overline{\langle \mathbf{x}_1 \rangle} = \frac{a_1(\gamma_2 + k_3)}{a_2k_2 + \gamma_1(\gamma_2 + k_3) + \gamma_2k_1 + k_1k_3}, \quad (5.32a)$$

$$\overline{\langle \mathbf{x}_2 \rangle} = \frac{\gamma_2 + k_3}{a_2} \overline{\langle \mathbf{x}_1 \rangle}. \quad (5.32b)$$

Similar to (5.20), the mean values are independent of statistical characteristics of  $\boldsymbol{\tau}_s$ . We can select  $k_1$ ,  $k_2$ , and  $k_3$  to have any desired mean level. Moreover, we have one degree of freedom (two means and three control gains) hence we can use this degree of freedom to minimize variance as in (5.5). The overall results for the mean and the variance of system as functions of feedback gains are similar to that in Fig. 5.3.

## 5.4 Conclusion

We studied statistical moments of a control system in which the controller and the plant are communicating in random times. We derived the exact solutions of mean and second-order moments as well as the stability conditions. We showed that these results can be used to design controllers for keeping the mean of states on a desired level. We demonstrate our method on different examples. Surprisingly, the mean is independent of transmission times statistical moments. In addition, we observed that under specific parameter regimes, rare transmissions of the control law not only save resources of the system but also reduce fluctuations. Further, we showed that noisy transmission times can reduce the fluctuations in  $\boldsymbol{x}$ .

This is important to note that the current framework only is applicable to a subclass of systems. In order to include all classes of such control loops (e.g. self-driven) we need to consider the hazard rate in equation (4.1) to be a function of  $\boldsymbol{x}$  as well. The future work will design the control law for such a case. Moreover, we considered a general form for the noise terms added to the plant in the time of applying control. This noise can be quantified with respect to its source [145–147]. Another avenue of research will be modeling this noise term mechanistically.

## Chapter 6

### STOCHASTIC HYBRID SYSTEMS WITH FAMILIES OF RANDOM DISCRETE EVENTS

We consider a class of TTSHS where the state evolves according to a linear dynamical system. This continuous time evolution is interspersed by discrete events that occur at random times and change (reset) the state based on a linear affine map. In particular, we consider two families of mutually independent discrete events, with the first family of resets occurring at exponentially-distributed times. The second family of resets is generally-distributed, in the sense that, the time intervals between successive events are independent and identically distributed random variables that follow an arbitrary continuous positively-valued probability density function. For this class of stochastic systems, we provide explicit conditions that lead to finite stationary moments, and the corresponding exact closed-form moment formulas. These results are illustrated on protein concentration. In summary, this chapter expands the class of stochastic hybrid systems for which statistical moments can be derived exactly without any approximations, and these results have applications for studying random phenomena in diverse areas.

#### 6.1 Model Formulation

The class of TTSHS under consideration have the following ingredients:

1. **Continuous dynamics:** The states of the system  $\mathbf{x} \in \mathbb{R}^{n \times 1}$  are governed by time-invariant ordinary differential equations

$$\frac{d\mathbf{x}(t)}{dt} = \hat{a} + A\mathbf{x}(t), \quad (6.1)$$

where vector  $\hat{a} \in \mathbb{R}^{n \times 1}$  and matrix  $A \in \mathbb{R}^{n \times n}$  are constant.

2. **Exponentially-distributed resets:** The first family of resets occur at exponentially distributed time intervals, i.e., Poisson arrival of events. Let the mean time interval in between these resets be denoted by  $1/h_1$  where  $h_1$  is a constant. Then, the probability of an event occurring in the next infinitesimal time interval  $(t, t + dt]$  is  $h_1 dt$ . Whenever these events occur the state is reset based on a linear affine map

$$\mathbf{x} \mapsto J_1 \mathbf{x} + \hat{r}_1, \quad (6.2)$$

where  $J_1 \in \mathbb{R}^{n \times n}$  and  $\hat{r}_1 \in \mathbb{R}^{n \times 1}$  are a constant matrix and vector, respectively.

3. **Generally-distributed resets:** The second family of resets occur in non exponentially distributed time intervals. Events occur at times  $\mathbf{t}_s$ ,  $s \in \{1, 2, \dots\}$ , and the time intervals

$$\boldsymbol{\tau}_s \equiv \mathbf{t}_s - \mathbf{t}_{s-1} \quad (6.3)$$

are independent and identically distributed (iid) random variables that follow an arbitrary continuous positively-valued probability density function  $f$ . Whenever the events occur, the state is reset as

$$\mathbf{x} \mapsto \mathbf{x}_{2+}. \quad (6.4)$$

We allow  $\mathbf{x}_{2+}$  to be a random variable, whose average value is related to its value just before the event as

$$\langle \mathbf{x}_{2+} \rangle = J_2 \mathbf{x} + \hat{r}_2. \quad (6.5)$$

Here  $\langle \cdot \rangle$  denotes the expected value operator,  $J_2 \in \mathbb{R}^{n \times n}$  and  $\hat{r}_2 \in \mathbb{R}^{n \times 1}$  are a constant matrix and vector, respectively. Furthermore, the covariance matrix of  $\mathbf{x}_{2+}$  is defined by

$$\langle \mathbf{x}_{2+} \mathbf{x}_{2+}^\top \rangle - \langle \mathbf{x}_{2+} \rangle \langle \mathbf{x}_{2+} \rangle^\top = Q_2 \mathbf{x} \mathbf{x}^\top Q_2^\top + B_2 \mathbf{x} \hat{c}_2^\top + \hat{c}_2 \mathbf{x}^\top B_2^\top + D_2. \quad (6.6)$$

Here  $Q_2 \in \mathbb{R}^{n \times n}$ ,  $D_2 \in \mathbb{R}^{n \times n}$ ,  $\hat{c}_2 \in \mathbb{R}^{n \times 1}$  are constant matrices. Moreover  $D_2 \in \mathbb{R}^{n \times n}$  is a constant symmetric positive semidefinite matrix.

Having mathematically defined the system, we next provide our main results on the statistical moments of  $\mathbf{x}(t)$ .

## 6.2 Steady-state Mean Level

To present the steady-state mean of  $\mathbf{x}$ , we define the following matrix and vector to simplify notation

$$A_{\bar{x}} \equiv A + h_1(J_1 - I_n), \quad \hat{a}_{\bar{x}} \equiv \hat{a} + \hat{r}_1. \quad (6.7)$$

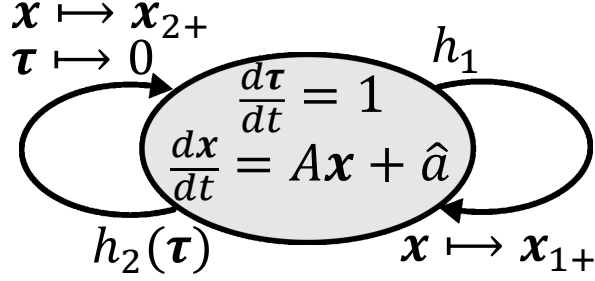


**Figure 6.1:** Schematic of a TTSHS with linear continuous dynamics and two families of random resets. The two families of resets occurs at random times and change the state based on the linear affine maps (6.2) and (6.4). For the first reset, events happen at exponentially-distributed time intervals, while for the second reset, time intervals are generally-distributed and drawn from an arbitrary probability distribution function. The timing of the latter family of resets is regulated by a timer  $\tau$  that measures the time since the last event, and the next event occurs at a hazard rate  $h_2(\tau)$ . In between events, the state evolve according to a linear time-invariant dynamical system.

**Theorem 6** Consider the TTSHS given by the linear continuous dynamics (6.1), and the two families of stochastic events defined in (6.2)-(6.6). For this system, the steady-state mean is

$$\begin{aligned} \overline{\langle \mathbf{x} \rangle} \equiv \lim_{t \rightarrow \infty} \langle \mathbf{x}(t) \rangle &= \left\langle e^{A_{\bar{x}}\tau} \int_0^\tau e^{-A_{\bar{x}}r} \hat{a}_{\bar{x}} dr \right\rangle \\ &+ \left\langle e^{A_{\bar{x}}\tau} \left( I_n - \langle J_2 e^{A_{\bar{x}}\tau_s} \rangle \right)^{-1} \left( \hat{r}_2 + J_2 \left\langle e^{A_{\bar{x}}\tau_s} \int_0^{\tau_s} e^{-A_{\bar{x}}r} \hat{a}_{\bar{x}} dr \right\rangle \right) \right\rangle, \end{aligned} \quad (6.8)$$

if and only if all the eigenvalues of  $J_2 \langle e^{A_{\bar{x}}\tau_s} \rangle$  are inside the unit circle.

**Proof:** The sketch of the proof is the following: we start by finding the moment dynamics of the system in between generally distributed events. Next, we solve moment dynamics for initial condition corresponding to  $\tau = 0$  (value of the states right after a generally distributed reset). Finally, taking mean over all  $\tau$  results in the steady-state mean of  $\mathbf{x}$ .

Based on forward Kolmogorov equation, we have the following for joint probability distribution of timer and the states  $p(\tau, x)$  in steady state

$$\begin{aligned} \frac{\partial p(\tau, x)}{\partial \tau} + \frac{\partial}{\partial x} ((\hat{a} + Ax)p(\tau, x)) = \\ + h_1 p(\tau, J_1^{-1}(x - \hat{r}_1)) - h_1 p(\tau, x) - h_2(\tau) p(\tau, x), \quad \tau > 0, \end{aligned} \quad (6.9)$$

where  $x$  is the vector of dummy variables for  $\mathbf{x}$ . Further the operator  $\frac{\partial}{\partial x}$  is defined as

$$\frac{\partial}{\partial x} = \left[ \frac{\partial}{\partial x_1}, \frac{\partial}{\partial x_2}, \dots, \frac{\partial}{\partial x_n} \right], \quad (6.10)$$

which is a vector of partial derivative operators.

By having the joint probability distribution, we define conditional mean  $\overline{\langle \mathbf{x} | \tau \rangle}$  as

$$\overline{\langle \mathbf{x} | \tau \rangle} \equiv \overline{\langle \mathbf{x} | \tau = \tau \rangle} = \frac{1}{p(\tau)} \int_0^{+\infty} xp(\tau, x) dx. \quad (6.11)$$

Taking derivative with respect to  $\tau$  from (6.11) results in

$$\frac{\partial \overline{\langle \mathbf{x} | \tau \rangle}}{\partial \tau} = - \frac{\frac{\partial p(\tau)}{\partial \tau}}{p^2(\tau)} \int_0^{+\infty} xp(\tau, x) dx + \frac{1}{p(\tau)} \int_0^{+\infty} x \frac{\partial p(\tau, x)}{\partial \tau} dx. \quad (6.12)$$

In order to calculate  $\frac{\partial \overline{\langle \mathbf{x} | \tau \rangle}}{\partial \tau}$  we need the expression of  $\frac{\partial p(\tau, x)}{\partial \tau}$  and  $\frac{\partial p(\tau)}{\partial \tau}$ . Substituting these expressions from (6.9) and (4.3) in (6.12) and after some algebraic steps we have

$$\frac{\partial \overline{\langle \mathbf{x} | \tau \rangle}}{\partial \tau} = (\hat{a} + \hat{r}_1) + (A + h_1(J_1 - I_n)) \overline{\langle \mathbf{x} | \tau \rangle}. \quad (6.13)$$

Thus the conditional mean can be derived as

$$\begin{aligned} \overline{\langle \mathbf{x} | \tau = \tau \rangle} &= e^{(A+h_1(J_1-I_n))\tau} \overline{\langle \mathbf{x}_+(\mathbf{t}_s) \rangle} \\ &+ e^{(A+h_1(J_1-I_n))\tau} \int_0^\tau e^{-(A+h_1(J_1-I_n))r} (\hat{a} + \hat{r}_1) dr. \end{aligned} \quad (6.14)$$

In order to calculate  $\overline{\langle \mathbf{x}_+(\mathbf{t}_s) \rangle}$  we use equation (6.5)

$$\begin{aligned} \overline{\langle \mathbf{x}(\mathbf{t}_s) \rangle} &= \left( I_n - J_2 \left\langle e^{(A+h_1(J_1-I_n))\tau_s} \right\rangle \right)^{-1} \times \\ &\left( \hat{r}_2 + J_2 \left\langle e^{(A+h_1(J_1-I_n))\tau_s} \int_0^{\tau_s} e^{-(A+h_1(J_1-I_n))r} (\hat{a} + \hat{r}_1) dr \right\rangle \right). \end{aligned} \quad (6.15)$$

using equation (4.3) to uncondition (6.14) with respect to  $\tau$  results in (6.8). ■

### 6.3 Steady-state Second-order Moments

To compute the second-order moments, we define a new vector  $\boldsymbol{\mu} \equiv \left[ \mathbf{x}^\top \quad \text{vec}(\mathbf{x}\mathbf{x}^\top)^\top \right]^\top \in \mathbb{R}^{(n+n^2) \times 1}$ , whose dynamics in between events is governed via

$$\frac{d\boldsymbol{\mu}}{dt} = \hat{a}_\mu + A_\mu \boldsymbol{\mu}, \quad (6.16)$$

where

$$A_\mu \equiv \left[ \begin{array}{c|c} A & 0 \\ \hline I_n \otimes \hat{a} + \hat{a} \otimes I_n & I_n \otimes A + A \otimes I_n \end{array} \right], a_\mu \equiv \left[ \begin{array}{c} \hat{a} \\ 0 \end{array} \right]. \quad (6.17)$$

Any time that an exponentially distributed event occurs, vector  $\boldsymbol{\mu}$  resets as

$$\boldsymbol{\mu} \mapsto J_{\mu 1} \boldsymbol{\mu} + \hat{r}_{\mu 1}, \quad J_{\mu 1} \equiv \left[ \begin{array}{c|c} J_1 & 0 \\ \hline 0 & J_1 \otimes J_1 \end{array} \right], \quad \hat{r}_{\mu 1} \equiv \left[ \begin{array}{c} \hat{r}_1 \\ \text{vec}(\hat{r}_1 \hat{r}_1^\top) \end{array} \right]. \quad (6.18)$$

Moreover, any time that a generally-distributed event occurs,  $\boldsymbol{\mu}$  resets as

$$\boldsymbol{\mu} \mapsto \boldsymbol{\mu}_{2+}. \quad (6.19)$$

Based on (6.6)

$$\langle \mathbf{x}_{2+} \mathbf{x}_{2+}^\top \rangle = \langle \mathbf{x}_{2+} \rangle \langle \mathbf{x}_{2+} \rangle^\top + Q_2 \mathbf{x} \mathbf{x}^\top Q_2^\top + B_2 \mathbf{x} \hat{c}_2^\top + \hat{c}_2 \mathbf{x}^\top B_2^\top + D_2. \quad (6.20)$$

Further from (6.5),  $\langle \mathbf{x}_{2+} \rangle \langle \mathbf{x}_{2+} \rangle^\top$  can be written as

$$\langle \mathbf{x}_{2+} \rangle \langle \mathbf{x}_{2+} \rangle^\top = J_2 \mathbf{x} \mathbf{x}^\top J_2^\top + J_2 \mathbf{x} \hat{r}_2^\top + \hat{r}_2 \mathbf{x}^\top J_2^\top + \hat{r}_2 \hat{r}_2^\top. \quad (6.21)$$

By combining these two equations and using (4.33),  $\langle \boldsymbol{\mu}_{2+} \rangle$  is given by

$$\langle \boldsymbol{\mu}_{2+} \rangle = J_{\mu 2} \boldsymbol{\mu} + \hat{r}_{\mu 2}, \quad (6.22)$$

where

$$J_{\mu 2} \equiv \left[ \begin{array}{c|c} J_2 & 0 \\ \hline B_2 \otimes \hat{c}_2 + J_2 \otimes \hat{r}_2 & J_2 \otimes J_2 + Q_2 \otimes Q_2 \\ + \hat{c}_2 \otimes B_2 + \hat{r}_2 \otimes J_2 & \end{array} \right], \hat{r}_{\mu 2} \equiv \left[ \begin{array}{c} \hat{r}_2 \\ \text{vec}(D_2 + \hat{r}_2 \hat{r}_2^\top) \end{array} \right]. \quad (6.23)$$

Deterministic dynamics (6.16), and stochastic resets (6.18) and (6.22) are similar to (6.1), (6.2) and (6.5). Hence with a similar analysis as in Theorem 4, the following theorem provides the necessary and sufficient conditions for having finite second-order moments of  $\mathbf{x}$ . As done prior to Theorem 4, we define

$$A_{\bar{\mu}} \equiv A_{\mu} + h_1(J_{\mu 1} - I_{n^2+n}), \quad \hat{a}_{\bar{\mu}} \equiv \hat{a}_{\mu} + \hat{r}_{\mu 1}. \quad (6.24)$$

**Theorem 7** *Suppose that the states of the system given by (6.1)-(6.6) satisfies the hypothesis of Theorem 4. Then*

$$\begin{aligned} \overline{\langle \boldsymbol{\mu} \rangle} \equiv \lim_{t \rightarrow \infty} \langle \boldsymbol{\mu} \rangle &= \langle e^{A_{\bar{\mu}} \tau} \rangle (I_{n^2+n} - J_{\mu 2} \langle e^{A_{\bar{\mu}} \tau_s} \rangle)^{-1} \times \\ &\left( \hat{r}_{\mu 2} + J_{\mu 2} \left\langle e^{A_{\bar{\mu}} \tau_s} \int_0^{\tau_s} e^{-A_{\bar{\mu}} r} \hat{a}_{\bar{\mu}} dr \right\rangle \right) + \left\langle e^{A_{\bar{\mu}} \tau} \int_0^{\tau} e^{-A_{\bar{\mu}} r} \hat{a}_{\bar{\mu}} dr \right\rangle, \end{aligned} \quad (6.25)$$

*if and only if all the eigenvalues of the matrix  $(J_2 \otimes J_2 + Q_2 \otimes Q_2) \langle e^{A_{\mu} \tau_s} \otimes e^{A_{\mu} \tau_s} \rangle$  are inside the unit circle.*

The proof of this theorem is similar to that of Theorem 3 and 4.

## 6.4 Noise in Protein Concentration

Here we consider an example of such a system drawn from cellular biology. Let  $\mathbf{x}(t) \in \mathbb{R}$  denote the concentration of a given protein inside a single cell at time  $t$ . We model the time evolution of  $\mathbf{x}$  using a TTSHS that incorporates three noise mechanisms:

1. Stochastic production of protein molecules in bursts of gene activity, as has been experimentally seen [86, 90, 94].
2. Timer controlled cell-division events occur at random times. Whenever, cell division occurs, both the cell volume and the number of protein molecules reduce by half (assuming symmetric division). Thus, in the sense of average concentrations, there is no change

$$\langle \mathbf{x}_+(\mathbf{t}_s) \rangle = \mathbf{x}(\mathbf{t}_s), \quad (6.26)$$

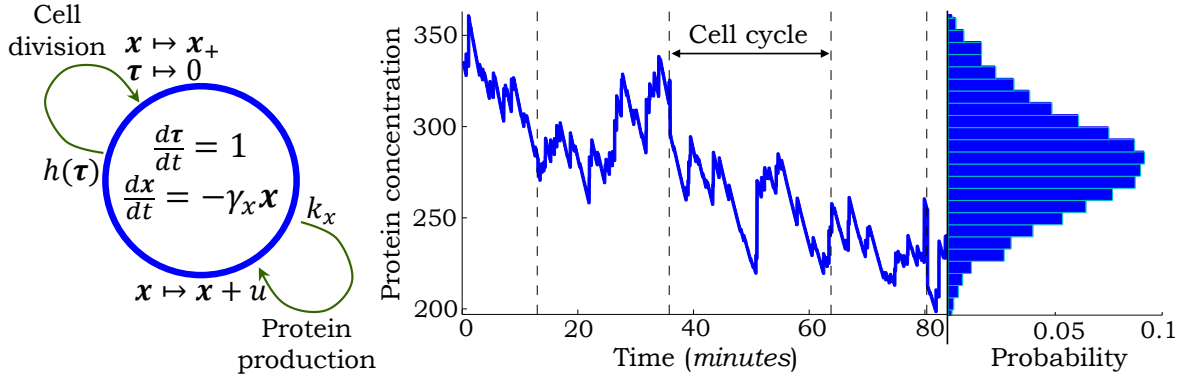


**Figure 6.2: Modeling stochasticity in the level of protein concentration using TTSHS.** *Left:* Time evolution of the protein level  $\mathbf{x} \in \mathbb{R}$  in a single cell is modeled via a SHS with two stochastic resets representing production of proteins in bursts and cell-division events. The latter is controlled by a timer  $\tau$ , and whenever it occurs the state is reset via (6.26)-(6.27). In between events, protein concentrations decay exponentially with rate  $\gamma_x$  due to cellular growth. *Right:* A sample trajectory of  $\mathbf{x}$  is shown with cell division events (dashed lines). The steady-state distribution of  $\mathbf{x}$  obtained via a large number Monte Carlo simulations is shown on the right.

3. During cell division, protein molecules are partitioned between two daughter cells based on a binomial distribution, i.e., each molecule has an equal probability of being in one of the two cells [20, 148]. This binomial partitioning process introduces noise in the concentration that can be represented by

$$\langle \mathbf{x}_+^2(\mathbf{t}_s) - \langle \mathbf{x}_+(\mathbf{t}_s) \rangle^2 \rangle = b\mathbf{x}(\mathbf{t}_s). \quad (6.27)$$

for some positive constant  $c$ . The linear dependence in (6.27) comes from the fact that the variance of a binomially distributed random variable is proportion to its mean.

Before considering the stochastic case, we first consider deterministic protein production, where the concentration evolves as

$$\dot{\mathbf{x}}(t) = k_x u - \gamma_x \mathbf{x}(t). \quad (6.28)$$

Here  $k_x$  and  $u$  denote the frequency and size of protein bursts, resulting in a net production rate of  $k_x u$  in the deterministic model. The concentration is diluted at a

rate  $\gamma_x$ , which is the rate of exponential growth in cell volume. Cell-division events are assumed to occur randomly at times  $\mathbf{t}_s$ , where  $\tau_s \equiv \mathbf{t}_s - \mathbf{t}_{s-1}$  follows an arbitrary positively-valued distribution. The mean cell-division time is intimately connected to the growth rate via

$$\langle \tau_s \rangle = \frac{\ln(2)}{2\gamma_x} \quad (6.29)$$

[72]. The TTSHS defined by (6.26)-(6.28) is of the form discussed in this section. Hence, steady-state analysis yields the following mean and noise

$$\overline{\langle \mathbf{x} \rangle} = \frac{k_x u}{\gamma_x}, \quad CV^2 = \frac{\ln(2)b}{2\overline{\langle \mathbf{x} \rangle}}, \quad (6.30)$$

respectively. The noise in the protein concentration level only depends on  $\langle \tau_s \rangle$ , which enters the equation via  $\gamma_x$  (see (6.29)). Thus remarkably, making the timing of cell division more random (for a fixed mean) will not result in higher stochasticity in the protein concentration.

Next, we consider stochastic production of proteins, which involves adding a second family of resets in the above TTSHS model. As pointed earlier, production of proteins is assumed to occur in bursts that happen at random times. In particular, burst events are assumed to occur at exponentially distributed times with rate  $k_x$ . Whenever the event occurs the concentration changes as

$$\mathbf{x}(\mathbf{t}_s) \mapsto \mathbf{x}(\mathbf{t}_s) + u. \quad (6.31)$$

The overall model with both stochastic production and cell division events is shown in Fig. 6.2. In between events, the concentration is diluted as

$$\dot{\mathbf{x}}(t) = -\gamma_x \mathbf{x}(t). \quad (6.32)$$

Steady-state analysis of the above moment equations yields

$$\overline{\langle \mathbf{x} \rangle} = \frac{k_x u}{\gamma_x}, \quad CV_x^2 = \frac{\ln(2)b}{2\overline{\langle \mathbf{x} \rangle}} + \frac{1}{2} \frac{u}{\overline{\langle \mathbf{x} \rangle}}, \quad (6.33)$$

providing the first results connecting the protein noise level to randomness in the underlying bursty synthesis and cell division events. As before, the noise only depends on  $\langle \tau_s \rangle$  and independent of its higher-order statistics.

## 6.5 Conclusion

We have studied statistical moments for a class of TTSHS with two families of resets, allowing the second family to occur at generally-distributed time intervals. Exact solutions of the first- and second-order moments were derived, and applied to the biological problem of stochastic gene expression. Our analysis reports for the first time, formulas for the mean and the noise in the level of a protein concentration in terms of underlying parameters and random processes. This is straightforward to expand these results to a system with multiple families of resets, each having Poisson arrivals. However, having more than one family of generally-distributed resets is convoluted and will be the subject of future investigation.

## Chapter 7

### MULTI-MODE STOCHASTIC HYBRID SYSTEMS WITH RENEWAL TRANSITIONS

In this chapter, a class of stochastic hybrid systems comprising of multiple operation modes is studied. In each mode, the state evolves according to a linear stochastic differential equation. We allow for stochastic switching between operational modes with switching times controlled by an underlying renewal process such that the time spent in each mode is a random variable with an arbitrary given probability distribution. We present a novel method to derive exact analytical solutions for the statistical moments, and illustrate the applicability of the method on an example drawn from systems biology. More specifically, we study how random switching of a gene between transcriptionally active and inactive states drives stochastic variation in the level of the expressed protein. Our results show that while randomness in gene switching times has no effect on the mean protein level, it critically impacts the magnitude of fluctuations in the protein level. This effect is further amplified for proteins with high decay rate. We finally discuss how noise in protein can be used to infer the underlying gene expression mechanisms.

#### 7.1 Model Formulation

The class of systems under study include:

1. **Operation modes:** The system, contains  $m$  operative modes. In each mode, the states  $\mathbf{x} \in \mathbb{R}^{n \times 1}$  are governed via a set of Stochastic Differential Equations (SDEs)

$$d\mathbf{x} = (\hat{a}_i + A_i\mathbf{x})dt + E_id\boldsymbol{\omega}_n, \quad i = \{1, \dots, m\}, \quad (7.1)$$

where  $A_i \in \mathbb{R}^{n \times n}$ ,  $E_i \in \mathbb{R}^{n \times n}$ , and  $\hat{a}_i \in \mathbb{R}^{n \times 1}$ . Moreover,  $\boldsymbol{\omega}_n$  denotes  $n$ -dimensional Wiener process where

$$\langle d\boldsymbol{\omega}_n \rangle = 0, \quad \langle d\boldsymbol{\omega}_n d\boldsymbol{\omega}_n^\top \rangle = I_n dt. \quad (7.2)$$

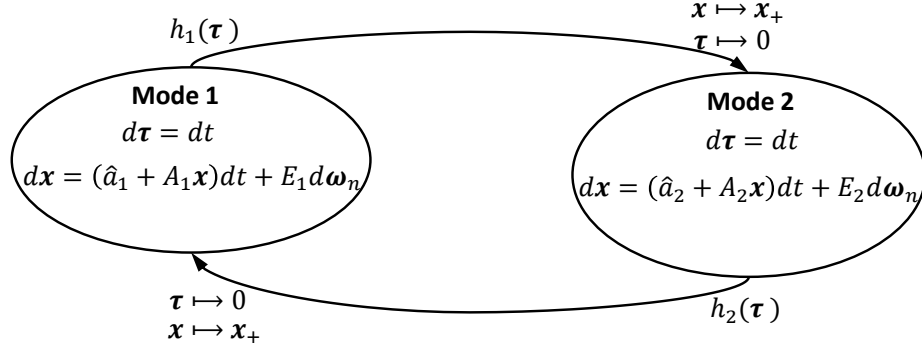


**Figure 7.1: Schematic of stochastic hybrid systems with two operation modes.** In each mode the states are governed via a set of stochastic differential equations according to (7.1). Resets happen at random times. Any time that an event occurs the states change their value and the system switches to another operation mode. The states after reset depend on the states before reset (eq. 7.4). A timer  $\tau$  measures the time since the last even, and rest to zero after each event occurs.

2. **Reset intensity:** When random events occur, the states will change and the system will switch to another mode. Assuming that random events happen at times  $\mathbf{t}_s$ ,  $s \in \{2, 3, \dots\}$ , the time interval between the events is defined as  $\tau_s \equiv \mathbf{t}_s - \mathbf{t}_{s-1}$ . The set of time intervals  $\tau_s$  can be divided into  $m$  subsets denoting reset time intervals between  $m$  different modes. In the rest of this paper for simplicity of notation and mathematical derivations we consider the case of  $m = 2$  (Fig. 7.1). However the obtained results are general and can be applied to any  $m$ . In this case system toggles between two modes and  $\tau_{s_i}$  is defined as

$$\tau_{s_i} \equiv \mathbf{t}_s - \mathbf{t}_{s-1} = \begin{cases} i = 1 & \text{from mode 1 to 2,} \\ i = 2 & \text{from mode 2 to 1.} \end{cases} \quad (7.3)$$

3. **Reset maps:** When a reset happens, the states change as

$$\mathbf{x}(\mathbf{t}_s) \mapsto \mathbf{x}_+(\mathbf{t}_s). \quad (7.4)$$

We assume that  $\mathbf{x}_+(\mathbf{t}_s)$  is a random variable in which its expectation is a linear affine map of  $\mathbf{x}(\mathbf{t}_s)$ . These maps depend on  $i$  as

$$\langle \mathbf{x}_+(\mathbf{t}_s) \rangle = J_i \mathbf{x}(\mathbf{t}_s) + \hat{r}_i, \quad i = \{1, 2\}, \quad (7.5)$$

where  $J_i \in \mathbb{R}^{n \times n}$  and  $\hat{r}_i \in \mathbb{R}^{n \times 1}$ . Further, the covariance matrix of  $\mathbf{x}_+(\mathbf{t}_s)$  depends on  $\mathbf{x}(\mathbf{t}_s)$  as

$$\begin{aligned} \langle \mathbf{x}_+(\mathbf{t}_s) \mathbf{x}_+^\top(\mathbf{t}_s) \rangle - \langle \mathbf{x}_+(\mathbf{t}_s) \rangle \langle \mathbf{x}_+(\mathbf{t}_s) \rangle^\top &= Q_i \mathbf{x}(\mathbf{t}_s) \mathbf{x}^\top(\mathbf{t}_s) Q_i^\top + B_i \mathbf{x}(\mathbf{t}_s) \hat{c}_i^\top \\ &\quad + \hat{c}_i \mathbf{x}^\top(\mathbf{t}_s) B_i^\top + D_i, \quad i = \{1, 2\}. \end{aligned} \quad (7.6)$$

Here  $Q_i \in \mathbb{R}^{n \times n}$ ,  $B_i \in \mathbb{R}^{n \times n}$ ,  $D_i \in \mathbb{R}^{n \times n}$ , and  $\hat{c}_i \in \mathbb{R}^{n \times 1}$ .

## 7.2 Statistical Moments of Multi-mode Stochastic Hybrid System

Similar to previous chapters, we introduce a timer  $\tau$  that measures the time since the last event. The timer increases with time between the events

$$d\tau = dt, \quad (7.7)$$

and resets to zero whenever a new event occurs

$$\tau \mapsto 0. \quad (7.8)$$

Note that we have two modes in the system, and the time intervals that the system resides in each of them is independent from the other. Thus we further divide set of  $\tau$  into two subsets  $\tau_1$  and  $\tau_2$  indicating the accumulation of time in mode 1 and 2, respectively ( $\tau = \{\tau_1, \tau_2\}$ ).

With this definition we can connect the probability of occurrence of an event to probability density function of the time intervals between the events. Let the probability that a transmission occurs in the next infinitesimal time  $(t, t + dt]$  be  $h_i(\tau)dt$ , where

$$h_i(\tau) \equiv \frac{f_i(\tau)}{1 - \int_{y=0}^{\tau} f_i(y)dy}, \quad i = \{1, 2\}, \quad (7.9)$$

Then, the time interval between events  $\tau_{s_i}$  follows a probability density function  $f_i$

$$\tau_{s_i} \sim f_i(\tau) = h_i(\tau)e^{-\int_{y=0}^{\tau} f_i(y)dy}, \quad i = \{1, 2\} \quad (7.10)$$

[116–118], and timers follow the following density function [119]

$$\tau_i \sim p_i(\tau) = \frac{1}{\langle \tau_{s_i} \rangle} e^{-\int_{y=0}^{\tau} f_i(y)dy}, \quad i = \{1, 2\}. \quad (7.11)$$

Finally, note that the probability that the system resides in each mode is independent of the states of system and is given by

$$\begin{aligned} \text{Probability of being in mode 1} &= \frac{\langle \tau_{s_1} \rangle}{\langle \tau_{s_1} \rangle + \langle \tau_{s_2} \rangle}, \\ \text{Probability of being in mode 2} &= \frac{\langle \tau_{s_2} \rangle}{\langle \tau_{s_1} \rangle + \langle \tau_{s_2} \rangle}. \end{aligned} \quad (7.12)$$

### 7.2.1 Steady-state Mean Level

By introducing the timer, we can derive the steady-state mean of  $\mathbf{x}$  in the following theorem.

**Theorem 8** *The steady-state mean of states of stochastic hybrid system in (7.1)-(7.6) is given by*

$$\begin{aligned} \overline{\langle \mathbf{x} \rangle} &= \frac{\langle \tau_{s_1} \rangle}{\langle \tau_{s_1} \rangle + \langle \tau_{s_2} \rangle} \left( \langle e^{A_1 \tau_{s_1}} \rangle (I_n - J_2 \langle e^{A_2 \tau_{s_2}} \rangle J_1 \langle e^{A_1 \tau_{s_1}} \rangle)^{-1} \left( J_2 \langle e^{A_2 \tau_{s_2}} \rangle \left\langle e^{A_1 \tau_{s_1}} \int_0^{\tau_{s_1}} e^{-A_1 l} \hat{a}_1 dl \right\rangle + J_2 \langle e^{A_2 \tau_{s_2}} \rangle \hat{r}_1 \right. \right. \\ &\quad \left. \left. + \left\langle e^{A_2 \tau_{s_2}} \int_0^{\tau_{s_2}} e^{-A_2 l} \hat{a}_2 dl \right\rangle + \hat{r}_2 \right) + \left\langle e^{A_1 \tau_{s_1}} \int_0^{\tau_{s_1}} e^{-A_1 l} \hat{a}_1 dl \right\rangle \right) \\ &+ \frac{\langle \tau_{s_2} \rangle}{\langle \tau_{s_1} \rangle + \langle \tau_{s_2} \rangle} \left( \langle e^{A_2 \tau_{s_2}} \rangle \left( I_n - J_1 \langle e^{A_1 \tau_{s_1}} \rangle J_2 \langle e^{A_2 \tau_{s_2}} \rangle \right)^{-1} \left( J_1 \langle e^{A_1 \tau_{s_1}} \rangle \left\langle e^{A_2 \tau_{s_2}} \int_0^{\tau_{s_2}} e^{-A_2 l} \hat{a}_2 dl \right\rangle + J_1 \langle e^{A_1 \tau_{s_1}} \rangle \hat{r}_2 \right. \right. \\ &\quad \left. \left. + \left\langle e^{A_1 \tau_{s_1}} \int_0^{\tau_{s_1}} e^{-A_1 l} \hat{a}_1 dl \right\rangle + \hat{r}_1 \right) + \left\langle e^{A_2 \tau_{s_2}} \int_0^{\tau_{s_2}} e^{-A_2 l} \hat{a}_2 dl \right\rangle \right). \end{aligned} \quad (7.13)$$

if and only if  $\langle e^{A_i \tau_{s_i}} \rangle$ ,  $i = \{1, 2\}$  is finite, and all the eigenvalues of the matrix  $J_1 \langle e^{A_1 \tau_{s_1}} \rangle J_2 \langle e^{A_2 \tau_{s_2}} \rangle$  are inside unit circle.

**Proof:** Proof of this theorem consists of two parts, we start with assuming that the system is residing in mode 1, hence the states of the system right before the  $s^{th}$  event is

$$\mathbf{x}(\mathbf{t}_s) = e^{A_1 \tau_{s_1}} \mathbf{x}_+(\mathbf{t}_{s-1}) + \int_0^{\tau_{s_1}} e^{-A_1 l} \hat{a}_1 dl + \int_0^{\tau_{s_1}} E_1 d\omega_n. \quad (7.14)$$

By using (7.5), the mean of the states after the  $s^{th}$  event is

$$\langle \mathbf{x}_+(\mathbf{t}_s) \rangle = J_1 \left( \langle e^{A_1 \tau_{s_1}} \rangle \langle \mathbf{x}_+(\mathbf{t}_{s-1}) \rangle + \left\langle e^{A_1 \tau_{s_1}} \int_0^{\tau_{s_1}} e^{-A_1 l} \hat{a}_1 dl \right\rangle \right) + \hat{r}_1. \quad (7.15)$$

After the  $s^{th}$  event the system is residing in mode 2. Hence the states of the system before  $s + 1^{th}$  event is given by

$$\mathbf{x}(\mathbf{t}_{s+1}) = e^{A_2 \tau_{s_2}} \mathbf{x}_+(\mathbf{t}_s) + \int_0^{\tau_{s_2}} e^{-A_2 l} \hat{a}_2 dl + \int_0^{\tau_{s_2}} E_2 d\omega_n. \quad (7.16)$$

Again by using (7.5) we derive the values of states right after  $s + 1^{th}$  event

$$\langle \mathbf{x}_+(\mathbf{t}_{s+1}) \rangle = J_2 \left( \langle e^{A_2 \tau_{s_2}} \rangle \langle \mathbf{x}_+(\mathbf{t}_s) \rangle + \left\langle e^{A_2 \tau_{s_2}} \int_0^{\tau_{s_2}} e^{-A_2 l} \hat{a}_2 dl \right\rangle \right) + \hat{r}_2. \quad (7.17)$$

Substituting (7.15) into (7.17), we get

$$\begin{aligned} \langle \mathbf{x}_+(\mathbf{t}_{s+1}) \rangle &= J_2 \langle e^{A_2 \tau_{s_2}} \rangle J_1 \langle e^{A_1 \tau_{s_1}} \rangle \langle \mathbf{x}_+(\mathbf{t}_{s-1}) \rangle + J_2 \langle e^{A_2 \tau_{s_2}} \rangle \left\langle e^{A_1 \tau_{s_1}} \int_0^{\tau_{s_1}} e^{-A_1 l} \hat{a}_1 dl \right\rangle \\ &+ J_2 \langle e^{A_2 \tau_{s_2}} \rangle \hat{r}_1 + \left\langle e^{A_2 \tau_{s_2}} \int_0^{\tau_{s_2}} e^{-A_2 l} \hat{a}_2 dl \right\rangle + \hat{r}_2. \end{aligned} \quad (7.18)$$

Note that after  $s + 1^{th}$  event we have returned to mode 1. Hence in order to have a finite recursive equation, all the eigenvalues of  $J_2\langle e^{A_2\tau_{s_2}}\rangle J_1\langle e^{A_1\tau_{s_1}}\rangle$  should be inside the unit circle. In this limit, the mean of states right after returning to mode 1 in steady-state is

$$\begin{aligned} \overline{\langle \mathbf{x}_+(\mathbf{t}_s) \rangle} &= V_1 J_2 \langle e^{A_2\tau_{s_2}} \rangle \left\langle e^{A_1\tau_{s_1}} \int_0^{\tau_{s_1}} e^{-A_1 l} \hat{a}_1 dl \right\rangle \\ &+ V_1 J_2 \langle e^{A_2\tau_{s_2}} \rangle \hat{r}_1 + V_1 \left\langle e^{A_2\tau_{s_2}} \int_0^{\tau_{s_2}} e^{-A_2 l} \hat{a}_2 dl \right\rangle + V_1 \hat{r}_2, \end{aligned} \quad (7.19)$$

where

$$V_1 = (I_n - J_2 \langle e^{A_2\tau_{s_2}} \rangle J_1 \langle e^{A_1\tau_{s_1}} \rangle)^{-1}. \quad (7.20)$$

By having the steady state initial condition of being in mode 1, we can calculate the mean of states for any time  $\tau_1 = \tau$

$$\begin{aligned} \overline{\langle \mathbf{x} |_{\tau_1=\tau} \rangle} &= e^{A_1\tau} \int_0^\tau e^{-A_1 l} \hat{a}_1 dl + e^{A_1\tau} V_1 (J_2 \langle e^{A_2\tau_{s_2}} \rangle \left\langle e^{A_1\tau_{s_1}} \int_0^{\tau_{s_1}} e^{-A_1 l} \hat{a}_1 dl \right\rangle \\ &+ J_2 \langle e^{A_2\tau_{s_2}} \rangle \hat{r}_1 + \left\langle e^{A_2\tau_{s_2}} \int_0^{\tau_{s_2}} e^{-A_2 l} \hat{a}_2 dl \right\rangle + \hat{r}_2). \end{aligned} \quad (7.21)$$

In the next part, we repeat our analysis by assuming that system is residing in mode 2. Such analysis results in another recursive formula which is converging if all the eigenvalues of  $J_1\langle e^{A_1\tau_{s_1}}\rangle J_2\langle e^{A_2\tau_{s_2}}\rangle$  are inside the unit circle. Note that eigenvalues of  $J_2\langle e^{A_2\tau_{s_2}}\rangle J_1\langle e^{A_1\tau_{s_1}}\rangle$  and  $J_1\langle e^{A_1\tau_{s_1}}\rangle J_2\langle e^{A_2\tau_{s_2}}\rangle$  are equal. In this case we can calculate the steady-state mean of states for any time  $\tau_2 = \tau$  as

$$\begin{aligned} \overline{\langle \mathbf{x} |_{\tau_2=\tau} \rangle} &= e^{A_2\tau} \int_0^\tau e^{-A_2 l} \hat{a}_2 dl e^{A_2\tau} V_2 (J_1 \langle e^{A_1\tau_{s_1}} \rangle \left\langle e^{A_2\tau_{s_2}} \int_0^{\tau_{s_2}} e^{-A_2 l} \hat{a}_2 dl \right\rangle \\ &+ J_1 \langle e^{A_1\tau_{s_1}} \rangle \hat{r}_2 + \left\langle e^{A_1\tau_{s_1}} \int_0^{\tau_{s_1}} e^{-A_1 l} \hat{a}_1 dl \right\rangle + \hat{r}_1), \end{aligned} \quad (7.22)$$

where

$$V_2 = (I_n - J_1 \langle e^{A_1\tau_{s_1}} \rangle J_2 \langle e^{A_2\tau_{s_2}} \rangle)^{-1}. \quad (7.23)$$

Finally, taking expected value with respect to  $\tau_i$ ,  $i = \{1, 2\}$  from (7.21) and (7.22) by using (7.11) and then using (7.12) results in (7.13) and that completes our proof. ■

In general, matrices cannot commute, thus,  $J_2\langle e^{A_2\tau_{s_2}}\rangle J_1\langle e^{A_1\tau_{s_1}}\rangle$  is not equal to  $J_1\langle e^{A_1\tau_{s_1}}\rangle$

$J_2 \langle e^{A_2 \tau_{s_2}} \rangle$ . This implies an important property of these systems: even if each mode is stable, it does not result in stability of the whole system. Note that the states of the system at a given time depends on the entire history of the resets.

### 7.2.2 Steady-state Second-order Moments

We use the method that we introduced in chapter 3 to convert dynamics of the second-order moments to a similar form as in (7.1) and (7.4). The dynamics of  $\boldsymbol{\mu}$  between the events is given by

$$d\boldsymbol{\mu} = (\hat{a}_{\mu_i} + A_{\mu_i} \boldsymbol{\mu}(t))dt + (E_{\mu_i})d\mathbf{w}_{n^2+n}, \quad (7.24)$$

where

$$A_{\mu_i} = \left[ \begin{array}{c|c} A_i & 0 \\ \hline I_n \otimes \hat{a}_i + \hat{a}_i \otimes I_n & I_n \otimes A_i + A_i \otimes I_n \end{array} \right], \quad \hat{a}_{\mu_i} = \left[ \begin{array}{c} \hat{a}_i \\ \hline \text{vec}(E_i E_i^\top) \end{array} \right]. \quad (7.25)$$

Note that we did not show  $E_{\mu_i}$  because this matrix has no role in the steady-state mean of  $\boldsymbol{\mu}$  [149]. Moreover, when a reset occurs, the states of  $\boldsymbol{\mu}$  reset as

$$\boldsymbol{\mu}(\mathbf{t}_s) \mapsto \boldsymbol{\mu}_+(\mathbf{t}_s), \quad (7.26)$$

where

$$\langle \boldsymbol{\mu}_+(\mathbf{t}_s) \rangle = J_{\mu_i} \boldsymbol{\mu}(\mathbf{t}_s) + \hat{r}_{\mu_i}, \quad J_{\mu_i} = \left[ \begin{array}{c|c} J_i & 0 \\ \hline M_i & N_i \end{array} \right], \quad \hat{r}_{\mu_i} = \left[ \begin{array}{c} \hat{r}_i \\ \hline \text{vec}(D_i D_i^\top) \end{array} \right], \quad (7.27a)$$

$$M_i = B_i \otimes \hat{c}_i + \hat{c}_i \otimes B_i + J_i \otimes \hat{r}_i + \hat{r}_i \otimes J_i, \quad N_i = J_i \otimes J_i + Q_i \otimes Q_i.$$

Deterministic dynamics (7.24) and stochastic resets (7.26) are similar to (7.1) and (7.4). Hence with a similar analysis as in Theorem 6, the following theorem provides the necessary and sufficient conditions for having the steady-state second-order moments of  $\mathbf{x}$ .

**Theorem 9** *Suppose that the multi-mode stochastic hybrid system in (7.1)-(7.6) satisfies the hypothesis of Theorem 1, then the steady-state mean of  $\mathbf{x}\mathbf{x}^\top$  is finite if and only if all the eigenvalues of the matrix*

$$(J_1 \otimes J_1 + Q_1 \otimes Q_1) \langle e^{A_1 \tau_{s_1}} \otimes e^{A_1 \tau_{s_1}} \rangle (J_2 \otimes J_2 + Q_2 \otimes Q_2) \langle e^{A_2 \tau_{s_2}} \otimes e^{A_2 \tau_{s_2}} \rangle \quad (7.28)$$

are inside the unite circle.

**Proof:** First let us define

$$\mathbf{y}_i \equiv e^{A_i \tau_{s_i}} \int_0^{\tau_{s_i}} e^{-A_i l} \hat{u}_i dl. \quad (7.29)$$

Similar to Theorem 6 we prove Theorem 7 in two parts. Assume that system is residing in mode 1, then  $\mathbf{x}\mathbf{x}^\top$  right after  $s^{th}$  event is related to  $\mathbf{x}(\mathbf{t}_{s-1}^+) \mathbf{x}_+^\top(\mathbf{t}_{s-1})$  as

$$\begin{aligned} \text{vec}(\langle \mathbf{x}_+(\mathbf{t}_s) \mathbf{x}_+^\top(\mathbf{t}_s) \rangle) = & \\ & (J_1 \otimes J_1 + Q_1 \otimes Q_1) \langle e^{A_1 \tau_{s_1}} \otimes e^{A_1 \tau_{s_1}} \rangle \text{vec}(\langle \mathbf{x}_+(\mathbf{t}_{s-1}) \mathbf{x}_+^\top(\mathbf{t}_{s-1}) \rangle) \\ & + (J_1 \otimes J_1 + Q_1 \otimes Q_1) (\langle e^{A_1 \tau_{s_1}} \otimes \mathbf{y}_1 \rangle \langle \mathbf{y}_1 \otimes e^{A_1 \tau_{s_1}} \rangle) \langle \mathbf{x}_+(\mathbf{t}_{s-1}) \rangle \\ & + ((B_1 \otimes \hat{c}_1 + J_1 \otimes \hat{r}_1) \langle I_n \otimes e^{A_1 \tau_{s_1}} \rangle) \\ & + (\hat{c}_1 \otimes B_1 + \hat{r}_1 \otimes J_1) \langle e^{A_1 \tau_{s_1}} \otimes I_n \rangle \langle \mathbf{x}_+(\mathbf{t}_{s-1}) \rangle \\ & + \text{vec}(Q_1 \langle \mathbf{y}_1 \mathbf{y}_1^\top \rangle Q_1^\top + J_1 \langle \mathbf{y}_1 \mathbf{y}_1^\top \rangle J_1^\top + B_1 \langle \mathbf{y}_1 \rangle \hat{c}_1^\top \\ & + J_1 \langle \mathbf{y}_1 \rangle \hat{r}_1^\top + \hat{c}_1 \langle \mathbf{y}_1^\top \rangle B_1^\top + \hat{r}_1 \langle \mathbf{y}_1^\top \rangle J_1^\top + E_1 + \hat{r}_1 \hat{r}_1^\top). \end{aligned} \quad (7.30)$$

Next,  $\mathbf{x}\mathbf{x}^\top$  right after  $s + 1^{th}$  event is related to  $\mathbf{x}_+(\mathbf{t}_s) \mathbf{x}_+^\top(\mathbf{t}_s)$  as

$$\begin{aligned} \text{vec}(\langle \mathbf{x}_+(\mathbf{t}_{s+1}) \mathbf{x}_+^\top(\mathbf{t}_{s+1}) \rangle) = & \\ & (J_2 \otimes J_2 + Q_2 \otimes Q_2) \langle e^{A_2 \tau_{s_2}} \otimes e^{A_2 \tau_{s_2}} \rangle \text{vec}(\langle \mathbf{x}_+(\mathbf{t}_s) \mathbf{x}_+^\top(\mathbf{t}_s) \rangle) \\ & + (J_2 \otimes J_2 + Q_2 \otimes Q_2) (\langle e^{A_2 \tau_{s_2}} \otimes \mathbf{y}_2 \rangle + \langle \mathbf{y}_2 \otimes e^{A_2 \tau_{s_2}} \rangle) \langle \mathbf{x}_+(\mathbf{t}_s) \rangle \\ & + ((B_2 \otimes \hat{c}_2 + J_2 \otimes \hat{r}_2) \langle e^{A_2 \tau_{s_2}} \rangle) \\ & + (\hat{c}_2 \otimes B_2 + \hat{r}_2 \otimes J_2) \langle e^{A_2 \tau_{s_2}} \rangle \langle \mathbf{x}_+(\mathbf{t}_s) \rangle \\ & + \text{vec}(Q_2 \langle \mathbf{y}_2 \mathbf{y}_2^\top \rangle Q_2^\top + J_2 \langle \mathbf{y}_2 \mathbf{y}_2^\top \rangle J_2^\top + B_2 \langle \mathbf{y}_2 \rangle \hat{c}_2^\top \\ & + J_2 \langle \mathbf{y}_2 \rangle \hat{r}_2^\top + \hat{c}_2 \langle \mathbf{y}_2^\top \rangle B_2^\top + \hat{r}_2 \langle \mathbf{y}_2^\top \rangle J_2^\top + E_2 + \hat{r}_2 \hat{r}_2^\top). \end{aligned} \quad (7.31)$$

Combining these two equations we obtain a recursive formula in which is converging in steady-state if all the eigenvalues of  $(J_2 \otimes J_2 + Q_2 \otimes Q_2) \langle e^{A_2 \tau_{s_2}} \otimes e^{A_2 \tau_{s_2}} \rangle (J_1 \otimes J_1 + Q_1 \otimes Q_1) \langle e^{A_1 \tau_{s_1}} \otimes e^{A_1 \tau_{s_1}} \rangle$  are inside unit circle. Similarly if we assume that the system resides in mode 2 then the steady-state values exists if all the eigenvalues of

$(J_1 \otimes J_1 + Q_1 \otimes Q_1)\langle e^{A_1\tau_{s_1}} \otimes e^{A_1\tau_{s_1}} \rangle (J_2 \otimes J_2 + Q_2 \otimes Q_2)\langle e^{A_2\tau_{s_2}} \otimes e^{A_2\tau_{s_2}} \rangle$  are inside the unit circle. The eigenvalues of these two matrices are the same. The rest of proof is similar to that of Theorem 6. ■

Finally,  $\overline{\langle \boldsymbol{\mu} \boldsymbol{\mu}^\top \rangle}$  can be obtained from (7.13) by replacing  $A_i$ ,  $\hat{a}_i$ ,  $J_i$ , and  $\hat{r}_i$  in (7.13) with their respective  $A_{\mu_i}$ ,  $\hat{a}_{\mu_i}$ ,  $J_{\mu_i}$ , and  $\hat{r}_{\mu_i}$ ,  $i = \{1, 2\}$ . In the next section, we apply our results on a biological example.

### 7.3 Noise in Gene Switching

A main source of noise in biological systems is occurrence of random events such as protein synthesis, binding, etc. [49, 51, 52]. One such important event is stochastic gene switching: a gene becomes active for a short period of time followed by a period of silence [89–92, 105, 148].

To explore the contribution of gene switching on protein concentration, we used the multi-mode stochastic hybrid system introduced in here. Let  $\boldsymbol{x}(t)$  denotes a protein concentration level inside the cell at time  $t$ . We assume that production occurs in exponentially distributed time intervals with rate  $k_x$  and we use a Langevin approximation of this reaction [140]. Further we consider that protein decays with a rate  $\gamma_x$ . When gene is active, the dynamics of protein concentration can be written as

$$d\boldsymbol{x} = (k_x - \gamma_x \boldsymbol{x})dt + \sqrt{k_x} d\boldsymbol{w}_1, \quad (7.32)$$

and when gene is inactive, protein dynamics only include decay

$$d\boldsymbol{x} = -\gamma_x \boldsymbol{x}dt. \quad (7.33)$$

Note that decay of protein concentration is mainly caused by cell growth. Since cell growth is a cellular process which is the summation of many random events, we did not consider any noise in the decay of proteins [119, 150, 151]. The dynamics of this system are in the form of (7.1) with

$$A_1 = A_2 = -\gamma_x, \quad \hat{a}_1 = k_x, \quad E_1 = \sqrt{k_x}, \quad \hat{a}_2 = 0, \quad E_2 = 0. \quad (7.34)$$

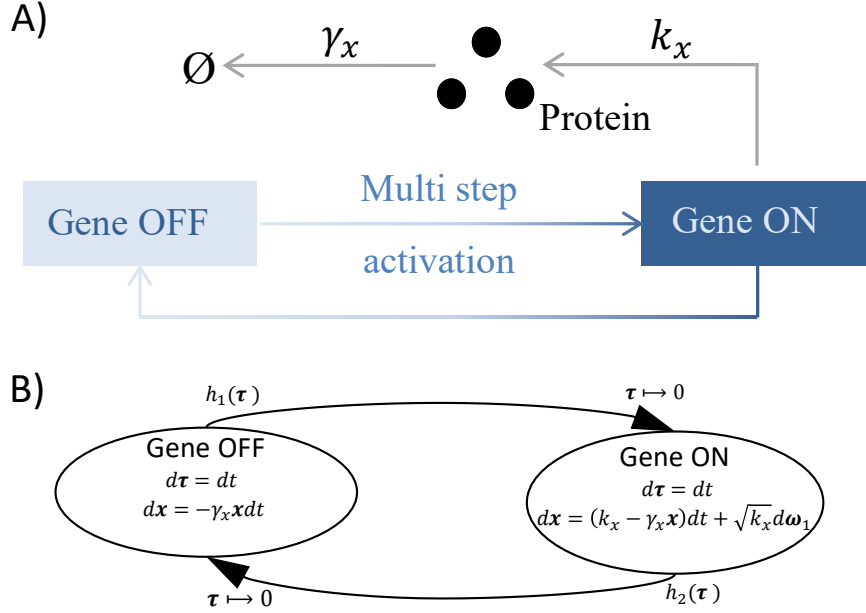


**Figure 7.2: The fundamental process of gene switching can be modeled through multi-mode framework.** A) Promoter randomly switches between active and inactive states. Protein synthesis only occurs when promoter is ON. Protein is subject to decay with a rate  $\gamma_x$ . B) The multi-mode system presented here is perfect for modeling promoter toggling. When gene is OFF the protein dynamics are only governed via decay. when promoter becomes active the protein synthesis is modeled through a Langevin equation with a rate  $k_x$ .

Moreover,  $J_1 = J_2 = 1$ , and  $\hat{r}_i = Q_i = B_i = D_i = \hat{c}_i = 0$ ,  $i = \{1, 2\}$  (Fig. 7.2). For having a clear connection to our biological example, we rename  $\tau_{s_1}$  and  $\tau_{s_2}$  as  $\tau_{on}$  and  $\tau_{off}$ , respectively.

Since  $A_1 = A_2 = -\gamma_x < 0$ , then both  $\langle e^{-\gamma_x \tau_{off}} \rangle$  and  $\langle e^{-\gamma_x \tau_{on}} \rangle$  exist. Moreover, because  $J_1 = J_2 = 1$  then  $\langle e^{-\gamma_x \tau_{off}} \rangle \langle e^{-\gamma_x \tau_{on}} \rangle < 1$ , hence we can use (7.13) to derive the steady-state mean of protein concentration

$$\overline{\langle \mathbf{x} \rangle} = \frac{\langle \tau_{on} \rangle}{\langle \tau_{on} \rangle + \langle \tau_{off} \rangle} \frac{k_x}{\gamma_x}. \quad (7.35)$$

The mean of protein concentration is independent of the probability density function of gene-switching time intervals. This means that the mean of protein contains no information about the underlying processes that leads to gene activation.

In the next step, we derive the second-order moment of protein to explore how variations in gene-switching time intervals affect the fluctuations in protein count. First, we use (7.25) to derive the matrices needed for calculating the second-order moment

$$A_{\mu_1} = \begin{bmatrix} -\gamma_x & 0 \\ 0 & -2\gamma_x \end{bmatrix}, \hat{a}_{\mu_1} = \begin{bmatrix} k_x \\ k_x \end{bmatrix}, A_{\mu_2} = \begin{bmatrix} -\gamma_x & 0 \\ 2k_x & -2\gamma_x \end{bmatrix}, \hat{a}_{\mu_2} = 0, J_{\mu_1} = J_{\mu_2} = I_2. \quad (7.36)$$

Further, here  $J_{\mu_i} = I_2$  and  $\hat{r}_{\mu_i} = 0$ ,  $i = \{1, 2\}$ . Since  $-\gamma_x < 0$  then the conditions of Theorem 7 are satisfied and we can derive the second-order moment as

$$\begin{aligned} \overline{\langle \mathbf{x}^2 \rangle} &= \frac{k_x^2}{\gamma_x^3} \frac{(\langle e^{-\gamma_x \tau_{off}} \rangle - 1)(\langle e^{-\gamma_x \tau_{on}} \rangle - 1)}{(\langle e^{-\gamma_x \tau_{off}} \rangle \langle e^{-\gamma_x \tau_{on}} \rangle - 1)(\langle \tau_{on} \rangle + \langle \tau_{off} \rangle)} \\ &+ \frac{k_x^2}{\gamma_x^2} \frac{(\langle e^{-\gamma_x \tau_{off}} \rangle \langle e^{-\gamma_x \tau_{on}} \rangle - 1) \langle \tau_{on} \rangle}{(\langle e^{-\gamma_x \tau_{off}} \rangle \langle e^{-\gamma_x \tau_{on}} \rangle - 1)(\langle \tau_{on} \rangle + \langle \tau_{off} \rangle)} + \frac{k_x}{2\gamma_x} \frac{\langle \tau_{on} \rangle}{\langle \tau_{on} \rangle + \langle \tau_{off} \rangle}. \end{aligned} \quad (7.37)$$

We use the coefficient of variation squared to quantify noise in  $\mathbf{x}$

$$\begin{aligned} CV^2 &= \frac{\gamma_x (\langle e^{-\gamma_x \tau_{off}} \rangle \langle e^{-\gamma_x \tau_{on}} \rangle - 1) \langle \tau_{off} \rangle \langle \tau_{on} \rangle}{(\langle e^{-\gamma_x \tau_{off}} \rangle \langle e^{-\gamma_x \tau_{on}} \rangle - 1) \gamma_x \langle \tau_{on} \rangle^2} \\ &+ \frac{(\langle \tau_{on} \rangle + \langle \tau_{off} \rangle) (\langle e^{-\gamma_x \tau_{off}} \rangle - 1) (\langle e^{-\gamma_x \tau_{on}} \rangle - 1)}{(\langle e^{-\gamma_x \tau_{off}} \rangle \langle e^{-\gamma_x \tau_{on}} \rangle - 1) \gamma_x \langle \tau_{on} \rangle^2} + \frac{1}{2} \frac{1}{\langle \mathbf{x} \rangle}. \end{aligned} \quad (7.38)$$

The first two terms in the right-hand side of this equation show the contribution of random gene switching times in protein noise, the last term quantifies the contribution of random synthesis events. While the mean of protein is independent of statistical characteristic of switching times, the protein fluctuations depend on the entire distribution of  $\tau_{on}$  and  $\tau_{off}$ .

Next, based on the measurements inside the living cells [22], we assume that gene deactivation reaction happens in exponentially distributed time intervals and we explore the effect of noise in gene activation time interval. Fig. 7.3 shows that making gene-activation reaction more noisy increases  $CV^2$ . Further, we can approximate the results in the limit of fast gene switching as

$$CV^2 \approx \frac{1}{2} \frac{\langle \tau_{on} \rangle^2 \gamma_x}{\langle \tau_{on} \rangle + \langle \tau_{off} \rangle} (1 + CV_{\tau_{on}}^2) + \frac{1}{2} \frac{1}{\langle \mathbf{x} \rangle}, \quad (7.39)$$

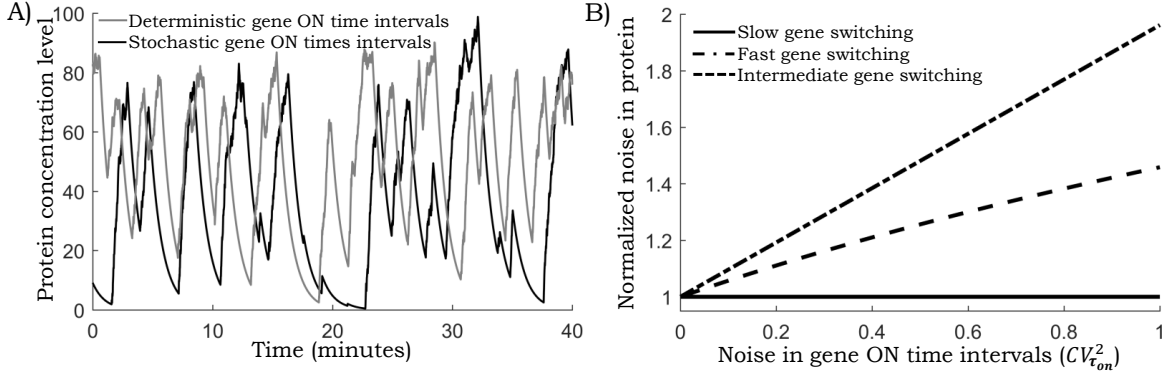


**Figure 7.3: The noise in protein concentration is highly affected by the gene-switching time intervals.** A) Noise in gene ON time intervals will not change the mean of a protein. Moreover, it does not have an obvious effect on the protein time trend. B) The noise in protein is highly affected by the gene switching noise. While the mean of protein only depends on the ratio of gene ON and OFF times, noise is affected by the magnitude of the ON and OFF time intervals as well. For this plot the protein production rate is selected to be  $k_x = 100$ , decay rate is  $\gamma_x = 1 \text{ min}^{-1}$ , and mean ON and OFF time intervals are equal  $\langle \tau_{on} \rangle = \langle \tau_{off} \rangle$ .

where  $CV_{\tau_{on}}^2 \equiv \langle \tau_{on}^2 \rangle / \langle \tau_{on} \rangle^2 - 1$  denotes the coefficient of variation squared of gene-activation time intervals. This equation clearly shows that the noise in gene activation reaction increases the noise in protein concentration. Moreover, this equation quantifies the contribution of decay rate on noise, i.e., higher decay rate means higher noise. Additionally, this equation shows that noise in  $\mathbf{x}$  depends on both fluctuations and amplitude of gene-switching time intervals (Fig. 7.3).

## 7.4 Conclusion

We studied statistical moments of a class of stochastic hybrid systems with multiple operation modes. We derived exact solution of the first and second order moments as well as necessary and sufficient conditions for having finite moments. While we only present our derivations for a two mode system, the results can be generalized to a any arbitrary number of modes.

We used the framework presented here to calculate the mean and the noise in protein concentration. We find that the randomness in gene-activation time intervals increases the noise in protein while having no effect on the mean. Hence noise can be used to infer protein expression parameters systematically. Noise in gene-activation time intervals is an indicator of the number of steps that needs to be taken to activate a gene [22]. Previously through a numerical model we explored this connection on experimental data obtained from mouse [22]. Here we provide the exact solutions that can be used to infer mechanisms behind gene switching in different types of cells.

## Chapter 8

### LINEAR NOISE APPROXIMATION FOR A CLASS OF STOCHASTIC HYBRID SYSTEMS

The usual problem of moment dynamics equations is that in general for non-linear systems, the lower order moments are dependent on the higher orders [152]. Hence the system of equations cannot be solved. The common method to solve this issue is to express the higher order moments as functions (mainly nonlinear) of lower order moments. This procedure is called as *moment closure* [153–157] and the approximated results are usually solved numerically.

However there exists two methods that give analytic results for the approximated moment dynamics. The first method is to linearize both continuous dynamics and discrete events of a system and then write the moment dynamics for a linear SHS using the extended generator [28]. This method is easy to implement yet ad-hoc and there exists no general theorem that guarantees the obtained results are a good approximation of the moments. The other method is through the omega expansion using LNA [158–160]. This method leads to the stochastic variables being distributed according to a Gaussian distribution with the mean given by the deterministic dynamics. The method has many salient features, namely (i) the mean and variance obtained are positive, (ii) the error of estimating these moments reduces with increase in the system size [161, 162], (iii) complex multivariable systems can be effectively reduced in dimensionality by considering timescale separation [163]. In this chapter we answer the question: Do these methods (linearization vs omega expansion with LNA) give the same moment dynamics equations for SHS, and if so for what sub-class of SHS?

To address this question we first give a one dimension example for which linearization method and the system size expansion methods are elucidated. We then

extend the result for a SHS having stochastic resets that do not scale with system size and show that the moment dynamics equations for LNA and linearization are the same. Finally, we study the single dimensional class of SHS where this condition is relaxed and direct application of LNA is not possible. For this model, we introduce a new method to derive and approximate the moments.

### 8.1 Comparison of Linearization and LNA in a Simple Genetic Circuit

Let the number of a species be denoted by  $\mathbf{x}$ . The stochastic synthesis of this species is mathematically described as

$$\text{Prob.}(\mathbf{x}(t + dt) = \mathbf{x} + 1) = \Omega h\left(\frac{\mathbf{x}}{\Omega}\right) dt. \quad (8.1)$$

Here the production rate is represented by  $h\left(\frac{\mathbf{x}}{\Omega}\right)$ , and  $\Omega$  is the system size. Further between two production events it follows the deterministic dynamics

$$\frac{d\mathbf{x}}{dt} = -\gamma_x \mathbf{x}. \quad (8.2)$$

Here  $\gamma_x$  is the dilution rate of the species. We assume that dilution is deterministic because cell growth is a cellular process which is the result of many events and hence can be modeled deterministically [119, 150, 151]. Next,  $\mathbf{x}$  is split into the deterministic and stochastic components for LNA with the ansatz

$$\mathbf{x} = \Omega\phi + \Omega^{1/2}\epsilon. \quad (8.3)$$

Here  $\epsilon$  is a stochastic process. The deterministic component  $\phi$  is solution of the system

$$\frac{d\phi}{dt} = h(\phi) - \gamma_x \phi. \quad (8.4)$$

The probability that the random variable  $\mathbf{x}$  takes the value  $n$  at time  $t$  is given by  $p(x, t)$ , which follows the chemical master equation

$$\frac{dp(x, t)}{dt} = \Omega h\left(\frac{n}{\Omega}\right) (p(x-1, t) - p(x, t)) + \frac{\partial (\gamma_x x p(x, t))}{\partial x}. \quad (8.5)$$

The left hand side can be expressed as

$$\frac{dp(x, t)}{dt} = \frac{\partial \Pi}{\partial t} + \frac{d\epsilon}{dt} \frac{\partial \Pi}{\partial \epsilon} = \frac{\partial \Pi}{\partial t} - \Omega^{1/2} \frac{d\phi}{dt} \frac{\partial \Pi}{\partial \epsilon}. \quad (8.6)$$

Here  $\Pi(\epsilon, t)$  is the probability that  $\epsilon$  takes value  $\epsilon$  at time  $t$ . Note that we have dropped the argument for the sake of simplicity. The master equation in the new variables  $\epsilon$  and  $\phi$  is given by

$$\frac{\partial \Pi}{\partial t} - \Omega^{1/2} \frac{d\phi}{dt} \frac{\partial \Pi}{\partial \epsilon} = \Omega (E^{-1} - 1) h\left(\frac{n}{\Omega}\right) \Pi + \frac{1}{\Omega^{1/2}} \frac{\partial(\gamma_x n \Pi)}{\partial \epsilon}. \quad (8.7)$$

The deterministic reaction is represented by the second term on the right hand side. The first term on the right hand side represents stochastic reactions with the operator  $E$  changing  $n$  to  $n + 1$  and hence  $\epsilon$  to  $\epsilon + \Omega^{-1/2}$ . The operator  $E^{-1}$  can be expanded as [158]

$$E^{-1} = 1 + (-1)\Omega^{-1/2} \frac{\partial}{\partial \epsilon} + \frac{(-1)^2}{2!} \Omega^{-1} \frac{\partial^2}{\partial \epsilon^2} \dots \quad (8.8)$$

Note that the transition intensity  $h$  is a function of the intensive variable  $\mathbf{x}/\Omega = \phi + \Omega^{-1/2}\epsilon$ . In order to proceed we expand the transition intensity linearly with respect to the fluctuations  $\Omega^{-1/2}\epsilon$  about the deterministic solution  $\phi$  as

$$h\left(\frac{\mathbf{x}}{\Omega}\right) = h(\phi) + \frac{dh(\phi)}{d\phi} \Omega^{-1/2} \epsilon. \quad (8.9)$$

Next substituting (8.3), (8.8), and (8.9) in (8.7) and truncating to the order  $\Omega^0$  the master equation is

$$\begin{aligned} \frac{\partial \Pi}{\partial t} = & \left( \frac{\partial \Pi}{\partial \epsilon} \epsilon + \Pi \right) \gamma_x + \Omega^{1/2} \frac{\partial \Pi}{\partial \epsilon} \left( \frac{d\phi}{dt} + \gamma_x \phi - h(\phi) \right) \\ & - \left( -\frac{h(\phi)}{2} \frac{\partial^2 \Pi}{\partial \epsilon^2} + \frac{dh(\phi)}{d\phi} \left( \frac{\partial \Pi}{\partial \epsilon} \epsilon + \Pi \right) \right). \end{aligned} \quad (8.10)$$

As the deterministic dynamics state follows

$$\frac{d\phi}{dt} + \gamma_x \phi - h(\phi) = 0, \quad (8.11)$$

hence the previous equation can be simplified. The reduced master equation is

$$\frac{\partial \Pi}{\partial t} = \left( \frac{\partial \Pi}{\partial \epsilon} \epsilon + \Pi \right) \gamma_x - \left( -\frac{h(\phi)}{2} \frac{\partial^2 \Pi}{\partial \epsilon^2} + \frac{dh(\phi)}{d\phi} \left( \frac{\partial \Pi}{\partial \epsilon} \epsilon + \Pi \right) \right). \quad (8.12)$$

Finally we obtain the moment dynamics of the  $i^{\text{th}}$  moment by multiplying (8.12) by  $\epsilon^i$  and integrating with respect to  $\epsilon$ . Thus the first order moment dynamics is

$$\frac{d\langle\epsilon\rangle}{dt} = \langle\epsilon\rangle \left( \frac{dh(\phi)}{d\phi} - \gamma_x \right). \quad (8.13)$$

With the initial condition,  $\langle\epsilon(0)\rangle = 0$ , the stochastic component  $\langle\epsilon\rangle = 0, \forall t \geq 0$ . Similarly, the dynamics of the second order moment is

$$\frac{d\langle\epsilon^2\rangle}{dt} = h(\phi) + 2\langle\epsilon^2\rangle \left( \frac{dh(\phi)}{d\phi} - \gamma_x \right). \quad (8.14)$$

At steady-state the second order moment is given by

$$\langle\bar{\epsilon}^2\rangle = \frac{h(\bar{\phi})}{2 \left( \gamma_x - \frac{dh(\bar{\phi})}{d\phi} \right)}. \quad (8.15)$$

We define the steady state production rate as  $h(\bar{\phi})$  and feedback strength as  $|\frac{dh(\bar{\phi})}{d\phi}|$ , where  $|\cdot|$  denotes the absolute value. We then quantify the noise with the coefficient of variation (CV). Noting that from (8.3), the variance of  $\epsilon$  ( $\sigma_\epsilon^2$ ) can be related to coefficient of variation squared of  $\mathbf{x}$  at steady-state as

$$CV_{\mathbf{x}}^2 = \frac{\sigma_\epsilon^2}{\Omega \bar{\phi}^2}. \quad (8.16)$$

Finally the noise in  $\mathbf{x}$  is

$$CV_{\mathbf{x}}^2 = \frac{\gamma_x}{2(\gamma_x - \frac{dh(\bar{\phi})}{d\phi})\langle\mathbf{x}\rangle}. \quad (8.17)$$

To compare with the linearization technique we first linearize the propensity function about  $\frac{\langle\mathbf{x}\rangle}{\Omega} = \phi$  as

$$h\left(\frac{\mathbf{x}}{\Omega}\right) = h(\phi) + \frac{dh(\phi)}{d\phi} \frac{\mathbf{x} - \langle\mathbf{x}\rangle}{\Omega}. \quad (8.18)$$

We then write the extended moment generator for a system with stochastic and deterministic dynamics as [28]

$$\frac{d\langle(\psi(\mathbf{x}, t))\rangle}{dt} = \langle(L\psi)(\mathbf{x}, t)\rangle, \quad (8.19)$$

$$(L\psi)(x, t) \equiv \frac{\partial\psi(x, t)}{\partial n} (-\gamma_x x) + \frac{\partial\psi(x, t)}{\partial t} + (\psi(x+1, t) - \psi(x, t))\Omega h(\phi). \quad (8.20)$$

Here  $\psi : \mathbb{R} \times [0, \infty) \rightarrow \mathbb{R}$ , is a continuously differentiable function. To obtain the first and second order moment dynamics we substitute  $\psi(x, t)$  in (8.20) as  $x$  and  $x^2$  respectively

$$\frac{d\langle \mathbf{x} \rangle}{dt} = \Omega h(\phi) - \gamma_x \langle \mathbf{x} \rangle, \quad (8.21)$$

$$\frac{d\langle \mathbf{x}^2 \rangle}{dt} = -2\gamma_x \langle \mathbf{x}^2 \rangle + \Omega h(\phi) + 2\Omega h(\phi) \langle \mathbf{x} \rangle + 2 \frac{dh(\phi)}{d\phi} (\langle \mathbf{x}^2 \rangle - \langle \mathbf{x} \rangle^2). \quad (8.22)$$

Solving these equations for the steady-state moments gives the same noise expression as (8.17). Note that, if  $dh(\bar{\phi})/d\bar{\phi} > 0$  then it is a positive feedback with the noise amplifying compared to that without feedback. In this case for high enough magnitude of  $dh(\bar{\phi})/d\bar{\phi} \geq \gamma_x$ , the noise in  $\mathbf{x}$  does not reach a steady state and diverges. On the other hand  $dh(\bar{\phi})/d\bar{\phi} < 0$  represents negative feedback, and noise in protein copy number reduces with feedback strength  $|dh(\bar{\phi})/d\bar{\phi}|$ .

On a side note, the auto-regulatory motif studied here is biologically relevant. Inherent stochasticity in genetic circuits is associated with diseased states [164]. While in some cases heterogeneity in the cell is advantageous for its survival [165, 166]. Hence, there exists mechanisms of regulation of the protein levels on the cellular level [70, 112, 167, 168]. In the next section we present the general results of LNA for a class of SHS models.

## 8.2 Equivalence of the Omega Expansion and Linearization Method

Once we establish that the omega expansion and linearization are the same for a birth/death example, a natural question is whether the equivalence of these two methods holds for general SHS.

**Theorem 10** *Consider a SHS with  $m$  states governed via ordinary differential equation between events*

$$\frac{d\mathbf{x}}{dt} = \Omega g\left(\frac{\mathbf{x}}{\Omega}, t\right), \mathbf{x} \in \mathbb{R}^{n \times 1}, g : \mathbb{R}^{n \times 1} \times [0, \infty) \rightarrow \mathbb{R}^{n \times 1}. \quad (8.23)$$

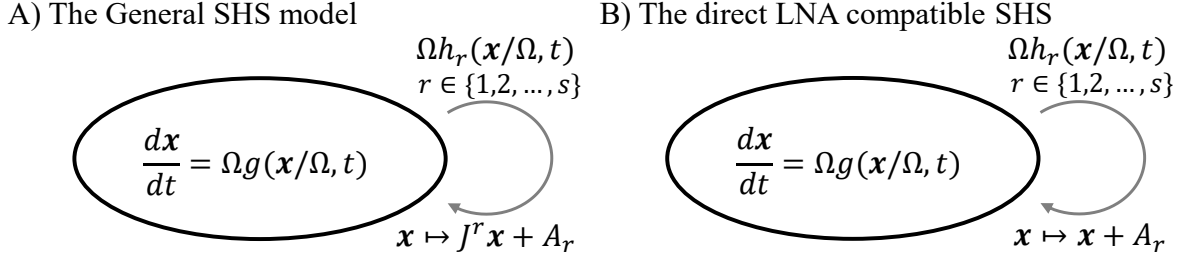


**Figure 8.1: The schematic of general SHS vs the ones in which linearization and LNA leads to the same results.** Continuous dynamics of the system are governed via a set of general ordinary differential equations  $g(\mathbf{x}/\Omega, t)$ . Different family of resets occur with transition intensity  $h_r(\mathbf{x}/\Omega, t)$ ,  $r \in \{1, \dots, s\}$ . Anytime that a reaction occurs the states of SHS change via a matrix  $J^r$  and a vector  $A_r$ . Note that for  $J^r \neq I_n$  the direct LNA using omega expansion is not valid.

Moreover this system consists of  $s$  stochastic events where reset map of each event  $r \in \{1, \dots, s\}$  is represented as

$$\mathbf{x} \mapsto \mathbf{x} + A_r, \quad A_r \in \mathbb{R}^{n \times 1}, h_r : \mathbb{R}^{n \times 1} \times [0, \infty) \rightarrow \mathbb{R} \quad (8.24)$$

and occurring with transition probabilities  $\Omega h_r(\mathbf{x}/\Omega, t)$ . For this SHS model, the omega expansion using LNA directly and the linearization approach gives the same first and second order moment dynamics.

**Proof:** The proof of this theorem is separated into two parts, one where we derive the moment equations of the system from the master equation proposed by Van Kampen. In this method we break the states into their respective deterministic and stochastic variables and write the moment equations for the stochastic components. For the linearization method, we use the extended generator of SHS systems to get the uncentered moment equations of the states. Finally we transform these to centered moments about the deterministic solution. Comparing these moments equations with those derived in the omega expansion, we see that they are same.

Let  $\phi_q$  and  $\epsilon_q$  be the deterministic part and the stochastic counterpart of the  $q^{th}$  state. We obtain the deterministic part as the solution of

$$\frac{d\phi_q}{dt} = \sum_{r=1}^s A_{qr} h_r(\phi_1, \dots, \phi_n) + g_q(\phi_1, \dots, \phi_n). \quad (8.25)$$

Note that for simplicity of notation, we drop the arguments of the functions  $h_r$  and  $g_q$  in the following analysis. We obtain the reduced master equation by truncating the expansion to  $\Omega^0$  as [158]

$$\begin{aligned} \frac{\partial \Pi}{\partial t} &= \sum_{r=1}^s \left( - \sum_{i=1}^n A_{ir} \frac{\partial}{\partial \epsilon_i} \sum_{j=1}^n \epsilon_j \frac{\partial h_r}{\partial \phi_j} \right) \Pi + \\ &\sum_{j=1}^n \left( - \sum_{i=1}^n \frac{\partial}{\partial \epsilon_i} \epsilon_j \frac{\partial g_i}{\partial \phi_j} \right) \Pi + \sum_{r=1}^s \left( \left( - \sum_{i=1}^n A_{ir} \frac{\partial}{\partial \epsilon_i} \right)^2 \frac{h_r}{2} \right) \Pi. \end{aligned} \quad (8.26)$$

Using this equation we obtain the first order moment equations of  $\epsilon_q$  as

$$\frac{d\langle \epsilon_q \rangle}{dt} = \sum_{r=1}^s A_{qr} \sum_{j=1}^n \langle \epsilon_j \rangle \frac{\partial h_r}{\partial \phi_j} + \sum_{j=1}^n \langle \epsilon_j \rangle \frac{\partial g_q}{\partial \phi_j}, \quad (8.27)$$

which for  $\langle \epsilon_j(0) \rangle = 0, \forall j \in \{1, \dots, m\}$ , implies that  $\langle \epsilon_q \rangle = 0, \forall t \geq 0$ . Further, it follows that the dynamics of  $\langle \mathbf{x}_q \rangle$  is that of  $\Omega \phi_q$ , shown in (8.25). The second order moment is

$$\frac{d\langle \epsilon_q^2 \rangle}{dt} = 2 \sum_{r=1}^s A_{qr} \sum_{i=1}^n \frac{\partial h_r}{\partial \phi_i} \langle \epsilon_i \epsilon_q \rangle + 2 \sum_{i=1}^n \frac{\partial g_q}{\partial \phi_i} \langle \epsilon_i \epsilon_q \rangle + \sum_{r=1}^s A_{qr}^2 f_r, \quad (8.28)$$

$$\begin{aligned} \frac{d\langle \epsilon_q \epsilon_l \rangle}{dt} &= \sum_{r=1}^s \left( A_{qr} \sum_{j=1}^n \frac{\partial h_r}{\partial \phi_j} \langle \epsilon_j \epsilon_l \rangle + A_{lr} \sum_{j=1}^n \frac{\partial h_r}{\partial \phi_j} \langle \epsilon_j \epsilon_q \rangle \right) \\ &+ \left( \sum_{j=1}^n \frac{\partial g_q}{\partial \phi_j} \langle \epsilon_j \epsilon_l \rangle + \sum_{j=1}^n \frac{\partial g_l}{\partial \phi_j} \langle \epsilon_j \epsilon_q \rangle \right) + \sum_{r=1}^s h_r A_{qr} A_{lr}. \end{aligned} \quad (8.29)$$

We then use the linearization method, which gives the following

$$\frac{d\langle (\mathbf{x}_q - \langle \mathbf{x}_q \rangle)^2 \rangle}{dt} = 2 \sum_{j=1}^n \left( \sum_{r=1}^s \frac{\partial h_r}{\partial \phi_j} A_{qr} + \frac{\partial g_q}{\partial \phi_j} \right) \langle (\mathbf{x}_q - \langle \mathbf{x}_q \rangle) (\mathbf{x}_j - \langle \mathbf{x}_j \rangle) \rangle + \sum_{r=1}^s \Omega h_r A_{qr}^2, \quad (8.30)$$

$$\begin{aligned}
\frac{d\langle(\mathbf{x}_q - \langle\mathbf{x}_q\rangle)(\mathbf{x}_l - \langle\mathbf{x}_l\rangle)\rangle}{dt} &= \sum_{r=1}^s \Omega h_r A_{qr} A_{lr} \\
&+ \sum_{j=1}^n \left( \sum_{r=1}^s \frac{\partial h_r}{\partial \phi_j} A_{qr} + \frac{\partial g_q}{\partial \phi_j} \right) \langle(\mathbf{x}_j - \langle\mathbf{x}_j\rangle)(\mathbf{x}_l - \langle\mathbf{x}_l\rangle)\rangle \\
&+ \sum_{j=1}^n \left( \sum_{r=1}^s \frac{\partial h_r}{\partial \phi_j} A_{lr} + \frac{\partial g_l}{\partial \phi_j} \right) \langle(\mathbf{x}_j - \langle\mathbf{x}_j\rangle)(\mathbf{x}_q - \langle\mathbf{x}_q\rangle)\rangle.
\end{aligned} \tag{8.31}$$

The fact that  $\mathbf{x}_j := \Omega\phi_j + \Omega^{1/2}\epsilon_j$ , means that (8.28) and (8.29) are centered moment equations. Comparing them with (8.30) and (8.31), we see that our centered moment dynamics from these two methods are the same. The final moment equations can be written in the form the matrix differential equation

$$\frac{dU}{dt} = B + \Delta U + U \Delta^T. \tag{8.32}$$

Here  $\Delta_{ij} = \sum_{r=1}^s A_{ir} \frac{\partial h_r}{\partial \phi_j} + \frac{\partial g_i}{\partial \phi_j}$ ,  $B_{ij} = \Omega \sum_{r=1}^s h_r A_{ir} A_{jr}$ ,  $U_{ij} = \langle(\mathbf{x}_i - \langle\mathbf{x}_i\rangle)(\mathbf{x}_j - \langle\mathbf{x}_j\rangle)\rangle$ .

■

The Lyapunov function derived from (8.32) at steady state has additional terms  $\frac{\partial g_i}{\partial \phi_j}$  compared to the Lyapunov function of biochemical reaction systems [160]. These terms represent the deterministic dynamics of the system in addition to the stochastic events. Note that the omega expansion with the LNA assumes that the fluctuations in the stochastic dynamics are of the order  $\Omega^{-1/2}$  with respect to the deterministic component (as seen in (8.3)). Hence in principle the noise as represented by the coefficient of variation  $\propto \Omega^{-1/2}$  and will tend to zero as  $\Omega \rightarrow \infty$ . Fluctuations of the order of the macroscopic variable ( $\Omega^0$ ) will be present in coefficient of variation for the resets of the form

$$\mathbf{x} \mapsto J^r \mathbf{x} + A_r, \quad A_r \in \mathbb{R}^{n \times 1}, \mathbf{x} \in \mathbb{R}^{n \times 1}, J^r \in \mathbb{R}^{n \times n}, \tag{8.33}$$

where  $J^r \neq I_n$  (Fig. 8.1). In the next section we propose an alternative approach to solving the moments of this system, where direct LNA via omega expansion is not applicable.

### 8.3 An Alternative Representation to Systems Where Direct LNA Fails

Consider a system with the dynamics

$$\text{Prob.}(\mathbf{x}(t + dt) = \mathbf{x} + 1) = \Omega h(\mathbf{x}/\Omega)dt, \quad (8.34)$$

$$\text{Prob.}(\mathbf{x}(t + dt) = h\mathbf{x} + a) = \Omega \gamma_x(\mathbf{x}/\Omega)dt. \quad (8.35)$$

As previously demonstrated, we break the state  $\mathbf{x}$  into two parts: one is the stochastic process which accounts for the macroscopic dynamics only  $\phi$ , and one which accounts for the stochasticity in production  $\epsilon$ , i.e.  $\mathbf{x} = \Omega\phi + \Omega^{1/2}\epsilon$ . By this definition, the following theorem provides an alternative representation of this system.

**Theorem 11** *For the system in (8.34)-(8.35) dynamics of  $\phi$  and  $\epsilon$  are as follows between events*

$$\frac{d\phi}{dt} = h(\phi), \quad \frac{d\epsilon}{dt} = -h(\phi)\Omega^{1/2}, \quad (8.36)$$

while the events are defined as

$$\text{Prob.} \left( \begin{array}{l} \phi(t + dt) = j\phi \\ \epsilon(t + dt) = j\epsilon + a\Omega^{-1/2} \end{array} \right) = \Omega \gamma_x(\phi + \Omega^{-1/2}\epsilon)dt, \quad (8.37)$$

$$\text{Prob.}(\epsilon(t + dt) = \epsilon + \Omega^{-1/2}) = \Omega h(\phi)dt. \quad (8.38)$$

**Proof:** For system in (8.34) and (8.35) we have  $p = \Pi(\phi, \epsilon, t)$ , thus

$$\frac{dp}{dt} = \frac{\partial \Pi}{\partial t} + \frac{d\epsilon}{dt} \frac{\partial \Pi}{\partial \epsilon} + \frac{d\phi}{dt} \frac{\partial \Pi}{\partial \phi} = \frac{\partial \Pi}{\partial t} - \Omega^{1/2} \frac{d\phi}{dt} \frac{\partial \Pi}{\partial \epsilon} + \frac{d\phi}{dt} \frac{\partial \Pi}{\partial \phi}. \quad (8.39)$$

We write the master equation as

$$\begin{aligned} & \frac{\partial \Pi}{\partial t} - \Omega^{1/2} \frac{d\phi}{dt} \frac{\partial \Pi}{\partial \epsilon} + \frac{d\phi}{dt} \frac{\partial \Pi}{\partial \phi} = \\ & \Omega \left( h(\phi + \Omega^{-1/2}(\epsilon - \Omega^{-1/2}))\Pi(\phi + \Omega^{-1/2}(\epsilon - \Omega^{-1/2})) \right. \\ & \quad \left. - h(\phi + \Omega^{-1/2}\epsilon)\Pi(\phi + \Omega^{-1/2}\epsilon) + \gamma_x \left( \frac{\phi}{j} + \Omega^{-1/2} \frac{\epsilon - a\Omega^{-1/2}}{j} \right) \times \right. \\ & \quad \left. \Pi \left( \frac{\phi}{j} + \Omega^{-1/2} \frac{\epsilon - a\Omega^{-1/2}}{j} \right) - \gamma_x(\phi + \Omega^{-1/2}\epsilon) \Pi(\phi + \Omega^{-1/2}\epsilon) \right). \end{aligned} \quad (8.40)$$

Now expanding this equation with respect to the deviation in  $\epsilon$ , we get

$$\begin{aligned}
\frac{\partial \Pi}{\partial t} - \Omega^{1/2} \frac{d\phi}{dt} \frac{\partial \Pi}{\partial \epsilon} + \frac{d\phi}{dt} \frac{\partial \Pi}{\partial \phi} &= \Omega \left( -\Omega^{-1/2} \frac{\partial}{\partial \epsilon} h(\phi + \Omega^{-1/2} \epsilon) \Pi(\phi + \Omega^{-1/2} \epsilon) \right. \\
&+ \frac{\Omega^{-1}}{2} \frac{\partial^2}{\partial \epsilon^2} h(\phi + \Omega^{-1/2} \epsilon) \Pi(\phi + \Omega^{-1/2} \epsilon) - a \Omega^{-1/2} \frac{\partial}{\partial \epsilon} \gamma_x \left( \frac{\phi}{j} + \Omega^{-1/2} \frac{\epsilon}{j} \right) \Pi \left( \frac{\phi}{j} + \Omega^{-1/2} \frac{\epsilon}{j} \right) \\
&+ a^2 \Omega^{-1} \frac{\partial^2}{\partial \epsilon^2} \gamma_x \left( \frac{\phi}{j} + \Omega^{-1/2} \frac{\epsilon}{j} \right) \Pi \left( \frac{\phi}{j} + \Omega^{-1/2} \frac{\epsilon}{j} \right) + \gamma_x \left( \frac{\phi}{j} + \Omega^{-1/2} \frac{\epsilon}{j} \right) \Pi \left( \frac{\phi}{j} + \Omega^{-1/2} \frac{\epsilon}{j} \right) \\
&\left. - \gamma_x(\phi + \Omega^{-1/2} \epsilon) \Pi(\phi + \Omega^{-1/2} \epsilon) \right).
\end{aligned} \tag{8.41}$$

Finally we can write the master equation for system described in (8.36)-(8.38), for which the results are identical to (8.41).  $\blacksquare$

As we mentioned earlier, the noise in the systems introduced above consist of fluctuations of the macroscopic scale. Direct LNA ignores such terms and hence the results obtained are erroneous, the transformation we introduced inherently accounts for these terms. This results in low errors of approximation. By having this alternative representation of the system we can now use the omega expansion to derive the moment dynamics of  $\phi$  and  $\epsilon$ . Note that the moment dynamics obtained from this method are still not closed. However they are in the standard form and any closure approximation can be applied to solve them. In the following, we applied this method to an example motivated by growth and division of living cells.

## 8.4 An Illustrative Example

Consider a system with the following dynamics

$$\text{Prob.}(\mathbf{x}(t + dt) = \mathbf{x} + 1) = \Omega k_x dt, \tag{8.42}$$

$$\text{Prob.}(\mathbf{x}(t + dt) = \mathbf{x}/2) = \gamma_x \mathbf{x} dt. \tag{8.43}$$

This system can be seen as the model of protein count progressing through many cell cycles and divisions. Protein molecules are produced in random events and any time a division event occurs, the molecules are halved in between daughter cells. We also consider that proteins are stable without degradation, due to the fact that many

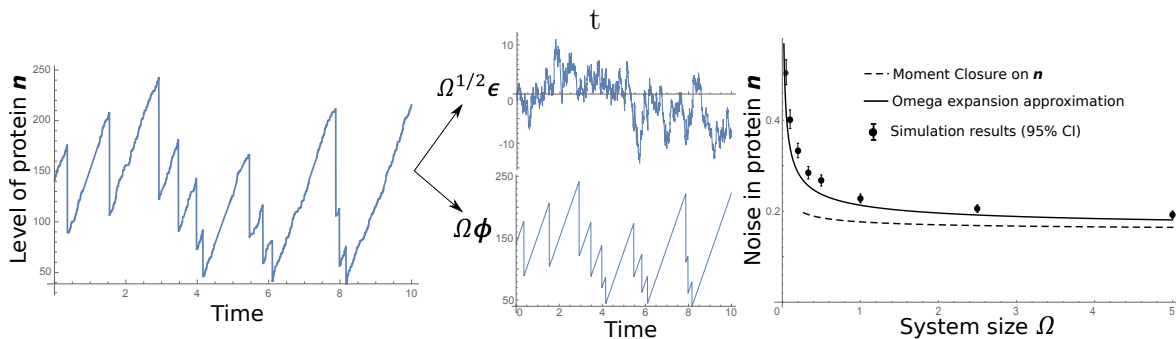


**Figure 8.2:** The fluctuations in protein  $x$  can be split into a macroscopic part and a stochastic production part. *Left.* The large fluctuations in proteins are reflected in the macroscopic part and the smaller fluctuations correspond to the stochastic production part. *Right.* The noise in protein ( $CV_x^2$ ) can be approximated well by our omega expansion technique when the system size increases. Note that this approximation is better than simply applying moment closure on the moment dynamics of  $x$ . The 95% confidence intervals are obtained via bootstrapping based on 5,000 realizations.

proteins have half-lives much longer than the cell division time [72–74]. As mentioned earlier LNA is not directly applicable in this case. Hence we use the alternative system introduced in Theorem 2 by choosing  $h(\phi) = k_x$ ,  $j = \frac{1}{2}$ , and  $a = 0$ . We assume the following scalings for the variables

$$\phi \sim \Omega^{-1/2}, \quad \epsilon \sim \Omega^{-1/4}. \quad (8.44)$$

Using these scalings, for large  $\Omega$ , we assume  $\phi \gg \Omega^{-1/2}\epsilon$  and hence we can approximate the moment dynamics to

$$\frac{d\langle\epsilon\rangle}{dt} = -\frac{\gamma_x\Omega}{2}\langle\epsilon\phi\rangle, \quad (8.45)$$

$$\frac{d\langle\epsilon^2\rangle}{dt} = k_x - \frac{3\gamma_x\Omega}{4}\langle\epsilon^2\phi\rangle, \quad (8.46)$$

$$\frac{d\langle\phi\rangle}{dt} = k_x - \frac{\gamma_x\Omega}{2}\langle\phi^2\rangle. \quad (8.47)$$

Due to the presence of the third order moment  $\langle\epsilon^2\phi\rangle$ , the moment dynamics of this system are not closed. From (8.44), this term exhibits scaling of  $\Omega^{-1}$ . Hence we

consider the following general form of this term at steady-state

$$\langle \overline{\epsilon^2 \phi} \rangle = \langle \overline{\epsilon^2} \rangle \langle \overline{\phi} \rangle + \eta \Omega^{-1}. \quad (8.48)$$

Here the coefficient  $\eta$  quantifies the correlation in this specific cross moment of  $\phi$  and  $\epsilon$ . The steady-state analysis of (8.45)-(8.47) gives

$$\langle \overline{\phi^2} \rangle = \frac{2k_x}{\gamma_x \Omega}, \quad \langle \overline{\epsilon \phi} \rangle = 0, \quad \langle \overline{\epsilon^2} \rangle = \sqrt{\frac{(1 + CV_\phi^2) \gamma_x}{2k_x \Omega}} \left( \frac{4k_x}{3\gamma_x} - \eta \right). \quad (8.49)$$

We can see that the scalings of  $\epsilon$  and  $\phi$  in (8.44), are justified as  $\langle \overline{\epsilon^2} \rangle \propto \Omega^{-1/2}$  and  $\langle \overline{\phi^2} \rangle \propto \Omega^{-1}$ . Here  $CV_\phi^2$  is the coefficient of variation squared of  $\phi$ . The noise in  $\mathbf{x}$  can be derived as

$$CV_x^2 = CV_\phi^2 + \frac{\langle \overline{\epsilon^2} \rangle}{\Omega \langle \overline{\phi} \rangle^2} = CV_\phi^2 + \overbrace{\frac{\sqrt{2}(1 + CV_\phi^2)^{3/2} \gamma_x^{1/2}}{3\Omega^{1/2} k_x^{1/2}}}^{\text{from stochastic production}} - \overbrace{\eta \frac{(1 + CV_\phi^2)^{3/2} \gamma_x^{3/2}}{2\sqrt{2}\Omega^{1/2} k_x^{3/2}}}^{\text{from correlation of } \epsilon^2 \text{ and } \phi}. \quad (8.50)$$

For high values of  $\Omega$ , the correlation in  $\langle \overline{\epsilon^2 \phi} \rangle$  represented by  $\eta$  is small. Hence the noise can be approximated as

$$CV_x^2 \approx CV_\phi^2 + \frac{\sqrt{2}(1 + CV_\phi^2)^{3/2} \gamma_x^{1/2}}{3\Omega^{1/2} k_x^{1/2}}. \quad (8.51)$$

This expression shows that for  $\Omega \rightarrow \infty$ , the noise in  $\mathbf{x}$  tends to that in  $\phi$ . Note that in order to get the noise in  $\phi$  we need  $\langle \overline{\phi} \rangle$ . To this end, we use the scalings in the variables to reduce the moment dynamics of the second order moment to

$$\frac{d\langle \overline{\phi^2} \rangle}{dt} = 2k_x \langle \overline{\phi} \rangle - \frac{3\gamma_x \Omega}{4} \langle \overline{\phi^3} \rangle. \quad (8.52)$$

This equation involves the third order moment of  $\phi$  showing that the system of equations cannot be solved or closed. Hence we use the derivative matching approach which shows superior performance in many cases, to obtain the relationship of  $\langle \overline{\phi^3} \rangle$  in terms of the lower order moments [154, 155]

$$\langle \overline{\phi^3} \rangle \approx \frac{\langle \overline{\phi^2} \rangle^3}{\langle \overline{\phi} \rangle^3}. \quad (8.53)$$

Using this relationship we get the noise in  $\phi$  as

$$CV_{\phi}^2 = \frac{2 - \sqrt{3}}{\sqrt{3}}. \quad (8.54)$$

Finally we compare the approximate expression for noise in  $\mathbf{x}$  to that of simulations (Fig. 8.2). Note that the noise in  $\mathbf{x}$  from the simulations and analytical formula are very close for high system size  $\Omega$ . This is because the assumptions used to derive the analytical formula are valid at high  $\Omega$ . The correlation term is an important term which we have neglected to derive the noise approximation. This is a simplifying assumption which may be inaccurate in some regimes. Finally, a natural question is whether moment closure on the dynamics of  $\mathbf{x}$  without  $\phi$ ,  $\epsilon$  separation yields a better approximation of the noise. To see this, we compare our approach to the moment closure method and see that our approximation outperforms closure on  $\mathbf{x}$  (Fig. 8.2).

## 8.5 Conclusion

We compared the linearization and omega expansion through a birth/death regulation example. We observed that for this example these methods give the same results. We find that the direct LNA method does not work, for systems with stochastic transitions of the form  $\mathbf{x} \mapsto J^r \mathbf{x} + A_r$ ,  $J^r \neq I_n$  and it does for  $J^r = I_n$ . For the latter systems we showed that the linearization technique gives the same moment dynamics equations as the omega expansion.

## Chapter 9

### DISCUSSION

Moment analysis of Stochastic Hybrid Systems (SHS) often relies on deriving a set of differential equations for the time evolution of moments [28, 78]. For linear stochastic systems, moments can be obtained exactly by solving these set of differential equations. However, nonlinearities within SHS, such as the transition intensity (4.1), lead to unclosed dynamics in the sense that time evolution of lower-order moments depends on higher-order moments. In such cases, moment computations are performed by either employing approximate closure schemes [152–156, 169–173], or constraints imposed by positive semidefiniteness of moment matrices [174–176].

Here we introduced two main methods for deriving the exact solutions of moments. In the first method we model arrival of events using phase-type processes [25], and show that the resulting systems has closed moment dynamics. In the second method, instead of relying on moment dynamics, we used an alternative approach to derive exact analytical expressions for the first two steady-state moments of TTSHS. Finally, applying the theory of TTSHS to the biological example of gene expression resulted in novel formulas for the mean and variance in the level of a gene product, and how these levels are impacted by stochasticity in cell-cycle times and the molecular partitioning process. Further, we extend our method to consider TTSHS where continuous dynamics follow a stochastic differential equation, or multi-mode TTSHS that allow for stochastic switching between linear systems. Finally, we proposed an alternative approximation for the case of nonlinear SHS. We showed the applicability of the method with an example motivated from the biologically relevant protein partitioning during cell division.

## BIBLIOGRAPHY

- [1] M. H. A. Davis, “Piecewise-deterministic markov processes: A general class of non-diffusion stochastic models,” *Journal of the Royal Statistical Society. Series B (Methodological)*, vol. 46, pp. 353–388, 1984.
- [2] O. L. V. Costa, “Stationary distributions for piecewise-deterministic markov processes,” *Journal of Applied Probability*, vol. 27, pp. 60–73, 1990.
- [3] M. H. A. Davis, *Markov models and optimization*. Chapman and Hall, 1993.
- [4] O. L. V. Costa and F. Dufour, “Stability and ergodicity of piecewise deterministic markov processes,” *SIAM Journal on Control and Optimization*, vol. 47, pp. 1053–1077, 2008.
- [5] X. Feng, K. A. Loparo, Y. Ji, and H. J. Chizeck, “Stochastic stability properties of jump linear systems,” *IEEE Transactions on Automatic Control*, vol. 37, pp. 38–53, 1992.
- [6] D. P. D. Farias, J. C. Geromel, J. B. R. D. Val, and O. L. V. Costa, “Output feedback control of markov jump linear systems in continuous-time,” *IEEE Transactions on Automatic Control*, vol. 45, pp. 944–949, 2000.
- [7] O. L. V. Costa, M. D. Fragoso, and R. P. Marques, *Discrete-Time Markov Jump Linear Systems*. Springer Science and Business Media, 2008.
- [8] B. De Saporta, F. Dufour, and H. Zhang, *Numerical methods for simulation and optimization of piecewise deterministic markov processes*. John Wiley & Sons, 2015.
- [9] D. Antunes, J. Hespanha, and C. Silvestre, “Volterra integral approach to impulsive renewal systems: Application to networked control,” *IEEE Transactions on Automatic Control*, vol. 57, pp. 607–619, 2012.
- [10] J. P. Hespanha, “Modeling and analysis of networked control systems using stochastic hybrid systems,” *Annual Reviews in Control*, vol. 38, pp. 155–170, 2014.
- [11] D. Antunes, J. Hespanha, and C. Silvestre, “Stability of networked control systems with asynchronous renewal links: An impulsive systems approach,” *Automatica*, vol. 49, pp. 402–413, 2013.

- [12] T. Gommans, D. Antunes, T. Donkers, P. Tabuada, and M. Heemels, “Self-triggered linear quadratic control,” *Automatica*, vol. 50, pp. 1279–1287, 2014.
- [13] W. P. M. H. Heemels, K. H. Johansson, and P. Tabuada, “An introduction to event-triggered and self-triggered control,” in *51st IEEE Conference on Decision and Control*, 2012, pp. 3270–3285.
- [14] D. J. Antunes and B. A. Khashoeei, “Consistent event-triggered methods for linear quadratic control,” in *2016 IEEE 55th Conference on Decision and Control*, 2016, pp. 1358–1363.
- [15] A. Anta and P. Tabuada, “To sample or not to sample: Self-triggered control for nonlinear systems,” *IEEE Transactions on Automatic Control*, vol. 55, pp. 2030–2042, 2010.
- [16] M. Soltani and A. Singh, “Control design and analysis of a stochastic network control system,” *arXiv preprint:1704.00236*, 2017.
- [17] B. A. Khashoeei, D. J. Antunes, and W. P. M. H. Heemels, “Output-based event-triggered control with performance guarantees,” *IEEE Transactions on Automatic Control*, vol. 62, pp. 3646–3652, 2017.
- [18] M. Soltani and A. Singh, “Moment-based analysis of stochastic hybrid systems with renewal transitions,” *Automatica*, vol. 84, pp. 62–69, 2017.
- [19] D. Antunes and A. Singh, “Quantifying gene expression variability arising from randomness in cell division times,” *Journal of Mathematical Biology*, vol. 71, pp. 437–463, 2015.
- [20] M. Soltani, C. A. Vargas-Garcia, D. Antunes, and A. Singh, “Intercellular variability in protein levels from stochastic expression and noisy cell cycle processes,” *PLOS Computational Biology*, p. e1004972, 2016.
- [21] M. Soltani and A. Singh, “Moment dynamics for linear time-triggered stochastic hybrid systems,” *IEEE 55th Conference on Decision and Control*, pp. 3702–3707, 2016.
- [22] B. Daigle, M. Soltani, L. Petzold, and A. Singh, “Inferring single-cell gene expression mechanisms using stochastic simulation,” *Bioinformatics*, vol. 31, pp. 1428–1435, 2015.
- [23] A. Singh, “Modeling noise mechanisms in neuronal synaptic transmission,” *bioRxiv*, 2017.
- [24] D. Antunes, J. Hespanha, and C. Silvestre, “Impulsive systems triggered by superposed renewal processes,” in *Proc. of the 49th IEEE Conf. on Decision and Control, Atlanta, GA*, 2010, pp. 1779–1784.

- [25] H. C. Tijms, *Stochastic models: an algorithmic approach*. John Wiley & Sons, 1994.
- [26] P. Buchholz, J. Kriege, and I. Felko, *Input Modeling with Phase-Type Distributions and Markov Models*, ser. SpringerBriefs in Mathematics. Springer, 2014.
- [27] S. Lagershausen, *Performance Analysis of Closed Queueing Networks*, ser. Lecture Notes in Economics and Mathematical Systems. Springer, 2013.
- [28] J. P. Hespanha and A. Singh, “Stochastic models for chemically reacting systems using polynomial stochastic hybrid systems,” *International Journal of Robust and Nonlinear Control*, vol. 15, pp. 669–689, 2005.
- [29] J. P. Hespanha, “Polynomial stochastic hybrid systems,” in *Hybrid Systems : Computation and Control (HSCC) 2005*, Zurich, Switzerland, 2005.
- [30] W. J. Blake, M. Kaern, C. R. Cantor, and J. J. Collins, “Noise in eukaryotic gene expression,” *Nature*, vol. 422, pp. 633–637, 2003.
- [31] J. M. Raser and E. K. O’Shea, “Noise in gene expression: Origins, consequences, and control,” *Science*, vol. 309, pp. 2010 – 2013, 2005.
- [32] G. Neuert, B. Munsky, R. Z. Tan, L. Teytelman, M. Khammash, and A. van Oudenaarden, “Systematic identification of signal-activated stochastic gene regulation,” *Science*, vol. 339, pp. 584–587, 2013.
- [33] E. Libby, T. J. Perkins, and P. S. Swain, “Noisy information processing through transcriptional regulation,” *Proceedings of the National Academy of Sciences*, vol. 104, pp. 7151–7156, 2007.
- [34] H. B. Fraser, A. E. Hirsh, G. Giaever, J. Kumm, and M. B. Eisen, “Noise minimization in eukaryotic gene expression,” *PLOS Biology*, vol. 2, p. e137, 2004.
- [35] B. Lehner, “Selection to minimise noise in living systems and its implications for the evolution of gene expression,” *Molecular Systems Biology*, vol. 4, p. 170, 2008.
- [36] R. Losick and C. Desplan, “Stochasticity and cell fate,” *Science*, vol. 320, pp. 65–68, 2008.
- [37] A. P. Arkin, J. Ross, and H. H. McAdams, “Stochastic kinetic analysis of developmental pathway bifurcation in phage  $\lambda$ -infected *Escherichia coli* cells,” *Genetics*, vol. 149, pp. 1633–1648, 1998.
- [38] L. S. Weinberger, J. Burnett, J. Toettcher, A. Arkin, and D. Schaffer, “Stochastic gene expression in a lentiviral positive-feedback loop: HIV-1 Tat fluctuations drive phenotypic diversity,” *Cell*, vol. 122, pp. 169–182, 2005.

- [39] L. S. Weinberger, R. D. Dar, and M. L. Simpson, “Transient-mediated fate determination in a transcriptional circuit of HIV,” *Nature Genetics*, vol. 40, pp. 466–470, 2008.
- [40] A. Singh and L. S. Weinberger, “Stochastic gene expression as a molecular switch for viral latency,” *Current Opinion in Microbiology*, vol. 12, pp. 460–466, 2009.
- [41] R. D. Dar, N. N. Hosmane, M. R. Arkin, R. F. Siliciano, and L. S. Weinberger, “Screening for noise in gene expression identifies drug synergies,” *Science*, vol. 344, pp. 1392–1396, 2014.
- [42] A. Eldar and M. B. Elowitz, “Functional roles for noise in genetic circuits,” *Nature*, vol. 467, pp. 167–173, 2010.
- [43] J. Veening, W. K. Smits, and O. P. Kuipers, “Bistability, epigenetics, and bet-hedging in bacteria,” *Annual Review of Microbiology*, vol. 62, pp. 193–210, 2008.
- [44] E. Kussell and S. Leibler, “Phenotypic diversity, population growth, and information in fluctuating environments,” *Science*, vol. 309, pp. 2075–2078, 2005.
- [45] N. Balaban, J. Merrin, R. Chait, L. Kowalik, and S. Leibler, “Bacterial persistence as a phenotypic switch,” *Science*, vol. 305, pp. 1622–1625, 2004.
- [46] M. A. Sánchez-Romero and J. Casadesús, “Contribution of phenotypic heterogeneity to adaptive antibiotic resistance,” *Proceedings of the National Academy of Sciences*, vol. 111, pp. 355–360, 2014.
- [47] T. M. A. Neildez-Nguyen, A. Parisot, C. Vignal, P. Rameau, D. Stockholm, J. Picot, V. Allo, C. Le Bec, C. Laplace, and A. Paldi, “Epigenetic gene expression noise and phenotypic diversification of clonal cell populations,” *Differentiation*, vol. 76, pp. 33–40, 2008.
- [48] A. Paldi, “Stochastic gene expression during cell differentiation: order from disorder?” *Cellular and Molecular Life Sciences*, vol. 60, pp. 1775–1778, 2003.
- [49] A. Raj and A. van Oudenaarden, “Nature, nurture, or chance: stochastic gene expression and its consequences,” *Cell*, vol. 135, pp. 216–226, 2008.
- [50] M. Kærn, T. C. Elston, W. J. Blake, and J. J. Collins, “Stochasticity in gene expression: from theories to phenotypes,” *Nature Reviews Genetics*, vol. 6, pp. 451–464, 2005.
- [51] A. Magklara and S. Lomvardas, “Stochastic gene expression in mammals: lessons from olfaction,” *Trends in Cell Biology*, vol. 23, pp. 449–456, 2014.
- [52] B. Munsky, B. Trinh, and M. Khammash, “Listening to the noise: random fluctuations reveal gene network parameters,” *Molecular Systems Biology*, vol. 5, p. 318, 2009.

- [53] G. Lambert and E. Kussell, “Quantifying selective pressures driving bacterial evolution using lineage analysis,” *Physical Review X*, vol. 5, p. 011016, 2015.
- [54] R. Tsukanov, G. Reshes, G. Carmon, E. Fischer-Friedrich, N. S. Gov, I. Fishov, and M. Feingold, “Timing of z-ring localization in escherichia coli,” *Physical Biology*, vol. 8, p. 066003, 2011.
- [55] G. Reshes, S. Vanounou, I. Fishov, and M. Feingold, “Cell shape dynamics in escherichia coli,” *Biophysical Journal*, vol. 94, pp. 251–264, 2008.
- [56] ———, “Timing the start of division in e. coli: a single-cell study,” *Physical Biology*, vol. 5, p. 046001, 2008.
- [57] A. Roeder, V. Chickarmane, B. Obara, B. Manjunath, and E. M. Meyerowitz, “Variability in the control of cell division underlies sepal epidermal patterning in *Arabidopsis thaliana*,” *PLOS Biology*, vol. 8, p. e1000367, 2010.
- [58] A. Zilman, V. Ganusov, and A. Perelson, “Stochastic models of lymphocyte proliferation and death,” *PLOS ONE*, vol. 5, p. e12775, 2010.
- [59] E. D. Hawkins, J. F. Markham, L. P. McGuinness, and P. Hodgkin, “A single-cell pedigree analysis of alternative stochastic lymphocyte fates,” *Proceedings of the National Academy of Sciences*, vol. 106, pp. 13 457–13 462, 2009.
- [60] E. B. Stukalin, I. Aifuwa, J. S. Kim, D. Wirtz, and S. Sun, “Age-dependent stochastic models for understanding population fluctuations in continuously cultured cells,” *Journal of the Royal Society Interface*, vol. 10, p. 20130325, 2013.
- [61] D. Huh and J. Paulsson, “Random partitioning of molecules at cell division,” *Proceedings of the National Academy of Sciences*, vol. 108, pp. 15 004–15 009, 2011.
- [62] D. Gonze, “Modeling the effect of cell division on genetic oscillators,” *Journal of Theoretical Biology*, vol. 325, pp. 22–33, 2013.
- [63] J. Lloyd-Price, H. Tran, and A. S. Ribeiro, “Dynamics of small genetic circuits subject to stochastic partitioning in cell division,” *Journal of Theoretical Biology*, vol. 356, pp. 11–19, 2014.
- [64] C. J. Zopf, K. Quinn, J. Zeidman, and N. Maheshri, “Cell-cycle dependence of transcription dominates noise in gene expression,” *PLOS Computational Biology*, vol. 9, p. e1003161, 2013.
- [65] J. Narula, A. Kuchina, D.-y. D. Lee, M. Fujita, G. M. Süel, and O. A. Igoshin, “Chromosomal arrangement of phosphorelay genes couples sporulation and DNA replication,” *Cell*, vol. 162, pp. 328–337, 2015.

- [66] A. Schwabe and F. J. Bruggeman, “Contributions of cell growth and biochemical reactions to nongenetic variability of cells,” *Biophysical Journal*, vol. 107, pp. 301–313, 2014.
- [67] D. Huh and J. Paulsson, “Non-genetic heterogeneity from stochastic partitioning at cell division,” *Nature Genetics*, vol. 43, pp. 95–100, 2011.
- [68] J. Paulsson, “Model of stochastic gene expression,” *Physics of Life Reviews*, vol. 2, pp. 157–175, 2005.
- [69] V. Shahrezaei and P. S. Swain, “Analytical distributions for stochastic gene expression,” *Proceedings of the National Academy of Sciences*, vol. 105, pp. 17 256–17 261, 2008.
- [70] A. Singh and J. P. Hespanha, “Optimal feedback strength for noise suppression in autoregulatory gene networks,” *Biophysical Journal*, vol. 96, pp. 4013–4023, 2009.
- [71] T. Jia and R. V. Kulkarni, “Intrinsic noise in stochastic models of gene expression with molecular memory and bursting,” *Journal of Mathematical Biology*, vol. 106, p. 058102, 2011.
- [72] U. Alon, *An introduction to systems biology: design principles of biological circuits*. Chapman and Hall/CRC, 2011.
- [73] Y. Taniguchi, P. J. Choi, G. W. Li, H. Chen, M. Babu, J. Hearn, A. Emili, and X. S. Xie, “Quantifying E. coli proteome and transcriptome with single-molecule sensitivity in single cells,” *Science*, vol. 329, pp. 533–538, 2010.
- [74] B. Schwanhauser, D. Busse, N. Li, G. Dittmar, J. Schuchhardt, J. Wolf, W. Chen, and M. Selbach, “Global quantification of mammalian gene expression control,” *Nature*, vol. 473, pp. 337–342, 2011.
- [75] P. S. Swain, M. B. Elowitz, and E. D. Siggia, “Intrinsic and extrinsic contributions to stochasticity in gene expression,” *Proceedings of the National Academy of Sciences*, vol. 99, pp. 12 795–12 800, 2002.
- [76] O. G. Berg, “A model for the statistical fluctuations of protein numbers in a microbial population,” *Journal of Theoretical Biology*, vol. 71, pp. 587–603, 1978.
- [77] D. R. Rigney, “Stochastic model of constitutive protein levels in growing and dividing bacterial cells,” *Journal of Theoretical Biology*, vol. 76, pp. 453–480, 1979.
- [78] A. Singh and J. P. Hespanha, “Stochastic hybrid systems for studying biochemical processes,” *Philosophical Transactions of the Royal Society A*, vol. 368, pp. 4995–5011, 2010.

- [79] H. Wang, Z. Yuan, P. Liu, and T. Zhou, “Division time-based amplifiers for stochastic gene expression,” *Molecular BioSystems*, 2015.
- [80] A. Hilfinger and J. Paulsson, “Separating intrinsic from extrinsic fluctuations in dynamic biological systems,” *Proceedings of the National Academy of Sciences*, vol. 108, pp. 12 167–12 172, 2011.
- [81] A. Singh and M. Soltani, “Quantifying intrinsic and extrinsic variability in stochastic gene expression models,” *PLOS ONE*, vol. 8, p. e84301, 2013.
- [82] V. Shahrezaei, J. F. Ollivier, and P. S. Swain, “Colored extrinsic fluctuations and stochastic gene expression,” *Molecular Systems Biology*, vol. 4, 2008.
- [83] M. Scott, B. Ingalls, and M. Kaern, “Estimations of intrinsic and extrinsic noise in models of nonlinear genetic networks,” *CHAOS*, vol. 16, p. 026107, 2006.
- [84] E. M. Ozbudak, M. Thattai, I. Kurtser, A. D. Grossman, and A. van Oudenaarden, “Regulation of noise in the expression of a single gene,” *Nature Genetics*, vol. 31, pp. 69–73, 2002.
- [85] J. R. S. Newman, S. Ghaemmaghani, J. Ihmels, D. K. Breslow, M. Noble, J. L. DeRisi, and J. S. Weissman, “Single-cell proteomic analysis of *S. cerevisiae* reveals the architecture of biological noise,” *Nature Genetics*, vol. 441, pp. 840–846, 2006.
- [86] A. Singh, B. Razooky, C. D. Cox, M. L. Simpson, and L. S. Weinberger, “Transcriptional bursting from the HIV-1 promoter is a significant source of stochastic noise in HIV-1 gene expression,” *Biophysical Journal*, vol. 98, pp. L32–L34, 2010.
- [87] A. Bar-Even, J. Paulsson, N. Maheshri, M. Carmi, E. O’Shea, Y. Pilpel, and N. Barkai, “Noise in protein expression scales with natural protein abundance,” *Nature Genetics*, vol. 38, pp. 636–643, 2006.
- [88] M. Jangi, P. L. Boutz, P. Paul, and P. A. Sharp, “Rbfox2 controls autoregulation in RNA-binding protein networks,” *Genes & Development*, vol. 28, pp. 637–651, 2014.
- [89] L.-H. So, A. Ghosh, C. Zong, L. A. Sepúlveda, R. Segev, and I. Golding, “General properties of transcriptional time series in *escherichia coli*,” *Nature Genetics*, vol. 43, pp. 554–560, 2011.
- [90] D. M. Suter, N. Molina, D. Gatfield, K. Schneider, U. Schibler, and F. Naef, “Mammalian genes are transcribed with widely different bursting kinetics,” *Science*, vol. 332, pp. 472–474, 2011.
- [91] R. D. Dar, B. S. Razooky, A. Singh, T. V. Trimeloni, J. M. McCollum, C. D. Cox, M. L. Simpson, and L. S. Weinberger, “Transcriptional burst frequency and burst size are equally modulated across the human genome,” *Proceedings of the National Academy of Sciences*, vol. 109, pp. 17 454–17 459, 2012.

- [92] A. Singh, “Transient changes in intercellular protein variability identify sources of noise in gene expression,” *Biophysical Journal*, vol. 107, pp. 2214–2220, 2014.
- [93] G. Hornung, R. Bar-Ziv, D. Rosin, N. Tokuriki, D. S. Tawfik, M. Oren, and N. Barkai, “Noise-mean relationship in mutated promoters,” *Genome Research*, vol. 22, pp. 2409–2417, 2012.
- [94] A. Raj, C. Peskin, D. Tranchina, D. Vargas, and S. Tyagi, “Stochastic mRNA synthesis in mammalian cells,” *PLOS Biology*, vol. 4, p. e309, 2006.
- [95] A. Singh, B. S. Razooky, R. D. Dar, and L. S. Weinberger, “Dynamics of protein noise can distinguish between alternate sources of gene-expression variability,” *Molecular Systems Biology*, vol. 8, p. 607, 2012.
- [96] K. B. Halpern, S. Tanami, S. Landen, M. Chapal, L. Szlak, A. Hutzler, A. Nizhberg, and S. Itzkovitz, “Bursty gene expression in the intact mammalian liver,” *Molecular Cell*, vol. 58, pp. 147–156, 2015.
- [97] C. R. Bartman, S. C. Hsu, C. C.-S. Hsiung, A. Raj, and G. A. Blobel, “Enhancer regulation of transcriptional bursting parameters revealed by forced chromatin looping,” *Molecular Cell*, vol. 62, pp. 237 – 247, 2016.
- [98] C. R. Brown and H. Boeger, “Nucleosomal promoter variation generates gene expression noise,” *Proceedings of the National Academy of Sciences*, vol. 111, pp. 17 893–17 898, 2014.
- [99] L. Cai and N. F. X. S. Xie, “Stochastic protein expression in individual cells at the single molecule level,” *Nature*, vol. 440, pp. 358–362, Sep. 2006.
- [100] A. Singh and J. J. Dennehy, “Stochastic holin expression can account for lysis time variation in the bacteriophage  $\lambda$ ,” *Journal of the Royal Society Interface*, vol. 11, p. 20140140, 2014.
- [101] S. Uphoff, N. D. Lord, B. Okumus, L. Potvin-Trottier, D. J. Sherratt, and J. Paulsson, “Stochastic activation of a dna damage response causes cell-to-cell mutation rate variation,” *Science*, vol. 351, pp. 1094–1097, 2016.
- [102] P. J. Choi, L. Cai, K. Frieda, and X. S. Xie, “A stochastic single-molecule event triggers phenotype switching of a bacterial cell,” *Science*, vol. 322, pp. 442–446, 2008.
- [103] T. M. Norman, N. D. Lord, J. Paulsson, and R. Losick, “Stochastic switching of cell fate in microbes,” *Annual Review of Microbiology*, vol. 69, pp. 381–403, 2015.

- [104] C. C.-S. Hsiung, C. R. Bartman, P. Huang, P. Ginart, A. J. Stonestrom, C. A. Keller, C. Face, K. S. Jahn, P. Evans, L. Sankaranarayanan, B. Giardine, R. C. Hardison, A. Raj, and G. A. Blobel, “A hyperactive transcriptional state marks genome reactivation at the mitosis g1 transition,” *Genes & Development*, vol. 30, pp. 1423–1439, 2016.
- [105] J. Yu, J. Xiao, X. Ren, K. Lao, and X. S. Xie, “Probing gene expression in live cells, one protein molecule at a time,” *Science*, vol. 311, pp. 1600–1603, 2006.
- [106] S. O. Skinner, H. Xu, S. Nagarkar-Jaiswal, P. R. Freire, T. P. Zwaka, and I. Golding, “Single-cell analysis of transcription kinetics across the cell cycle,” *eLife*, vol. 5, p. e12175, 2016.
- [107] O. Padovan-Merhar, G. P. Nair, A. G. Biaesch, A. Mayer, S. Scarfone, S. W. Foley, A. R. Wu, L. S. Churchman, A. Singh, and A. Raj, “Single mammalian cells compensate for differences in cellular volume and DNA copy number through independent global transcriptional mechanisms,” *Molecular Cell*, vol. 58, pp. 339–352, 2015.
- [108] M. Thattai, “Universal poisson statistics of mrnas with complex decay pathways,” *Biophysical Journal*, vol. 110, pp. 301–305, 2016.
- [109] A. N. Boettiger, “Analytic Approaches to Stochastic Gene Expression in Multicellular Systems,” *Biophysical Journal*, vol. 105, no. 12, pp. 2629–2640, 2013.
- [110] J. Rausenberger and M. Kollmann, “Quantifying origins of cell-to-cell variations in gene expression,” *Biophysical Journal*, vol. 95, pp. 4523–4528, 2008.
- [111] K. H. Kim and H. M. Sauro, “Measuring retroactivity from noise in gene regulatory networks,” *Biophysical Journal*, vol. 100, pp. 1167–1177, 2011.
- [112] M. Soltani, P. Bokes, Z. Fox, and A. Singh, “Nonspecific transcription factor binding can reduce noise in the expression of downstream proteins,” *Physical Biology*, vol. 12, p. 055002, 2015, undergraduate student marked with \*.
- [113] Y. Li, D. Liu, C. López-Paz, B. J. Olson, and J. G. Umen, “A new class of cyclin dependent kinase in chlamydomonas is required for coupling cell size to cell division,” *eLife*, vol. 5, p. e10767, 2016.
- [114] K. M. Schmoller, J. J. Turner, M. Koivomagi, and J. M. Skotheim, “Dilution of the cell cycle inhibitor Whi5 controls budding-yeast cell size,” *Nature*, vol. 526, pp. 268–272, 2015.
- [115] K. M. Schmoller and J. M. Skotheim, “The biosynthetic basis of cell size control,” *Trends in Cell Biology*, vol. 25, pp. 793–802, 2015.

- [116] S. M. Ross, “Reliability theory,” in *Introduction to Probability Models*, 10th ed. Academic Press, 2010, pp. 579–629.
- [117] M. Finkelstein, “Failure rate and mean remaining lifetime,” in *Failure Rate Modelling for Reliability and Risk*, ser. Springer Series in Reliability Engineering. Springer, 2008, pp. 9–44.
- [118] M. Evans, N. Hastings, and B. Peacock, *Statistical Distributions*, 3rd ed. Wiley, 2000.
- [119] C. A. Vargas-García, M. Soltani, and A. Singh, “Conditions for cell size homeostasis: A stochastic hybrid systems approach,” *IEEE Life Sciences Letters*, vol. 2, pp. 47–50, 2016.
- [120] H. D. Macedo and J. N. Oliveira, “Typing linear algebra: A biproduct-oriented approach,” *Science of Computer Programming*, vol. 78, pp. 2160–2191, 2013.
- [121] F. Zhang and Q. Zhang, “Eigenvalue inequalities for matrix product,” *IEEE Transactions on Automatic Control*, vol. 51, pp. 1506 – 1509, 2006.
- [122] R. A. Horn and C. R. Johnson, *Topics in Matrix Analysis*. Cambridge University Press, 1991.
- [123] M. Di Ventra, S. Evoy, J. R. Heflin, and D. J. Lockwood, Eds., *Introduction to Nanoscale Science and Technology*, ser. Nanostructure Science and Technology. Springer US, 2004.
- [124] K. L. Ekinici, Y. T. Yang, and M. L. Roukes, “Ultimate limits to inertial mass sensing based upon nanoelectromechanical systems,” *Journal of Applied Physics*, vol. 95, pp. 2682–2689, 2004.
- [125] J. Tamayo, P. M. Kosaka, J. J. Ruz, A. San Paulo, and M. Calleja, “Biosensors based on nanomechanical systems,” *Chemical Society Reviews*, vol. 42, pp. 1287–1311, 2013.
- [126] D. Liberzon and D. Netic, “Input-to-state stabilization of linear systems with quantized state measurements,” *IEEE Transactions on Automatic Control*, vol. 52, pp. 767–781, 2007.
- [127] A. Molin and S. Hirche, “On the optimality of certainty equivalence for event-triggered control systems,” *IEEE Transactions on Automatic Control*, vol. 58, pp. 470–474, 2013.
- [128] P. Tabuada, “Event-triggered real-time scheduling of stabilizing control tasks,” *IEEE Transactions on Automatic Control*, vol. 52, pp. 1680–1685, 2007.
- [129] J. Lunze and D. Lehmann, “A state-feedback approach to event-based control,” *Automatica*, vol. 46, pp. 211–215, 2010.

- [130] M. Mazo Jr., A. Anta, and P. Tabuada, “An iss self-triggered implementation of linear controllers,” *Automatica*, vol. 46, pp. 1310–1314, 2010.
- [131] X. Wang and M. D. Lemmon, “Self-triggered feedback control systems with finite-gain  $calL_2$  stability,” *IEEE Transactions on Automatic Control*, vol. 54, pp. 452–467, 2009.
- [132] J. H. Sandee, W. P. M. H. Heemels, and P. P. J. van den Bosch, “Case studies in event-driven control,” in *Hybrid Systems: Computation and Control*, A. Bemporad, A. Bicchi, and G. Buttazzo, Eds. Berlin, Heidelberg: Springer Berlin Heidelberg, 2007, pp. 762–765.
- [133] J. H. Sandee, “Event-driven control in theory and practice,” *Eindhoven Technical University*, pp. 53–60, 2006.
- [134] A. Bemporad, M. Heemels, and M. Johansson, Eds. Springer London, 2010.
- [135] A. Singh, “Noise suppression in cell-size control,” *bioRxiv*, 2017. [Online]. Available: <http://biorxiv.org/content/early/2017/01/05/098640>
- [136] E. D. Sontag, *Mathematical control theory: deterministic finite dimensional systems*. Springer Science & Business Media, 2013, vol. 6.
- [137] M. Nagahara, D. E. Quevedo, and J. stergaard, “Sparse packetized predictive control for networked control over erasure channels,” *IEEE Transactions on Automatic Control*, vol. 59, pp. 1899–1905, 2014.
- [138] L. Xiao, M. Johansson, H. Hindi, S. Boyd, and A. Goldsmith, *Joint Optimization of Wireless Communication and Networked Control Systems*. Springer Berlin Heidelberg, 2005, pp. 248–272.
- [139] Y. Wang, S. X. Ding, H. Ye, and G. Wang, “A new fault detection scheme for networked control systems subject to uncertain time-varying delay,” *IEEE Transactions on Signal Processing*, vol. 56, pp. 5258–5268, 2008.
- [140] D. T. Gillespie, “The chemical Langevin equation,” *Journal of Chemical Physics*, vol. 113, pp. 297–306, 2000.
- [141] H. Kobayashi, M. Kærn, M. Araki, K. Chung, T. S. Gardner, C. R. Cantor, and J. J. Collins, “Programmable cells: Interfacing natural and engineered gene networks,” *Proceedings of the National Academy of Sciences*, vol. 101, pp. 8414–8419, 2004.
- [142] P. Szymańska, N. Gritti, J. M. Keegstra, M. Soltani, and B. Munsky, “Using noise to control heterogeneity of isogenic populations in homogenous environments,” *Physical Biology*, vol. 12, p. 045003, 2015.

- [143] A. Borri, P. Palumbo, and A. Singh, “The impact of negative feedback in metabolic noise propagation,” *IET Systems Biology*, pp. 179–186, 2016.
- [144] A. Singh, “Negative feedback through mRNA provides the best control of gene-expression noise,” *IEEE Transactions on Nanobioscience*, vol. 10, pp. 194–200, 2011.
- [145] G. C. Goodwin, H. Haimovich, D. E. Quevedo, and J. S. Welsh, “A moving horizon approach to networked control system design,” *IEEE Transactions on Automatic Control*, vol. 49, pp. 1427–1445, 2004.
- [146] S. Tatikonda and S. Mitter, “Control under communication constraints,” *IEEE Transactions on Automatic Control*, vol. 49, pp. 1056–1068, 2004.
- [147] J. Xiong and J. Lam, “Stabilization of linear systems over networks with bounded packet loss,” *Automatica*, vol. 43, pp. 80–87, 2007.
- [148] I. Golding, J. Paulsson, S. Zawilski, and E. Cox, “Real-time kinetics of gene activity in individual bacteria,” *Cell*, vol. 123, pp. 1025–1036, 2005.
- [149] B. Øksendal, *Stochastic differential equations*. Springer, 2003.
- [150] A. Amir, “Cell size regulation in bacteria,” *Physical Review Letters*, vol. 112, p. 208102, 2014.
- [151] K. R. Ghusinga, C. A. Vargas-Garcia, and A. Singh, “A mechanistic stochastic framework for regulating bacterial cell division,” *Scientific Reports*, p. 30229, 2016.
- [152] A. Singh and J. P. Hespanha, “Models for multi-specie chemical reactions using polynomial stochastic hybrid systems,” in *Proc. of the 44th IEEE Conf. on Decision and Control, Seville, Spain, 2005*, pp. 2969–2974.
- [153] P. Smadbeck and Y. N. Kaznessis, “A closure scheme for chemical master equations,” *Proceedings of the National Academy of Sciences*, vol. 110, pp. 14 261–14 265, 2013.
- [154] A. Singh and J. P. Hespanha, “Approximate moment dynamics for chemically reacting systems,” *IEEE Transactions on Automatic Control*, vol. 56, pp. 414–418, 2011.
- [155] M. Soltani, C. A. Vargas-Garcia, and A. Singh, “Conditional moment closure schemes for studying stochastic dynamics of genetic circuits,” *IEEE Transactions on Biomedical Systems and Circuits*, vol. 9, pp. 518–526, 2015.
- [156] K. R. Ghusinga, M. Soltani, A. Lamperski, S. V. Dhople, and A. Singh, “Approximate moment dynamics for polynomial and trigonometric stochastic systems,” in *IEEE 56th Conference on Decision and Control*, 2017, pp. 1864–1869.

- [157] J. Hespanha, “Modelling and analysis of stochastic hybrid systems,” *IEEE Proceedings Control Theory and Applications*, vol. 153, pp. 520–535, 2006.
- [158] N. Van Kampen, *Stochastic processes in physics and chemistry*. Elsevier, 2011.
- [159] R. Grima, “Linear-noise approximation and the chemical master equation agree up to second-order moments for a class of chemical systems,” *Phys. Rev. E*, vol. 92, p. 042124, 2015.
- [160] J. Elf and M. Ehrenberg, “Fast evaluation of fluctuations in biochemical networks with the linear noise approximation,” *Genome Research*, vol. 13, pp. 2475–2484, 2003.
- [161] R. Grima, “An effective rate equation approach to reaction kinetics in small volumes: theory and application to biochemical reactions in nonequilibrium steady-state conditions,” *Journal of Chemical Physics*, vol. 133, p. 035101, 2010.
- [162] R. Grima, P. Thomas, and A. Straube, “How accurate are the chemical langevin and fokker-planck equations?” *Journal of Chemical Physics*, vol. 135, p. 084103, 2011.
- [163] P. Thomas, A. V. Straube, and R. Grima, “The slow-scale linear noise approximation: an accurate, reduced stochastic description of biochemical networks under timescale separation conditions,” *BMC Systems Biology*, vol. 6, p. 39, 2012.
- [164] A. Brock, H. Chang, and S. Huang, “Non-genetic heterogeneity – a mutation-independent driving force for the somatic evolution of tumours,” *Nature Reviews Genetics*, vol. 10, pp. 336–342, 2009.
- [165] G. Balázsi, A. van Oudenaarden, and J. J. Collins, “Cellular decision making and biological noise: From microbes to mammals,” *Cell*, vol. 144, pp. 910–925, 2014.
- [166] T. M. Norman, N. D. Lord, J. Paulsson, and R. Losick, “Memory and modularity in cell-fate decision making,” *Nature*, vol. 503, pp. 481–486, 2013.
- [167] I. Lestas, G. Vinnicombe, and J. Paulsson, “Fundamental limits on the suppression of molecular fluctuations,” *Nature*, vol. 467, pp. 174–178, 2010.
- [168] M. Soltani, T. Platini, and A. Singh, “Stochastic analysis of an incoherent feed-forward genetic motif,” in *American Control Conference*, 2016, pp. 406–411.
- [169] P. Whittle, “On the use of the normal approximation in the treatment of stochastic processes,” *Journal of the Royal Statistical Society Series B*, vol. 19, pp. 268–281, 1957.

- [170] I. Krishnarajah, A. Cook, G. Marion, and G. Gibson, “Novel moment closure approximations in stochastic epidemics,” *Bulletin of Mathematical Biology*, vol. 67, pp. 855–873, 2005.
- [171] Z. Konkoli, “Modeling reaction noise with a desired accuracy by using the X level approach reaction noise estimator (XARNES) method,” *Journal of Theoretical Biology*, vol. 305, pp. 1–14, 2012.
- [172] R. Grima, “A study of the accuracy of moment-closure approximations for stochastic chemical kinetics,” *Journal of Chemical Physics*, vol. 136, p. 154105, 2012.
- [173] L. DeVille, S. Dhople, A. D. Domínguez-García, and J. Zhang, “Moment closure and finite-time blowup for piecewise deterministic markov processes,” *SIAM Journal on Applied Dynamical Systems*, vol. 15, pp. 526–556, 2016.
- [174] K. R. Ghusinga, C. A. Vargas-Garcia, A. Lamperski, and A. Singh, “Exact lower and upper bounds on stationary moments in stochastic biochemical systems,” *Physical Biology*, vol. 14, p. 04LT01, 2017.
- [175] A. Lamperski, K. R. Ghusinga, and A. Singh, “Analysis and control of stochastic systems using semidefinite programming over moments,” *arXiv preprint:1702.00422*, 2017.
- [176] K. R. Ghusinga, A. Lamperski, and A. Singh, “Moment analysis of stochastic hybrid systems using semidefinite programming,” *arXiv preprint*, p. 1802.00376v1, 2018.
- [177] M. Soltani and A. Singh, “Effects of cell-cycle-dependent expression on random fluctuations in protein levels,” *Royal Society Open Science*, vol. 3, p. 160578, 2016.

## **Appendix A**

### **DISCLAIMER**

Substantial parts of this thesis (theoretical results and figures) have been previously published in several proceedings and journals of IEEE, Public Library of Science, Automatica, and Royal Society [18,20,21,177]. Given that these publications has Open Access rights, the use of figures and results, completely contained within the papers, is permitted according to the creative commons license.